VARIABLE FREQUENCY MICROWAVE CURING OF POLYURETHANE

Diane C. Folz

Thesis submitted to the faculty of the Virginia Polytechnic Institute and State University
in partial fulfillment of the requirements for the degree of

Master of Science in
Materials Science and Engineering

David E. Clark
Gary S. Pickrell
Robert W. Hendricks

19 July 2011
Blacksburg, Virginia

Keywords: microwave processing, FTIR spectroscopy, attenuated total reflectance, cure rate, polymer coatings, wood coatings

VARIABLE FREQUENCY MICROWAVE CURING OF POLYURETHANE

Diane C. Folz

ABSTRACT

Historically, coatings were processed from natural oils, fats, and resins; the first well-known and widely used being *lacquer* [Meir-Westhues, 2007]. In the 20th century, synthetic resins were developed to achieve coatings with improved properties. Of these coating compositions, *polyurethanes* (PURs) were one of the most prevalent. Polyurethanes became possible in 1937 when Otto Bayer developed the diisocyanate polyaddition process [Randall et al, 2002]. Since that time, literally thousands of PUR compositions have been used commercially. The primary application of interest in this study is that of coatings for wood substrates.

It is well-known among materials researchers that there can be a number of differences between microwave and conventional materials treatment techniques [Clark et al, 1996], including enhanced reaction rates, lowered processing temperatures for some products, and selective interactions in composite systems. The primary goals of this research were to determine (1) whether microwave energy affected the cure rate in a water-based, aliphatic PUR, as compared with conventional curing techniques, and (2) if there was an effect of microwave frequency on the cure rate.

The primary tool for determining extent of cure in the PUR samples was Fourier transform infrared spectroscopy (FTIR). Using this characterization method, the changes in intensities of four bonds specific to the PUR composition were followed. It was determined that, in the particular PUR composition studied, microwave energy had an effect on the cure rate when compared with conventional heating, and that there was a frequency effect on the cure rate. Additionally, a deeper understanding of the use of FTIR spectroscopy techniques for studying cure kinetics was developed.

DEDICATION

I dedicate this thesis to my parents, Peter and Helen Folz.

ACKNOWLEDGEMENTS

First and foremost, my sincere thanks to my mentor, Dr. David E. Clark, for his years of support and encouragement. He didn't just open doors for me, but gave me that gentle push (and sometimes the kick in the pants) to get me to step over the threshold. I can't imagine having done this work without his leadership, guidance, and friendship.

Thank you also to co-advisor, Dr. Gary Pickrell. He kept my eyes on the ball always and helped me to see experimental design with clarity. The hours spent in conversation with Dr. Robert Hendricks, my third committee member, were entertaining and enlightening. I also appreciate the contributions that Drs. Bill Reynolds, Sean McGinnis, and Maureen Julian have made to my understanding of materials engineering.

To all the graduate students I've worked with over the years, I owe a great debt. They all paved the way for me and taught me as much about life as about research. In particular, Becky Schulz, Zak Fathi, Carlos Folgar, and Raghu Thridandapani – you are great friends, but also examples of excellence.

For Mulder, Dana, and Peel – they tolerated my moods and the late nights and never gave up on me. Finally, my deep gratitude to Patricia Mellodge, Sue Clark, and Tracey Keister – friends through it all!

TABLE OF CONTENTS

LIST OF FIGURES

LIST OF TABLES

LIST OF EQUATIONS

LIST OF SYMBOLS

α	=	absorption coefficient
a	=	fraction absorbed
A	=	absorbance
c	=	concentration of bonds represented
C_p	=	specific heat
cm	=	centimeter
cm^{-1}	=	wavenumber
$C\text{-}N_{str}$	=	carbon-nitrogen bond; stretching
$C{=}O_{str}$	=	carbon-oxygen double bond; stretching
dB	=	decibel
dBm	=	power ratio in decibels of the measured power referenced to one milliwatt
δ	=	loss angle
°	=	degrees
°C	=	degrees Celsius
D_p	=	depth of penetration
e^x	=	exponential function
E^2_{rms}	=	root mean square of the internal electric field
ε_o	=	permittivity of free space
ε'	=	dielectric constant
ε''	=	relative dielectric constant
ε''_{eff}	=	effective relative dielectric loss
ε''_d	=	dielectric loss due to dipolar polarization
ε''_i	=	dielectric loss due to ionic polarization
ε''_e	=	dielectric loss due to electronic polarization
ε''_s	=	dielectric loss due to interfacial polarization
ε''_c	=	dielectric loss due to dc conductivity
f	=	frequency
GHz	=	gigahertz
H^2_{rms}	=	root mean square of the internal magnetic field
A/m	=	ampere per meter (unit of magnetic field strength)
I_c	=	intensity of absorbance peak at cured state

I_m	=	measured intensity
I_λ^O	=	intensity of incident beam at wavelength, λ
I_λ^R	=	intensity of reflected beam at wavelength, λ
I_λ^T	=	intensity of transmitted beam at wavelength, λ
in	=	inches
kg/m^3	=	mass density
kJ/kg-°C	=	kilojoule per kilogram per degrees Celsius
km	=	kilometer
kW	=	kilowatt
L	=	liter
λ	=	wavelength
ℓ	=	pathlength
m	=	meter
mm	=	millimeter
μm	=	micron or micrometer
mol/L	=	moles per liter
mol	=	moles
mol	=	moles
ml	=	milliliter
ml	=	milliwatt
μ_0	=	permeability of free space
μ'	=	magnetic loss factor
μ''	=	relative magnetic loss factor
μ''_{eff}	=	effective relative magnetic loss factor
O-H$_{str}$	=	oxygen-hydrogen bond; stretching
ω	=	angular frequency
N-H$_{str}$	=	nitrogen-hydrogen bond; stretching
P$_a$	=	power absorbed per unit volume
P$_a$*	=	power absorbed
ρ	=	density
R	=	free radical
R'	=	functional group
R	=	reflectance

sec or s	=	second
t	=	time
T	=	temperature
T_{max}	=	maximum temperature
T_{soak}	=	soak temperature
T	=	transmittance
tanδ	=	loss tangent
θ_i	=	angle of incident beam
θ_r	=	angle of reflected beam
V/m	=	volts per meter
W	=	watt
W/m^2	=	watts per square meter
W/m^3	=	watts per cubic meter

LIST OF ACRONYMS

ATR	**=**	Attenuated Total Reflectance
CF	=	Central Frequency
DMA	**=**	Dynamic Mechanical Analyzer/Analysis
DSC	**=**	Differential Scanning Calorimeter/Calorimetry
EM	**=**	Electromagnetic
FEM	**=**	Finite Element Model
FP	**=**	Forward Power
FTIR	**=**	Fourier Transform Infrared Spectrometer/Spectroscopy
GL-4850	**=**	Water-based, Aliphatic Polyurethane, Van Technologies, Inc.
HAP	**=**	Hazardous Air Pollutant
HATR	**=**	Horizontal Attenuated Total Reflectance
IR	**=**	Infrared
PUR	**=**	Polyurethane
RP	=	Reverse Power
TE	**=**	Transverse Electric
TGA	**=**	Thermogravimetric Analyzer/Analysis
TM	**=**	Transverse Magnetic
TPU	**=**	Thermoplastic Polyurethane
TWT	**=**	Traveling Wave Tube
UR	**=**	Urethane
UV	**=**	Ultraviolet
VFM	**=**	Variable Frequency Microwave
VOC	**=**	Volatile Organic Compound

CHAPTER 1: INTRODUCTION

1.1 Goals and Objectives

1.1.1 Primary Goals

The primary goals of this work were to (1) determine whether microwave energy affected the cure rate in water-based, aliphatic polyurethane when compared with conventional curing techniques, and (2) to determine whether different microwave frequencies had different effects on the cure rate.

It is well-known among materials researchers that there can be a number of differences between microwave and conventional processing techniques [Clark et al, 1996], including:

- the reaction rates associated with microwave heat treatments are enhanced in some materials; in some cases, significantly;
- heat is generated by the interaction of the material with the electromagnetic radiation that results in volumetric heating, rather than heating by thermal conduction from the surface via an external heat source;
- because the degree of interaction with the electromagnetic energy is different for different types of materials, selective heating of specific phases or components is possible;
- heating with microwave energy is governed by the dielectric properties of the material, and by the frequency and power of the microwave field, as opposed to being controlled only by the surrounding thermal environment.

1.1.2 Objectives

There were three primary objectives established as crucial to achieving the project goals:

Objective 1: Establish the definition of cure for the specific polyurethane under study

In *THE POLYMER SCIENCE DICTIONARY,* Alger defines *cure*[1] as "the process of deliberately *crosslinking* a polymer to improve its properties, especially mechanical properties, such as stiffness" [Alger, 1997]. Curing is a critical stage in forming the polymer. It is through this process that the modulus increases, and the solubility and resistance to swelling increase (dimensional stability).

It is understood by manufacturers of high-grade musical instruments at Taylor Guitars that their ultraviolet (UV)-cured polyester resin coatings are not completely cured prior to leaving the

[1] Note: All italicized terms are defined in Appendix 1.

factory [Guzzetta & Baldwin, 2008]. There is an interest in finding a coating material and a method of cure for that coating so that the products can be cured completely before they leave the manufacturing floor. Additionally, there always is interest in the potential for lowering the amounts of volatile organic compounds (VOC) emitted by the coatings [Guzzetta & Baldwin, 2008], thus the interest in water-based polyurethanes that can be cured using and energy efficient microwave process.

The specific candidate coating material selected for this study was water-based, *aliphatic* urethane[2]. This particular product is design for maximum clarity as a protective topcoat on wood products. It is a non-yellowing composition with low VOC content and a negligible hazardous air pollutants (HAP) classification. Upon curing, it yields a clear coating with excellent mechanical properties, well-suited particularly for flooring and furniture applications or where a high-quality clear coating is desirable.

Objective 2: Establish the microwave processing method and parameters, and conduct processing experiments

Microwave processing techniques are being proposed as a possible replacement method for UV radiation curing of some wood coatings. The primary reasoning behind this proposal is the issue with "*strike-in*" associated with UV curing methods. This situation occurs when the coatings penetrate the wood surface and cannot be "seen" by the UV light. This phenomenon also could lead to limitations on curing coatings on complex shapes where the entire surface is not visible to the UV radiation. Microwave radiation, on the other hand, has the potential to penetrate many of these materials to cure the coating materials that have soaked into the pores of the substrate; also, to reach all the surfaces of complex shapes. Additionally, microwave energy has been shown to accelerate curing in polymer adhesives by as much as 10 to 20 times that of conventional methods [Lambda Technologies, 2010]. If the cure rate of the coatings can be increased with little or no impact on the substrate materials, then microwave energy can offer a viable alternative for curing coating materials for a wide range of industrial applications.

Several microwave processing techniques were available for this work, including single-mode and multimode fixed frequency microwave systems, and a low-power, variable frequency microwave system. **For this study, the relationship between cure rate of the selected polymer and microwave energy was evaluated for frequencies in the range from 6 to 18GHz** (specifically, 7, 12 and 17GHz) **using a variable frequency microwave oven[3].**

[2] Greenlight Coatings, Product Number GL-4850, Van Technologies, Inc., Duluth, MN.
[3] Variwave® Model 1500, Lambda Technologies, Inc., Morrisville, NC.

Objective 3: Identify the characterization and/or testing technique(s) to evaluate the effect of microwave radiation on the cure rate of polyurethane

The most common method for establishing a cure profile for a material is to measure the change in weight and phase versus time [Randall et al, 2002]. The cure kinetics most often are determined using thermal analysis techniques; specifically, *thermogravimetric analysis* (TGA) and *differential scanning calorimetry* (DSC). However, *Fourier transform infrared spectroscopy* (FTIR) is used most often when the reactions of specific compositional components are to be followed. This method works very well on both coatings and thin films.

A Thermo Electron FTIR spectrometer[4] was used to follow four peaks: the broad water peak at approximately 3450cm^{-1} [Barnes, 2002]**; the carbonyl peak at 1729cm^{-1}** [Smith, 1990]**; the aliphatic *amine* peaks at 1241 and 1148cm^{-1}** [Smith, 1990]**.** While there is a significant number of peaks in the range from about 1800 to 450 cm^{-1} that are due to the polymer cure, the three strong peaks selected showed the most change and were selected based on their prominence in the specific coating type being evaluated. While isothermal runs were conducted in the TGA-DSC, the primary method for determining the cure rate for various treatment methods was FTIR spectroscopy.

[4] Avatar FTIR Spectrometer Smart SpeculATR Stage Assemblies, Model 330, Thermo Fisher Scientific, Inc., West Palm Beach, FL.

CHAPTER 2: LITERATURE REVIEW

2.1 Polyurethane

Archaeology has uncovered some of the earliest uses of coatings by man; namely, cave paintings. This use of coatings is believed to have been a form of storytelling and of art [Szulga, 2003]. These early coatings used magnesium oxide, ochre, and charred wood as colorants and were often mixed into animal fats to enrich the colors. However, as time progressed, so did the understanding of the importance of coatings to the lifetime and even use of certain materials. Some of the earliest uses of coatings were as protection for wood from the elements. From tools to construction materials, paints rapidly became one of the most significant uses for coatings. Later, as synthesis of organic chemicals led the way to a multitude of polymer compositions, coatings took on the role of the ultimate protection for a wide range of materials.

Historically, coatings were processed from natural oils, fats, and resins, the first well-known and widely used being *lacquer*. One of the first lacquers was *shellac*, made from the natural secretions of the lac bug. The word 'lacquer' is derived from the Sanskrit word for 100,000 and referred to the great multitude of bugs needed to produce shellacs [Meir-Westhues, 2007].

In the 20th century, synthetic resins were developed to achieve coatings with improved properties. Of these coating compositions, *polyurethanes* (PURs) were one of the most prevalent. Polyurethanes became possible in 1937 when Otto Bayer developed the diisocyanate polyaddition process [Randall et al, 2002]. These first diisocyanate-based, single-component PURs were *aromatic* and tended to yellow with exposure to UV radiation. When *aliphatic* PURs were developed in the 1960s, the application of this material for coatings broadened substantially, as they could remain clear under exposure to UV light [Meir-Westhues, 2007]. Aliphatic PURs were prepared by combining diisocyanate with polyols. Coatings based on these compositions did not have to be baked in order to achieve good mechanical properties, as was required for the early aromatic compositions. The development of these aliphatic compositions was driven primarily by the automotive industry, due to the size of their products and the improbability of successfully baking them. This application demanded a composition that was durable, compatible with the paints, and that maintained a consistent appearance for several years. As more and more stringent environmental regulations have been enacted and as cost-optimization for coated products has become a priority, researchers have been working to develop solvent-free compositions (or having negligible VOCs) that are water-based, or that cure with more energy efficient processing methods [Randall et al, 2002].

With these improvements, the uses for PURs further increased and broadened. Compositions were developed that led to products ranging from the soles of shoes to foam insulation; from the basis for interior and exterior paints to coatings for a wide range of wood, glass, and metal products [Randall et al, 2002; Fried, 1995; Allen, 2006]. While the applications for PURs are wide-ranging, their application as a coating material was the basis for this study.

2.1.1 Polyurethane Chemistry

A *polyurethane* is defined as "a polymer which contains *urethane* (-NHCOO-) groups in the polymer chain" [Alger, 1997]. In many of these PUR compositions, the urethane group is only a minor component, with functional groups such as ether or amide present in significantly higher numbers.

The primary method used for forming the urethane groups (– NHCOO –) present in PURs is the diisocyanate polyaddition process [Randall et al, 2002]. The generic chemical reaction of the diisocyanate with the diol is presented in Equation (2.1). The step-growth polymerization reaction that leads to the linear polymer is shown in Equation (2.2) [Alger, 1997]. In these equations, R and R′ represent *free radicals* and *functional groups*, respectively, associated with the components specific to the particular composition.

$$\mathrm{R-NCO+HO-R'} \rightarrow \nsim \mathrm{RNHCO-OR'} \tag{2.1}$$

$$\mathrm{OCN-R-NCO+nHO-R'-OH} \rightarrow \nsim \mathrm{O-CONH-R-NHCO-O-R'} \nsim \mathrm{n} \tag{2.2}$$

In the water-based, aliphatic urethane used for this study, the crosslinking associated with the material was detected in the increased intensity of three peaks: two for aliphatic amines and one for carbonyls. Additionally, there was a confounded peak due to water, alcohol, and secondary urethanes that underwent a significant intensity decrease due to the loss of the solvents. A low-intensity peak associated with the *crosslinked* urethane remained visible (see further information in Chapter 4: Results and Discussion).

These PURs can exist in the form of a *thermoplastic* or *thermoset*, the primary difference being that a thermoset is so crosslinked that it does not soften significantly on heating [Alger, 1997]. A thermoplastic PUR product can be formed by a wide range of melt processing methods, such as injection molding or casting. Many of the thermoplastic PURs, known as TPUs, are elastomeric; they are segmented into hard and soft phases.

The chemistry of urethane-based material ranges from simple to highly complex. While the fundamental urethane group is common to this class of materials, there are many additives that can be used to formulate PURs with a wide range of properties (Fried, 1995; Randall, 2002; Szycher, 1990].

Aliphatic vs. Aromatic

Aromatic compounds are those in which the carbon atoms are connected via benzene rings [Randall et al, 2002]. They are one of the most common chemistries found in urethanes and polyurethanes, existing in forms ranging from elastomers to rigid thermosets. Characterized by low chemical and UV resistance, they tend to degrade and discolor in sunlight.

The carbon atoms in aliphatic urethanes and polyurethanes, on the other hand, are connected via straight or branched chains, rather than the benzene rings. The aliphatic compounds are characterized by UV and chemical stability. They do not discolor or break down easily in sunlight, making them desirable, especially for coating applications.

2.1.2. Curing Methods

Air Cure

Many PUR products on the market today are designed specifically to cure by evaporation of binders or suspension media, such as alcohols or water [Van Iseghem, 2006]. The air-cure products are designed specifically as coatings and are intended for use by the at-home end user. These products are used primarily for small jobs, such as low-volume furniture and floor finishing, and exterior weather protection for the home and garden [Allen, 2006]. Most of the products that are categorized as air curing refer to air "drying" (rather than true curing), are accomplished normally within 20 to 360 minutes of application. In fact, many of these products continue to cure (crosslink) for several weeks, or even months, following the air drying step [Van Iseghem, 2006; Guzzetta & Baldwin, 2008]. For the low-volume home consumer applications, the dry finishes are sufficient in that they are significantly cured to resist damage, such as scratching or discoloration.

Chemical Cure

Catalysts are used in PUR compositions for multiple reasons, including to aid in proper curing for a variety of applications and environments and, in some products, to serve as the primary method for complete cure [Randall et al, 2002; Fried, 1995]. These compositions are classified in several forms: 2-component, 1-component, and oil-modified or *alkyd* coatings. In

each of the composition types, the *catalysts* vary significantly; but in all, they are used specifically to "jump start" reactions in those compositions considered to have low reactivity. Typical catalysts include: triethylenediamine/glycols (many applications), tin salts (elastomers), lead naphthenate (spraying applications – poor choice environmentally), and N, N-dimorpholindiethylether (high moisture environments; adds to shelf life significantly). The cure time for these types of coatings varies widely and depends on the particular composition, especially that of the catalyst [Fried, 1995].

Thermal Cure

Thermal "curing" of PUR coatings normally is accomplished using infrared (IR) lamps or hot air (convection currents) methods [Martin Guitar Company, 2007; Randall et al, 2002]. Both of these techniques are relatively low cost and allow for slow cure rates, avoiding possible cracking of the coatings or warping of the substrates. For most PUR coatings, "slow" is a relative term in that they can be air dried in a few hours, or even minutes. However, these coatings are not truly cured; the curing process can take days, weeks, or even months to complete. In those cases where IR lamps or convection are selected, usually it is a method to accelerate the air or chemical cure processes. Temperatures rarely exceed 75 to 150°C [Martin Guitar Company, 2007; Fried, 1995], depending on the product. In these thermal cure processes, the goal is to "set" the product coatings so they can be handled soon after the thermal process cycles.

Ultraviolet (UV Radiation) Cure

Along with using UV radiation for curing PUR coatings has come the need for developing UV-specific coating chemistries [Van Iseghem, 2006]. As with all radiation curing techniques, the material must absorb the energy associated with the particular wavelength range to which it is exposed [Randall et al, 2002]. Many of the traditional PUR compositions could absorb in the IR range, but not in the UV range. Therefore, new coating compositions were developed that were tailored specifically to absorb in the UV range. These new coatings also had to fit easily into the coating operations used for thermally and IR-treated materials, especially for high-volume industrial operations.

Three types of UV-curable coating materials exist currently on the market: 100% solids, water-reduced coatings, and solvent-reduced coatings [Van Iseghem, 2006; Fried, 1995; Randall et al, 2002]. Of these choices, the solvent-reduced materials were most quickly accepted, but the water-reduced and 100% solids materials were significantly more desirable from an environmental perspective. Typical cure times range from seconds to hours, based on

composition and coating thickness. Table 2.1 outlines some of the characteristics associated with each of these UV-curable coating materials.

Table 2.1: Advantages and disadvantages associated with different types of UV-curable polyurethane coating materials [Van Iseghem, 2006; Randall et al, 2002; Fried, 1995].

Coating Classifications	Advantages	Disadvantages
100% Solids (Entirely chemical active - no water or solvent)	• Converts directly to solid upon UV exposure • Excess coating can be re-used • Rapid production rates • Small equipment footprint • Spray equipment doesn't clog and overspray doesn't cure (if no exposure to UV)	• Thickness builds quickly (difficult to control without training) • Low-gloss difficult to achieve • "Orange peel" can be noticed with lower quality coatings
Water-reduced (water to "thin" the solution – no solvents)	• Viable option for transition to UV coatings from conventional compositions • Good option from environmental perspective	• Soaks into porous substrates • If solids content is too low, can have "build" problems
Solvent-reduced	• Very easy transition from conventional coatings • Same equipment for application (only different for cure step) • Performs the same as conventional coatings, but cures much more quickly (higher throughput)	• Not good from a regulatory perspective – polluting (high VOC emissions) and can be toxic • Can have low solids loading if not carefully controlled in production

In general, most UV-curable coatings are difficult to sand, as they have higher hardness values than other types of coatings. Additionally, they can be very difficult to cure on some woods – sapwoods or woods with high oil contents, in particular, as the sap or oil tends to collect at the wood surface upon heating under high-intensity UV lamps. In the case of the 100% solids and the solvent-based materials, a dry substrate is required, necessitating a pre-heat step for most substrate materials [Van Iseghem, 2006; Randall et al, 2002].

One of the primary issues with UV curing of polymers is that UV radiation cures only what it "sees." In other words, any coating materials that penetrate the substrate will not be visible to the UV radiation [Van Iseghem, 2006; Guzzetta & Baldwin, 2008], a phenomenon referred to as

"strike-in." This material can be trapped beneath already cured layers and prove difficult to cure, or the curing process can cause damage to the coating material, substrate, or both.

2.2 Microwave Processing

2.2.1 Microwave-Material Interactions

Microwave frequencies are defined as corresponding to a frequency range of 0.3 and 300GHz (wavelengths of 1m to 1mm, respectively) [Metaxas, 1993]. This range puts them between the radio (RF) and IR frequencies in the electromagnetic (EM) spectrum, as seen in Figure 2.1 [New World Encyclopedia, 2011].

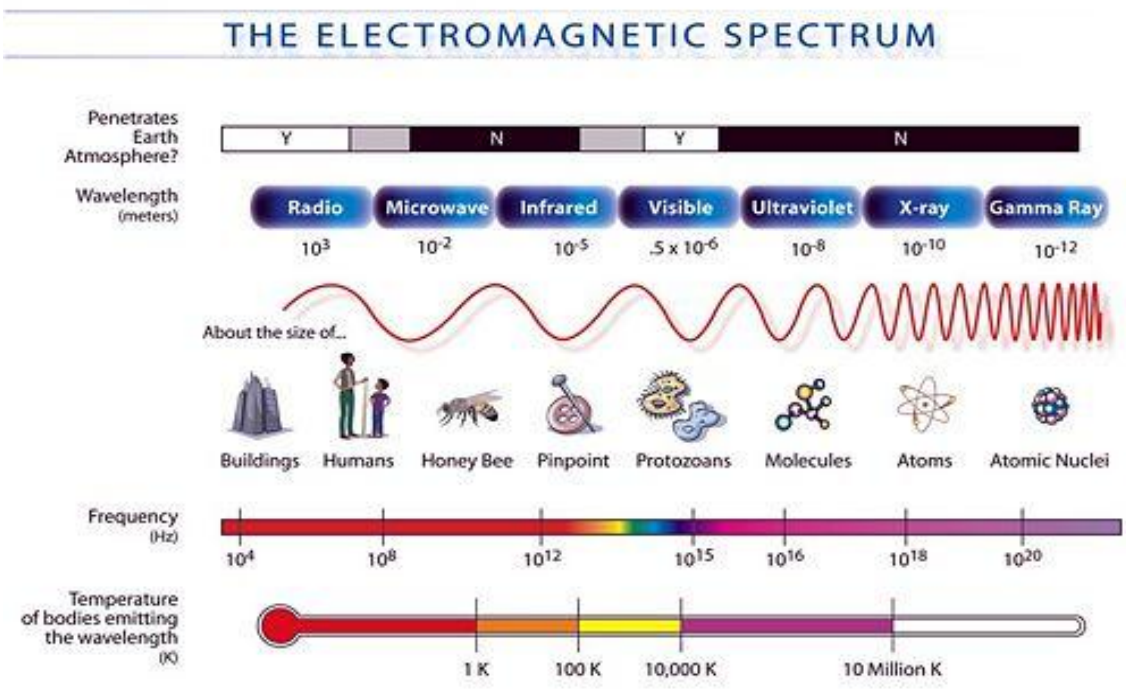

Figure 2.1: A depiction of the microwave frequency range as it falls in the electromagnetic spectrum [New World Encyclopedia, 2011; Used under fair use guidelines, 2011].

Materials are classified in four primary ways with respect to their interactions with microwave energy [Sutton, 1989] (with examples at room temperature): absorbing (i.e. silicon carbide), reflecting (i.e. bulk metal), transparent (i.e. alumina, cubic zirconia), and partially absorbing (silicon carbide particles or fibers interspersed in an alumina matrix). Figure 2.2 illustrates the change in the microwave field strength as it interacts with materials in each of these classifications. Note that dielectric properties of a material change with temperature [Thuery, 1992; Metaxas, 1993], thus the interactions with the microwaves also can change as the

temperature of the material changes. The polyurethane material is a microwave absorber and is represented by the behavior in case number three.

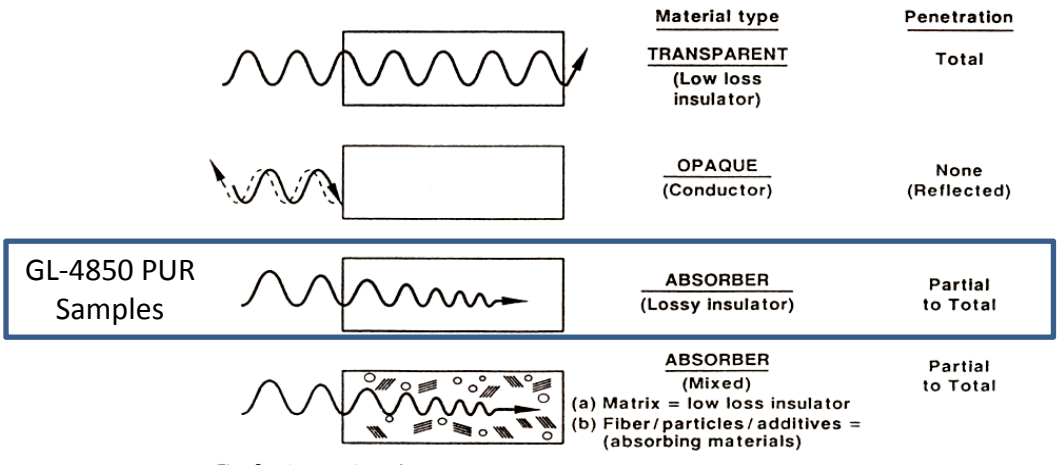

Figure 2.2: Illustration of the four ways in which microwaves interact with materials [adapted from Sutton, 1989; Used under fair use guidelines, 2011].

Microwaves can be absorbed by materials either through polarization or conduction mechanisms. Polarization involves short-range displacement of charge through formation and rotation of electric dipoles (or magnetic dipoles, if present). Conduction requires long-range transport of charge (compared to rotation) [Hench et al, 1990].

In addition to dipole rotation, other widely recognized polarization processes include interfacial, ionic, and electronic polarization. These processes are discussed in detail by Hench et al for typical ceramic materials; however, the same polarization mechanisms also are applicable to most electrically non-conducting polymers. Because several processes can contribute to the dielectric losses, and it is not always easy to differentiate experimentally between the loss mechanisms, losses typically are reported as effective losses, ε''_{eff}. To adequately characterize the response of materials to the electromagnetic spectrum, measurements should be made over a broad frequency range. Frequency ranges where each of these polarization mechanisms can contribute to losses may vary considerably over the EM spectrum, depending on the material. Because of the frequency dependence of absorption, a single frequency such as 2.45GHz cannot be used easily to heat all materials from room temperature. Efficiently heating a material that does not have an absorption mechanism close to 2.45GHz requires that the frequency of the EM radiation be changed, that the composition of the material be tailored to the frequency, or that

hybrid heating techniques can be employed that involve both conventional and microwave heating (i.e., radiant, laser, or UV combined with microwave radiation) [Clark et al, 2005].

The amount of heating a material undergoes is determined by how much and how fast energy can be absorbed, governed by the power per unit volume or power absorbed, shown in Equation (2.3). The first term on the right hand side is due to the electric field and the second term is due to the magnetic field [Clark et al, 2005; Thuery, 1992].

$$P_a = \omega \varepsilon_0 \varepsilon''_{eff} E^2_{rms} + \omega \mu_0 \mu''_{eff} H^2_{rms} \quad (\text{W/m}^3) \tag{2.3}$$

Where, P_a ≡ power absorbed (W/m^3),
ω ≡ angular frequency (Hz),
ε_0 ≡ permittivity of free space (8.85 x 10^{-12} F/m),
ε''_{eff} ≡ effective relative dielectric loss factor (unitless),
E^2_{rms} ≡ root mean square of the internal electric field (V/m),
μ_0 ≡ permeability of free space (1.26 x 10^{-6} H/m),
μ''_{eff} ≡ effective relative magnetic loss factor (unitless), and
H^2_{rms} ≡ root mean square of the internal magnetic field (A/m).

In a typical microwave processing experiment, the forward and reflected powers are measured and P_a is calculated based on the sample size. For many polymer and ceramic materials, the magnetic losses are considered insignificant and the primary energy absorption by the material is due to the absorption of the electric field [Clark et al, 2005]. In this case, Equation (2.3) reduces to the following:

$$P_a = \omega \varepsilon_0 \varepsilon''_{eff} E^2_{rms} \quad (\text{W/m}^3) \tag{2.4}$$

The overall relative dielectric loss can be expressed as

$$\varepsilon''_{eff} = \varepsilon''_c + \varepsilon''_s + \varepsilon''_d + \varepsilon''_i + \varepsilon''_e \quad (\text{unitless}) \tag{2.5}$$

where, ε''_c is the loss due to dc conductivity. The last four terms represent dielectric losses due to polarization mechanisms: ε''_s represents space charge or interfacial; ε''_d represents dipolar; ε''_i represents ionic, and ε''_e represents electronic. For materials in the microwave frequency range,

ε''_s and ε''_d are the most important. Sometimes, ε''_{eff} is replaced by $\varepsilon' tan\delta$, where δ is the loss angle, $tan\delta$ is the dissipation factor, and ε' is the dielectric constant. Materials with room temperature loss factors between 10^{-2} and 5 are good candidates for microwave heating; those with $\varepsilon''_{eff} < 10^{-2}$ are difficult to heat; and, those with $\varepsilon''_{eff} > 5$ experience most of the heating in the surface and not the bulk [Thuery, 1992].

The rate of temperature rise ($\Delta T/\Delta t$) in a material when microwave energy is absorbed is given by,

$$\frac{\Delta T}{\Delta t} = \frac{P_a}{\rho(C_p)} \quad (°C/sec) \tag{2.6}$$

where, ρ is density of the material (kg/m^3), and C_p is the specific heat (kJ/kg-°C) [Thuery, 1992]. If the density and specific heat are known for a particular material, it can be seen that the rate of temperature increase is proportional to the power absorbed by the material.

It must be noted that the electric field in the cavity that surrounds the sample material is not uniform in most multimode microwave ovens, which is why many home microwave ovens require turntables or mode stirrers. The cavity should be much larger than the wavelength of the microwaves, but if it is too large, the field will be weak in some locations and strong in others. Possible solutions to this problem, particularly in research applications, include the use of a single-mode microwave applicator with the capability of measuring the applied electric field, or use of a variable frequency microwave (VFM) oven.

2.2.2 Microwave Processing Equipment

Single-mode vs. Multimode Applicators

A mode can be defined as a particular distribution of the electromagnetic field in a transmission line or cavity [Metaxas, 1993]. A multimode cavity is one in which different patterns of electromagnetic waves are present, and the total electromagnetic field in the cavity is the summation of all the excited modes. This configuration makes the analysis of the field distribution difficult, especially after the introduction of a sample material, which can shift the energy distribution significantly. In a single-mode cavity, only one mode is excited, so the primary advantage is that the field distribution in the cavity can be determined precisely.

The single-mode microwave system generates a single, fixed frequency with a well-defined electromagnetic field [Metaxas, 1993]. The intensity (peak power) and position of the field within the cavity can be varied, but the shape and power distribution of the field remains the same. Because the exact nature of the EM field can be determined in a single-mode cavity, this

configuration often is used for research into microwave-materials interactions. An illustration of the microwave field within a 2.45GHz rectangular cavity is shown in Figure 2.3 [Folgar, 2010].

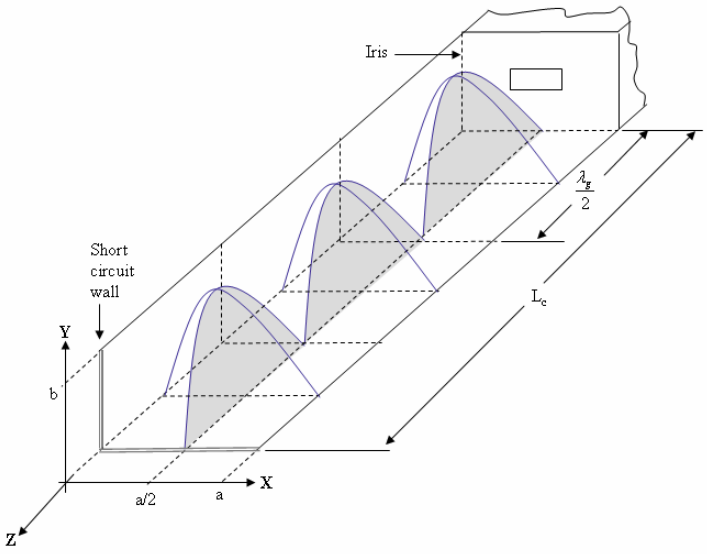

Figure 2.3: Illustration of a microwave field generated in a single-mode microwave cavity; in this case, a TE_{103} cavity at 2.45GHz [Folgar, 2010; Used under fair use guidelines, 2011].

The primary reasons for using multimode cavities are to enable heating of large samples/products and to have as uniform a field distribution/density as possible so as to provide consistent energy absorption throughout the a sample. A number of efforts have been made to map multimode cavities associated with 2.45GHz due to the use of this frequency in home model microwave ovens and in the food manufacturing industry [Chan et al, 2000; Schiffmann, 1997]. The theoretical distribution of EM energy within a particular cavity (or applicator) is determined primarily using Finite Element Modeling (FEM) techniques, or by calculating the transverse electric (TE) and transverse magnetic (TM) components of the specific hardware. Experimentally, the distribution of the electric field can be determined by using a probe technique in which the normal field distribution on the interior surface of the microwave cavity is measured (method is described in detail by Chan et al, 2000). Figure 2.4 (a) and (b) illustrate the different field patterns associated with calculation versus experimental methods.

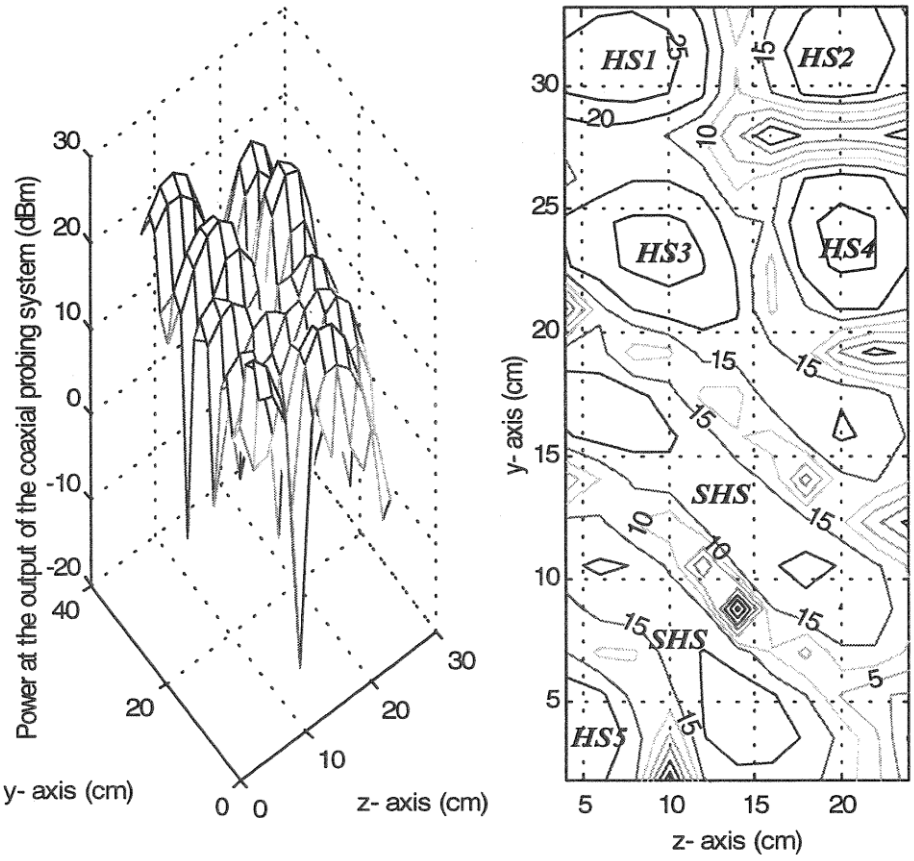

(a) (b)

Figure 2.4: Field patterns in a multimode microwave cavity: (a) calculated; (b) experimentally determined [Chan et al, 2000; Used under fair use guidelines, 2011]. Note: The "H designations" in (b) indicate areas of different peak powers.

Magnetrons (Fixed Frequency) vs. Traveling Wave Tubes (Variable Frequency)

The magnetron was attributed originally to Albert Hull, who conceived of the device in 1921 [Pozar, 2005]. Independent development took place in the same timeframe in Czechoslovakia, Japan, the United States, and France. However, the magnetron tube was developed in the 1930s and was the first practical microwave source [Pozar, 2005; Thuery, 1992]. It was the basis for the microwave radar used during World War II. Over the past three decades, these magnetron tubes have been replaced by solid state devices in low-power (<10kW) and low-frequency (<100GHz) microwave equipment.

These first uses of microwave energy were to carry an information signal, with thermal applications in which the EM wave carried energy coming much later (in the 1940s) [Thuery,

1992]. The first continuous wave magnetron was developed by Raytheon and patented in 1949. In 1951, the first microwave oven was patented in the United States. In 1962, Tad's, a restaurant in New York City, became the first establishment to serve food with no traditional kitchen! It was equipped completely with microwave ovens to cook the food that was served.

The magnetron, illustrated schematically in Figure 2.5, is comprised of a cylindrical anode with a cathode running along its axis [Thuery, 1992]. This cathode (usually tungsten) is heated in the magnetron assembly via a filament (wound around the cathode in the diagram). A magnetic field is generated parallel to the axis of the magnetron tube via an electromagnet (or permanent magnets), powered via a constant potential between the anode and cathode. The basic function of the magnetron is to generate a stream of electrons, emitted by the cathode and directed by the magnetic field, into a resonant microwave cavity specific to the emitted EM frequency.

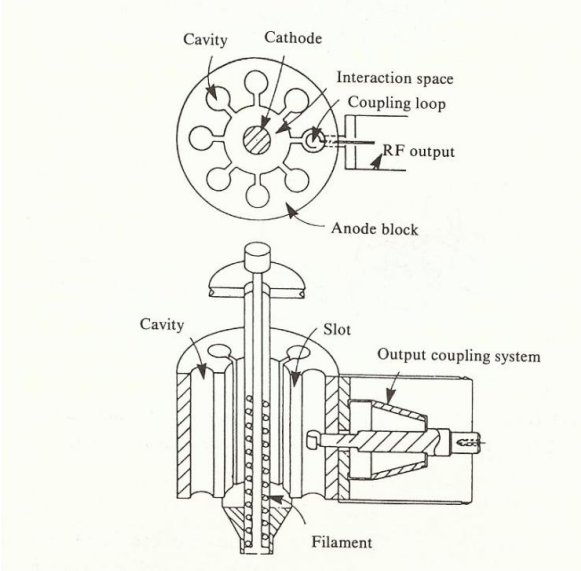

Figure 2.5: Schematic of a microwave magnetron [Thuery, 1992; Used under fair use guidelines, 2011].

Theoretically, magnetrons can be designed (by size of the resonant cavities in the anode and strength of the electric and magnetic fields) to emit any microwave frequency [Pozar, 2005; Thuery, 1992]; however, they are fixed frequency devices with limited power variations. The most common of the microwave frequencies is 2.45GHz; not because it is easier to manufacture or power, but because it is used almost exclusively by the food industry, by far the largest industrial application of microwave heating [Schiffmann, 1997]. The home-model microwave oven is designed to cook food via microwave interactions with water, the highest volume component in most processed food products. Although the dielectric loss of water is highest

around 18GHz, at 2.45GHz, the penetration depth of the microwave energy into water (and most natural and processed foods) allows for more uniform heating of the bulk product [Thuery, 1992].

The microwave generator in the variable frequency microwave oven used for this research was a *traveling wave tube* (TWT). In a TWT (Figure 2.6), the electron beam interacts with the traveling wave [Thuery, 1992]. The dimensions of the non-resonant structure force this interaction, resulting in bundles of electrons that are periodic over a wide bandwidth. In this way, a fluctuating wave is induced in the microwave cavity. This microwave generator produces significantly more modes than those that are detected in a field generated by a single frequency magnetron. The higher concentration of modes produces a more uniform microwave field throughout the cavity.

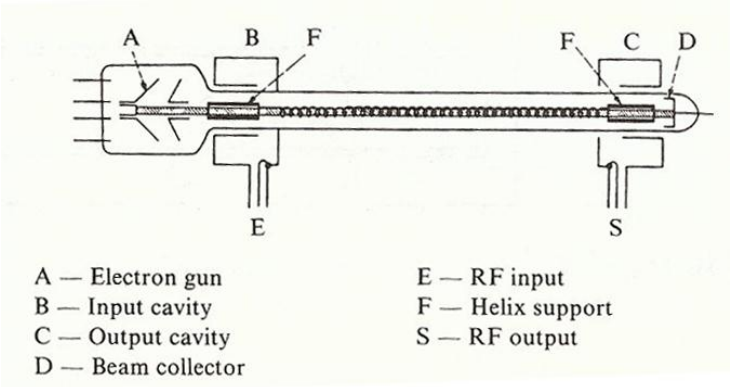

Figure 2.6: Schematic of a traveling wave tube (TWT) [Thuery, 1992; Used under fair use guidelines, 2011].

Some of the characteristics of the variable frequency microwave oven include [Lambda Technologies, 2011]:

- A uniform energy distribution in the cavity generated by sweeping across a central frequency and a defined bandwidth.
- The ability to reduce arcing with low-load or conductive loads in the cavity by designing rapid sweep cycles into the processing parameters.
- Selective heating of various components of the load by adjusting the frequency, bandwidth, sweep rate, or combination of the available controllable process parameters. This feature can lead to rapid cure with little or no change in the product properties or characteristics.

The Lambda Technologies VFM products are used internationally in polymer curing operations, especially in the semiconductor and electronic packaging industries. In studies performed by the company, the calculated and measured energy distributions were determined for

a multimode cavity housing 2.45GHz fixed frequency microwaves and a multimode cavity in which 4GHz to 8GHz was swept (Figure 2.7 (a) and (b), respectively) [Lambda Technologies, 2011]. Note that the VFM energy generated by the TWT produced a more uniform field, as compared to that of the fixed frequency oven. The fixed frequency set-up, on the other hand, shows significant variation in field intensity throughout the cavity.

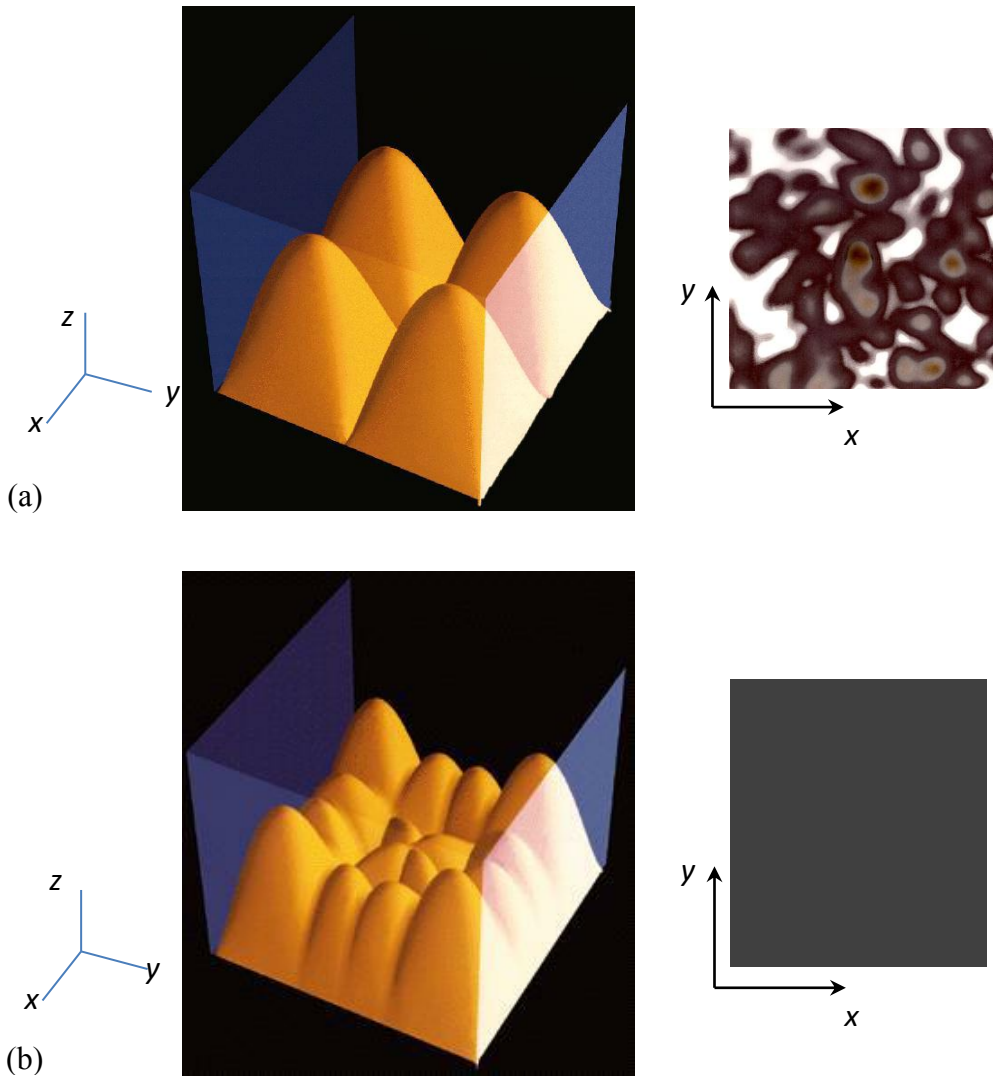

Figure 2.7: Fixed and variable frequency energy distributions generated in multimode cavities: (a) 2.45GHz; (b) 4 to 6GHz. Three-dimensional pictures were generated from calculated data, while the two-dimensional figures on the right represent the measured energy distributions [Lambda Technologies, 2011; Used under fair use guidelines, 2011]. (The x and y axes are in cm; the z axis is a model of relative power output, dBm). Note: There is no detectable variation in the measured power distribution throughout the cavity in (b).

2.3 Characterization Methods

The primary characterization and testing techniques used to evaluate curing in polymer materials are *thermogravimetric analysis-differential scanning calorimetry* (TGA-DSC), *Fourier transform infrared spectroscopy* (FTIR), and *dynamic mechanical analysis* (DMA) [Rabek, 1980; Bundle et al, 2002]. The first two methods are used for fundamental analyses of the materials properties associated with the polymers as they cure. The last is a mechanical property testing device that can relate the extent of crosslinking to the stiffness of the sample material. This method was not used, as the model available could not be used to evaluate the specific system in the liquid state. Both of the methods used in this study, DSC-TGA and FTIR, are discussed in more detail below.

2.3.1 Thermogravimetric Analysis (TGA) - Differential Scanning Calorimetry (DSC)

The main purpose for conducting thermal analyses is to relate temperature with the physical properties of materials. In fact, polymers provide the widest application for thermal analysis techniques [Menczel, 2009]. It is used to develop new process techniques, in predicting the service life of the polymer under various conditions, and it can be used to determine the stresses that a material has undergone, thermally and/or mechanically.

Thermogravimetric analysis is a tool that measures weight loss in a sample as a function of temperature, either dynamically or *isothermally*. It is used most often in polymer degradation studies; evaluation of the kinetics associated with the polymer breakdown when exposed to various thermal environments [Alger, 1997].

Differential scanning calorimetry is one of the most heavily used characterization tools for polymer materials [Menczel, 2009]. The DSC is used to measure the energy associated with *exothermic* and *endothermic* changes in materials. These changes can be related directly to changes in enthalpy. Through detection and measurement of these transitions, studies can be conducted on melting, crystallization, and morphology [Alger, 1997; Randall et al, 2002; Fried, 1995]. It also is possible to measure the rates of chemical reactions, such as polymerization, crosslinking, and degradation. Using this method, the energy to maintain the same temperature in the sample and a reference is measured and stored as a function of temperature and time.

Figure 2.8 (a) provides an illustration of the cross-section of a Netzsch TGA-DSC instrument. Basically, the system houses a microbalance that is capable of measuring changes that occur in a sample as a function of temperature. The specifics of the instrument and its set-up for use in this study will be discussed in more detail in Chapter 3: Experimental Procedures.

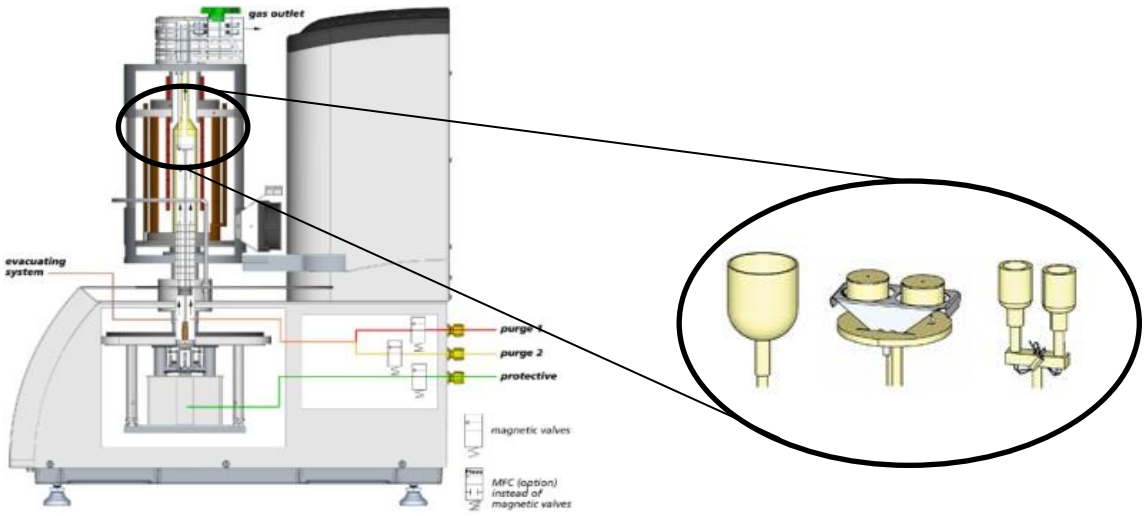

(a) (b)

Figure 2.8: Netzsch STA 449 Jupiter F3 Simultaneous TGA-DSC: (a) instrument cross-section schematic; (b) three possible crucible assembly configurations [Netzsch Corporation, 2011; Used under fair use guidelines, 2011].

While this method provides a great deal of information as to the changes taking place in polymers under certain conditions, it provides only one method of heating – conventional radiant heating. Calorimeters using microwave energy as a process catalyst do not yet exist commercially.

2.3.2 Fourier Transform Infrared Spectroscopy (FTIR)

Infrared spectroscopy offers a non-destructive method for determining the chemical bonding in a material, particularly in solids and films/coatings [Brundle et al, 1992]. New developments in FTIR spectrophotometers over the past 10 to 20 years have made this method simple to use for quick, quantitative or qualitative measurements of chemical composition for a wide range of materials. Fourier transform infrared spectroscopy serves as the primary tool for evaluating cure rate in this study.

Theory

Infrared spectroscopy involves studying the interaction of IR radiation with target materials [Smith, 1996]. Originally, IR measurements were made with dispersive spectroscopy methods in which equipment was used to generate spatially dispersed broadband frequencies into spectral components [Brundle et al, 1992; Thermo Nicolet Corporation, 2001]. These dispersive

spectrometers still are used to provide low-cost, qualitative data as to chemical composition of materials.

When evaluating the interaction of any form of light wave with a material, the relationships between the absorbed, transmitted, and reflected light are defined in the Kirchhoff relationship, shown in Equation (2.7) [Storm et al, 1998], which came about in 1860 when Kirchhoff introduced the concept of blackbody radiation [Kirchhoff, 1860].

$$\mathbf{a} + T + R = 1 \quad \text{(unitless)} \tag{2.7}$$

Where, $\mathbf{a}$ ≡ fraction absorbed,

T ≡ fraction transmitted (transmittance), and

R ≡ fraction reflected (reflectance).

For a specific wavelength,

$$I_\lambda^T = I_\lambda^O \frac{(1-R)^2 e^{-2\propto x}}{(1+R)^2 e^{-\propto x}} \quad (\text{W/m}^2) \tag{2.8}$$

where, I_λ^T ≡ intensity of the transmitted beam at wavelength, λ,

I_λ^O ≡ intensity of the incident beam at wavelength, λ, and

$\propto$ ≡ absorption coefficient (cm^{-1}).

.

When the spectral reflectance is negligible, the equation for I_λ^T becomes

$$I_\lambda^T = I_\lambda^O \text{e}^{-\alpha x} \quad (\text{W/m}^2) \tag{2.9}$$

In infrared spectroscopy, it is common practice to measure the beam transmitted through the sample and/or the beam reflected by the sample (as shown in Figure 2.9). If the reflectance is negligible or is known, the transmitted beam can be ratioed to the incident beam to provide either the transmittance or percent transmittance, shown in Equations (2.10) and (2.11) [Smith, 1996].

$$T_\lambda = \left(\frac{I_\lambda^T}{I_\lambda^O}\right) = \text{e}^{-\alpha x} \quad \text{(unitless)} \tag{2.10}$$

and

$$\% T_\lambda = \left(\frac{I_\lambda^T}{I_\lambda^O}\right) 100 \tag{2.11}$$

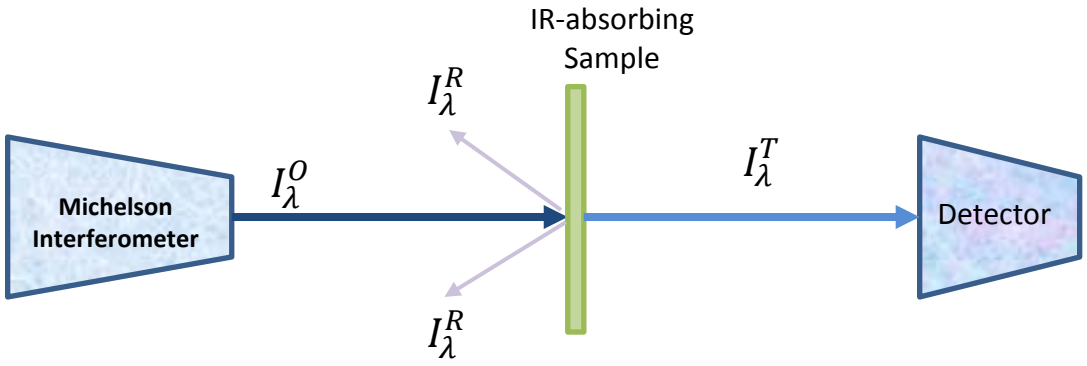

Figure 2.9: Schematic illustrating the FTIR transmission configuration for generating the infrared spectrum for a sample material.

In reflectance techniques, the IR beam is reflected off the sample rather than passing through it, as in transmission techniques [Smith, 1996]. The reflectance is calculated according to Equation (2.12) [Urban, 1996]. *Specular reflectance* occurs when the beam is reflected off of a smooth surface. Diffuse reflectance describes the conditions where the angle of incidence of the beam is fixed, but the reflected beam can vary between 0 and 360º, as with rough surfaces. These methods are illustrated in Figure 2.10. Percent reflectance is represented in Equation (2.12).

$$\% R_\lambda = \left(\frac{I_\lambda^R}{I_\lambda^O}\right) 100 \tag{2.12}$$

Where, R_λ ≡ reflectance at wavelength λ,

I_λ^R ≡ intensity of the reflected beam at wavelength λ, and

I_λ^O ≡ intensity of the incident beam at wavelength λ.

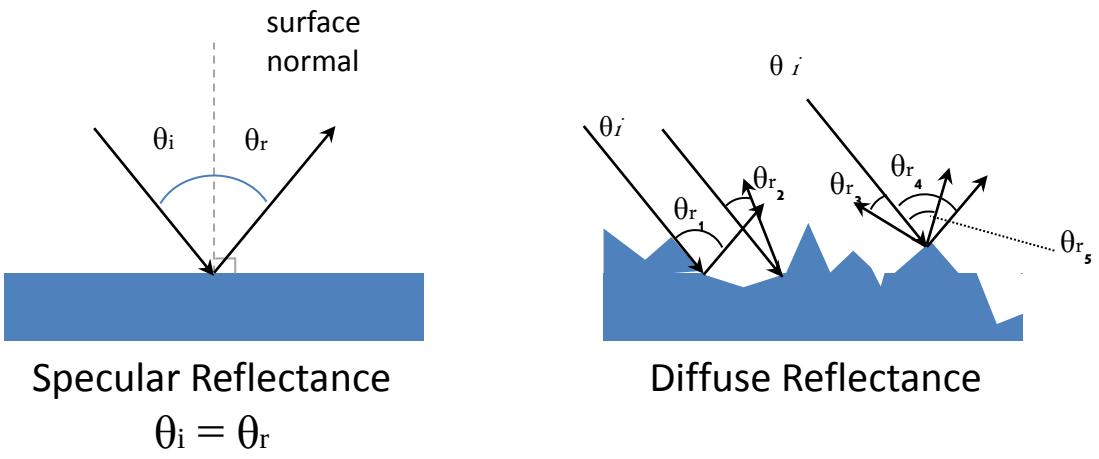

Figure 2.10: Schematic illustration of specular and diffuse reflectance in infrared spectroscopy [Adapted from Smith, 1996; Used under fair use guidelines, 2011].

Reflectance methods provide a tool to obtain spectra for a host of materials that cannot easily be placed into the IR beam (i.e., powders, sintered materials). Some of the advantages associated with FTIR reflectance techniques include the ease of use, simplified sample preparation (thickness, surface roughness, and concentration can vary widely), and nondestructive nature of the methods. However, there are a number of disadvantages associated with reflectance techniques that must be considered [Smith, 1996]:

- Reflectance can be significantly more expensive than transmittance or absorbance methods due to the cost of the accessories.
- The depth of penetration of the IR beam into the sample is based on the material properties of the samples, the surface roughness, and the angle of incidence of the impinging IR beam. These parameters usually are not known, thus the path length of the beam usually is not known. Due to these uncertainties, the absorbance is difficult to quantify when obtained using reflectance techniques.
- The bulk of the sample material is the dominant contributor to the spectrum when FTIR measurements are made in transmission modes; whereas, the surface is dominant in reflectance. This difference is due to the low typical penetration depth (in the range of 1 to10μm) of the incident IR beam in the reflectance mode.
- Reflectance spectra can differ significantly from those obtained in transmittance or absorbance modes, again due to the difference in depth of data collection in the samples.

If quantitative analysis of the sample is required, the absorbance must be known. The absorbance is equal to the exponent in Equation (2.10) and can be written as

$$A_\lambda = \alpha x = -\ln T_\lambda \quad \text{(unitless)} \tag{2.13}$$

Since T_λ in Equation (2.13) is measured by the machine, the absorbance is a calculated value. Beer's law (also known as the Beer-Lambert law and the Lambert-Beer law) allows the absorbance to be used in quantitative analyses [Smith, 1996; Brundle et al, 2002], as shown in Equation (2.14).

$$A_\lambda = \varepsilon \ell c \quad \text{(unitless)} \tag{2.14}$$

Where, $A_\lambda \equiv$ absorbance of infrared radiation by the bonds present in the material,
$\varepsilon \equiv$ absorptivity of the material ($L \cdot mol^{-1} \cdot cm^{-1}$),
$\ell \equiv$ the pathlength (cm), and
$c \equiv$ the concentration of the represented bonds ($mol \cdot L^{-1}$).

It should be noted that the absorptivity is different for different molecules and that it changes with wavenumber (x-axes on the spectrum). However, for a given molecule and wavenumber, it is a fundamental property of the molecule, and thus is distinct and unchanging. Molar absorptivity is a constant for a particular material and is directly proportional to the concentration. Absorbance is a unitless value represented as intensity along the y-axes on the spectra. It can be measured in terms of peak height, peak ratio, or peak area ratio when a quantitative analysis is required.

There are a number of techniques that can be used in FTIR to obtain the spectrum of a material, the most common being the transmittance method. In all FTIR measurements, the Michelson interferometer employs a beam splitter to halve the beam from the source. Measurements are accomplished using a series of mirrors aligned so that the detector can "see" all of the transmitted and reflected beams.

The FTIR spectroscopy method used to study the PUR coating materials in this work was that of Horizontal Attenuated Total Reflectance (HATR). It is a very specialized configuration of an FTIR method known as *Attenuated Total Reflectance* (ATR) that differs from standard transmission or reflectance in that it measures the magnitude of the transmitted beam after a small

portion of the incident beam is absorbed in the sample surface [Smith, 1996]. A typical ATR set-up is shown in Figure 2.11.

Central to the ATR methods is the use of a crystal with a known index of refraction through which a standing wave of radiation, referred to as an *evanescent wave*, is established [Smith, 1996]. This evanescent wave is unique; it is slightly larger than the crystal, and so it passes just beyond the surface of the crystal into the space beyond. When a sample is in contact with the crystal surface, the evanescent wave penetrates a short distance into the sample. If the sample is absorbing in the IR range, it will interact with the beam to produce a spectrum.

The depth of penetration of the absorbed portion of the beam is inversely proportional to the wavenumber, and the indices of refraction of the crystal and the sample, and is related to the angle of incidence of the IR radiation, as shown in Equation (2.15). It usually varies from about 0.1 to 5μm, depending on the absorption of the sample in the IR range [Smith, 1996].

$$D_p = \frac{1}{2\pi W n_c (sin^2\theta - n_s^2)^{\frac{1}{2}}} \qquad (\mu m) \qquad (2.15)$$

Where, $D_p \equiv$ depth of penetration (cm),

$W \equiv$ wavenumber (cm^{-1}),

$n_c \equiv$ index of refraction of the crystal,

$n_s \equiv$ index of refraction of the sample, and

$\theta \equiv$ the angle of incidence of the IR radiation on the crystal.

The ATR technique usually is performed with the crystal sandwiched between two pieces of the sample material [adapted from Mirabella, 1993; Smith, 1996]. The sample –crystal assembly then is mounted in the instrument so the incident IR beam is directed onto the end of the crystal (at an angle of 90º with respect to the facet) and propagates down its length, interacting with the sample all along the points of contact between the sample and the crystal.

The name attenuated total "reflectance"' can be misleading in that these techniques work with a beam "transmitted" through the crystal. This configuration allows Equations (2.10) and (2.13) to be used to calculate the absorbance. Quantitative data was not sought in this study, so Beer's law was not applied; however, absorbance was the default format for the data when the HATR method was selected.

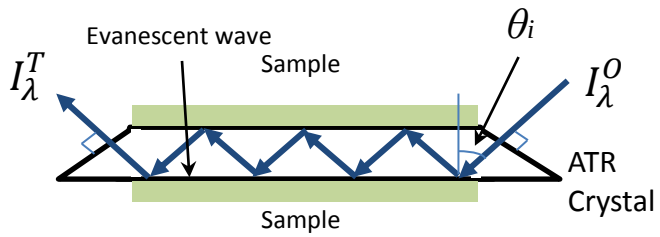

Figure 2.11: Typical ATR stage with sample mounted on each side of the crystal [adapted from Mirabella, 1993; Smith, 1996; Used under fair use guidelines, 2011].

For the ATR or HATR crystal to serve as a waveguide for the beam, it must be an IR-transparent crystal and the criterion for the critical angle of incidence (θ_c) of the beam on the crystal surface must be satisfied. The value of θ_c for zinc selenide (ZnSe) is about 38º, and the actual angle of incidence for the internally reflected beam on this crystal design is 45º.

A schematic cross-section of the HATR set-up in the Thermo Electron FTIR system used for this work is provided in Figure 2.12. Note the differences between the typical ATR and the HATR set-ups. In HATR, the sample is situated on only one side of the crystal, allowing for even simpler sample preparation. In the ATR set-up shown in Figure 2.11, the sample must be secured in some way to the crystal. This step is not required in HATR where the sample can simply be placed on top of the crystal surface and pressure can be applied to ensure good sample-crystal contact [Thermo Nicolet Corporation, 2001].

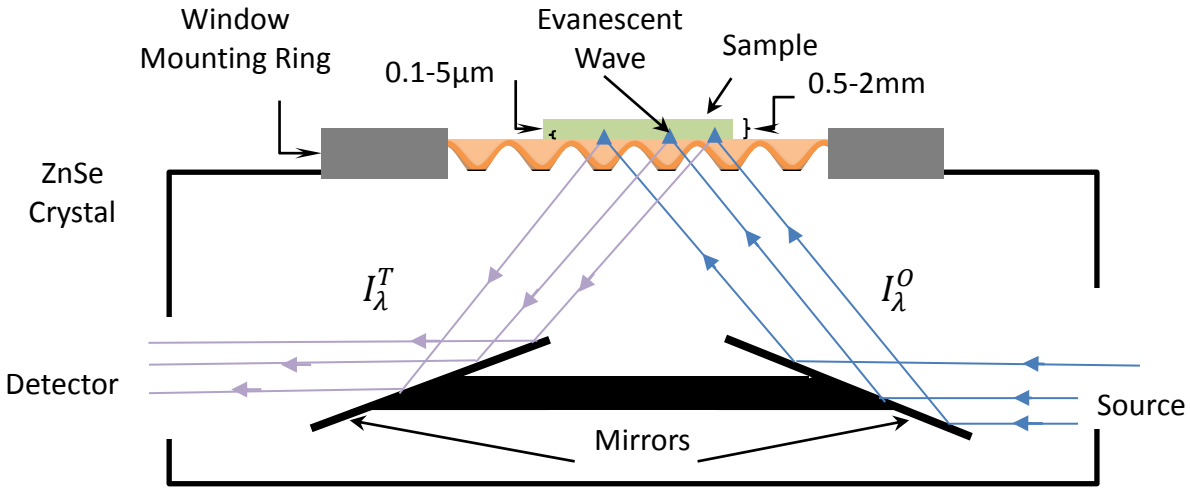

Figure 2.12: Schematic of the sample set-up for HATR-FTIR measurements in the Avatar 330 Smart SpeculATR Stage. Note that this schematic is presented in cross-section and is not drawn to scale [schematic by author, based on Simonis, 2011 and Thermo Nicolet, 2001; Used under fair use guidelines, 2011].

One of the major drawbacks associated with any ATR method, no matter the configuration, is the requirement for extremely good sample contact with the crystal surface. A strong signal to noise ratio (strong reflected beam signal with low noise) is required when measurements are made using evanescent waves due to the very short depth of penetration of the wave into the sample surface. This requirement is easy to understand from Figure 2.13. Gaps between the sample and the crystal would interfere with the generation of the evanescent wave, as indicated by the absence of the wave at one position in the schematic. If a significant number of gaps exist, then the reflected signal to the detector will be too weak to obtain a clear spectrum for the sample material [Smith, 1996; Mirabella, 1998].

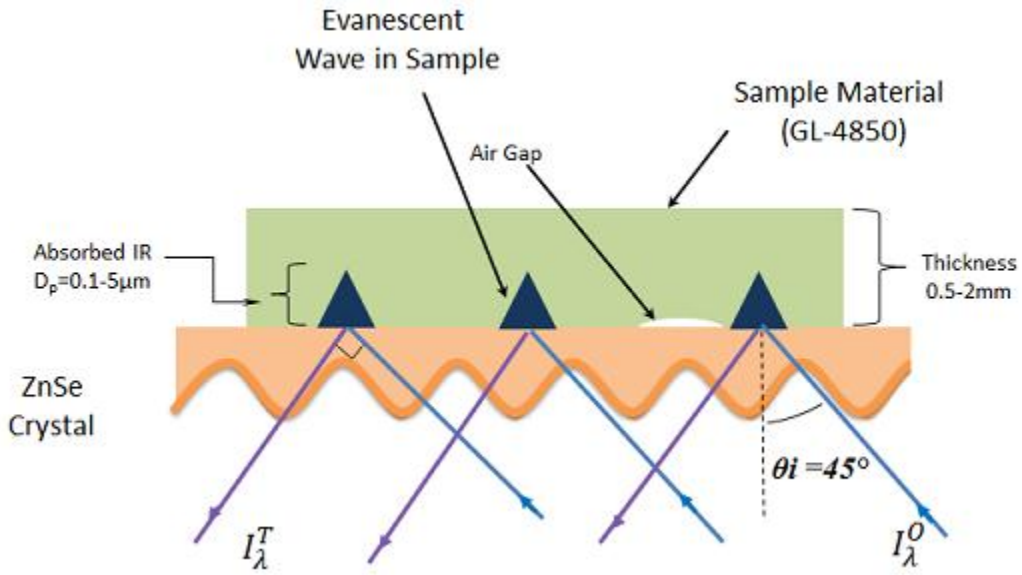

Figure 2.13: Close-up of the sample-HATR crystal interface. Note: This schematic is presented in cross-section and is not drawn to scale [schematic by author, based on Simonis, 2011 and Thermo Nicolet, 2001; Used under fair use guidelines, 2011].

Using HATR, the IR beam is focused on the bottom surface of the crystal sample stage (in this case, a ZnSe crystal). This crystal has a unique geometry on the underside, where the incident IR beam impinges on the "corrugated" bottom surface. The angle of the corrugation with respect to the incident beam produces an angle of incidence (θ_i) of 45° off normal.

The ATR crystal is designed is to act as a *waveguide*, channeling the IR beam down the length of the crystal and then out to the detector [Brundle et al, 1992]. At each point where the sample is in close contact with the beam traveling through the crystal, some of the energy is absorbed into the material (the evanescent wave), while the remainder continues to travel the

length of the crystal. The transmitted beam then exits the crystal faces on the sides facing the detector. However, as seen in Figure 2.13, the HATR crystal used in this study is a single-pass (or single-bounce) configuration in which the incident beam enters the crystal, interacts with the sample, and then exits the crystal after only one point of interaction.

Instrumentation

The advent of low-cost, high-speed computers that became available in the 1970s enabled the development of more robust spectroscopy equipment. This newer equipment incorporated the *Michelson interferometer*, a component capable of measuring the wavelengths of transmitted IR radiation. An interference pattern is generated which is measured by the detector and converted to the IR spectrum through a series of Fourier transform operations [Urban, 1996]. In this application, the Fourier transform is a mathematical algorithm that converts the intensity of the signal with time into an IR spectrum, represented as amplitude versus frequency [Alger, 1997].

A simple FTIR spectrometer layout is provided in Figure 2.14 [Thermo Nicolet Corporation, 2001]. As seen in the detailed schematic of a Michelson interferometer design (Figure 2.15), a beamsplitter is used to divide the IR beam into two paths – one which reflects off a fixed mirror, and another reflecting off a movable (translating) mirror. The differences in measured pathlengths when the beams rejoin generate interference, resulting in an *interferogram*.

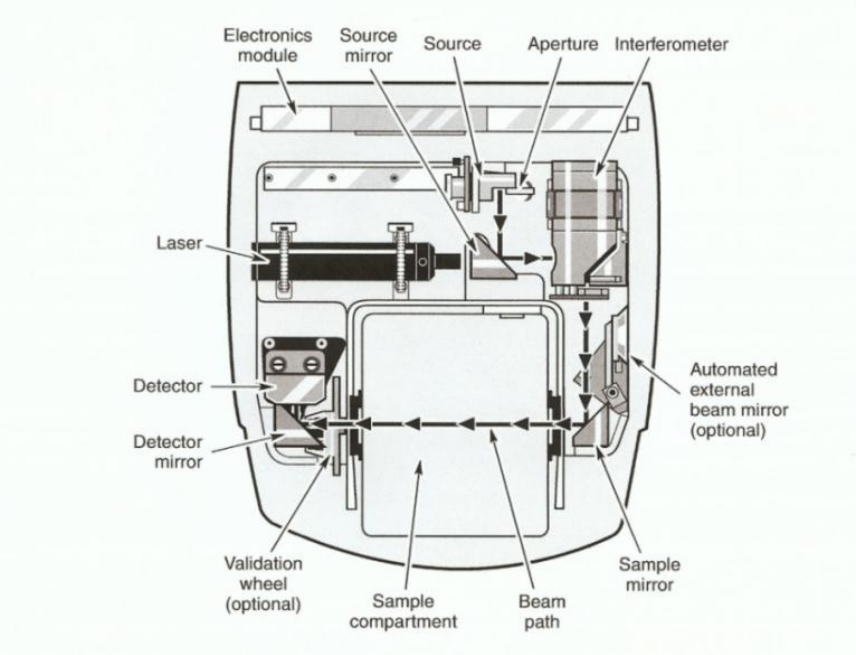

Figure 2.14: A design schematic for the Thermo Nicolet Avatar 330 FTIR [Thermo Nicolet Corporation, 2001; Used under fair use guidelines, 2011].

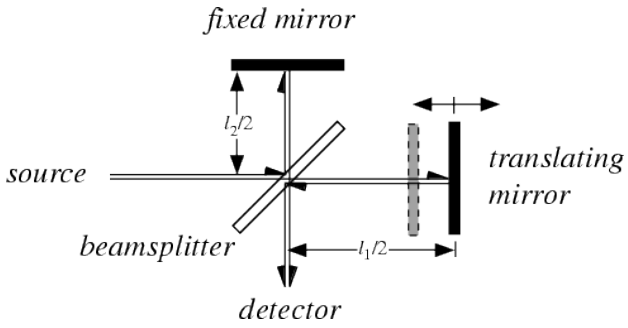

Figure 2.15: Schematic of a typical Michelson interferometer illustrating the basic components [University of Twente, 2011; Used under fair use guidelines, 2011].

The advantages of using the new generation of FTIR spectrophotometers over dispersive spectroscopy instruments include [Alger, 2005; Brundle et al, 1992; Fried, 1995; Thermo Nicolet Corporation, 2001]:

- Non-destructive nature of the measurements
- Internal instrument calibration allowing for more precise measurements
- High-speed scanning capabilities with up to a scan per second
- Increased signal-to-noise ratio leading to increased instrument sensitivity
- Mechanical simplicity leading to ease of use

Fundamental to the operation of the FTIR is the *interferogram* – a plot of the infrared light intensity versus the optical path difference [Smith, 1996]. The interferogram is generated by the instrument as the moving mirror is translated through its range of motion (a scan), and is then Fourier transformed into a spectrum. A typical interferogram is shown in Figure 2.16. The single beam spectrum is a plot of the response of the detector, considering only the contributions of the instrument itself and the environment at the time of measurement. This spectrum is also considered as the background spectrum and generally is taken regularly throughout the measurement period (once per 4 to 6 hours is common) so the sample spectra is a measure of the contribution of the sample only.

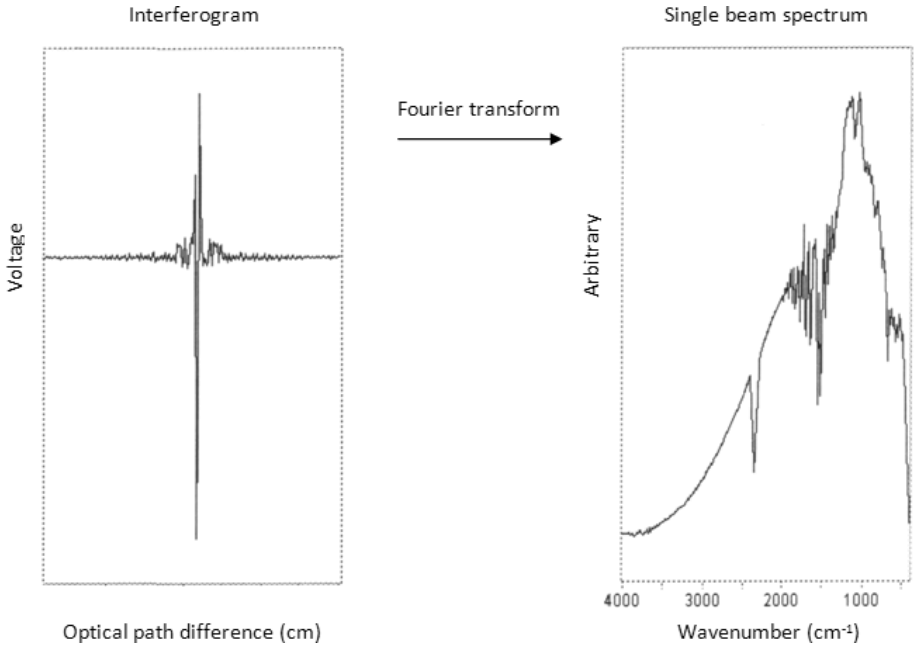

Figure 2.16: Typical interferogram produced in an FTIR spectrometer [Smith, 1996; Used under fair use guidelines, 2011].

The IR spectrum that is generated using FTIR spectrometers represents a sort of fingerprint of a material, with absorption or transmission peaks corresponding to the vibrational frequencies of the atomic bonds comprising the material. Using these characteristic spectra allows for qualitative identification of the sample material, as no two materials will generate the exact same spectra [Fried, 1995; Brundle et al, 1992].

Figure 2.17 shows the absorbance spectrum and the percent transmittance spectrum for deionized water. Note that these spectra appear to be mirror images of each other. Remember that the HATR-FTIR method is one that makes use of a transmitted IR beam and that the reflectance of the crystal is considered to be negligible. By using measurements of the incident and transmitted beams, the instrument calculates the percent transmittance value and back-calculates the absorbance using equation (2.13) [Thermo Electron, July 2011]. In the spectrum for percent transmittance, the values for the peaks are 41% at approximately 3300cm^{-1} and 65% at approximately 1650cm^{-1}. Applying Equations (2.10) and (2.13), corresponding values for absorbance are 0.38 and 0.19, respectively.

(a)

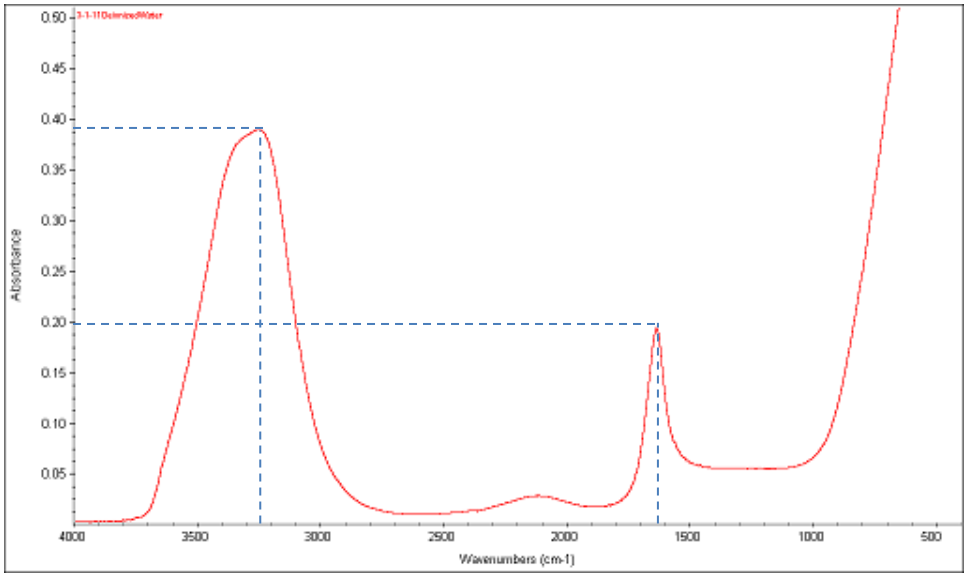

(b)

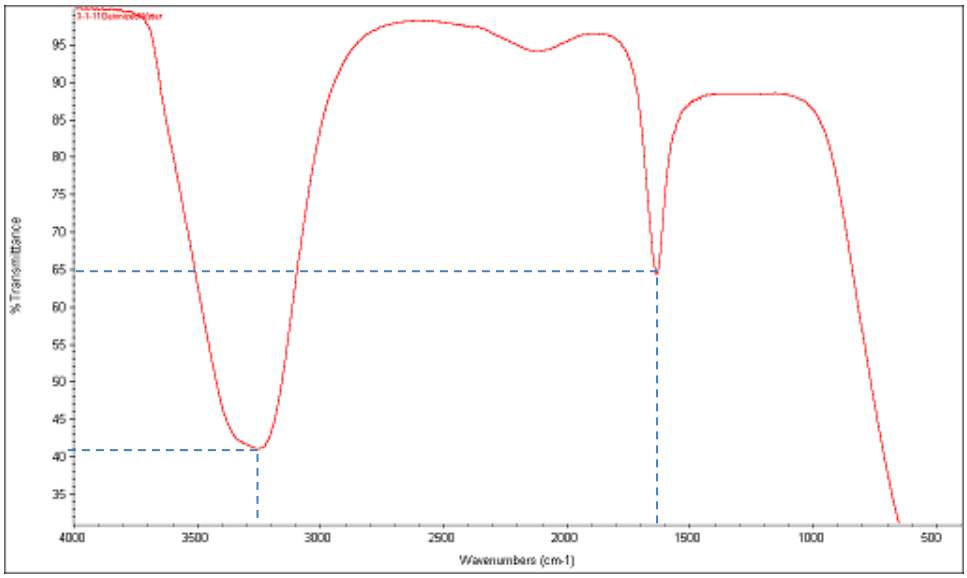

Figure 2.17: FTIR spectra for deionized water in varying modes for intensity vs. wavenumber (cm^{-1}): (a) absorbance; (b) % transmittance. Note: %T is measured by the interactions as described in Equation (2.12); the machine calculates the absorbance using Equation (2.10).

The use of FTIR spectroscopy methods allow for the tracking of changes to specific bonds in the material as a function of time, thus providing a means of studying the cure kinetics of a target material. These techniques measure the transmission of IR radiation through the material. [Alger, 2005; Brundle et al, 1992; Fried, 1995]. While it is possible to measure transmission across a broad range of the EM spectrum, measurements typically lie between 4000 and 400 cm^{-1}, referred to as the mid-IR range.

There are many different configurations used in IR spectroscopy. Measurements can be taken with the sample inserted directly in the IR beam so that the quantity of transmitted IR energy can be measured directly, or it can be taken indirectly through the use of internal reflection techniques. Further details relating the theory of microwave-material interactions and the characterization methods used to evaluate the cure rate of the water-based, aliphatic urethane used in this investigation are presented as needed in Chapter 3: Experimental Procedures.

CHAPTER 3: EXPERIMENTAL PROCEDURE

Figure 3.1 illustrates the experimental approach used to determine whether microwave energy and/or frequency affected the cure rate in the water-based, aliphatic urethane material (GL-4850) under study. The time steps refer to the amount of time samples were exposed to the cure method (i.e. air, thermal, microwave), divided into regular intervals. The number of time steps used for each method was based on complete cure. Note that, for a sample to be considered as completely cured, its FTIR spectra experienced only small intensity changes in a comparison of consecutive time steps in the major peaks being evaluated.

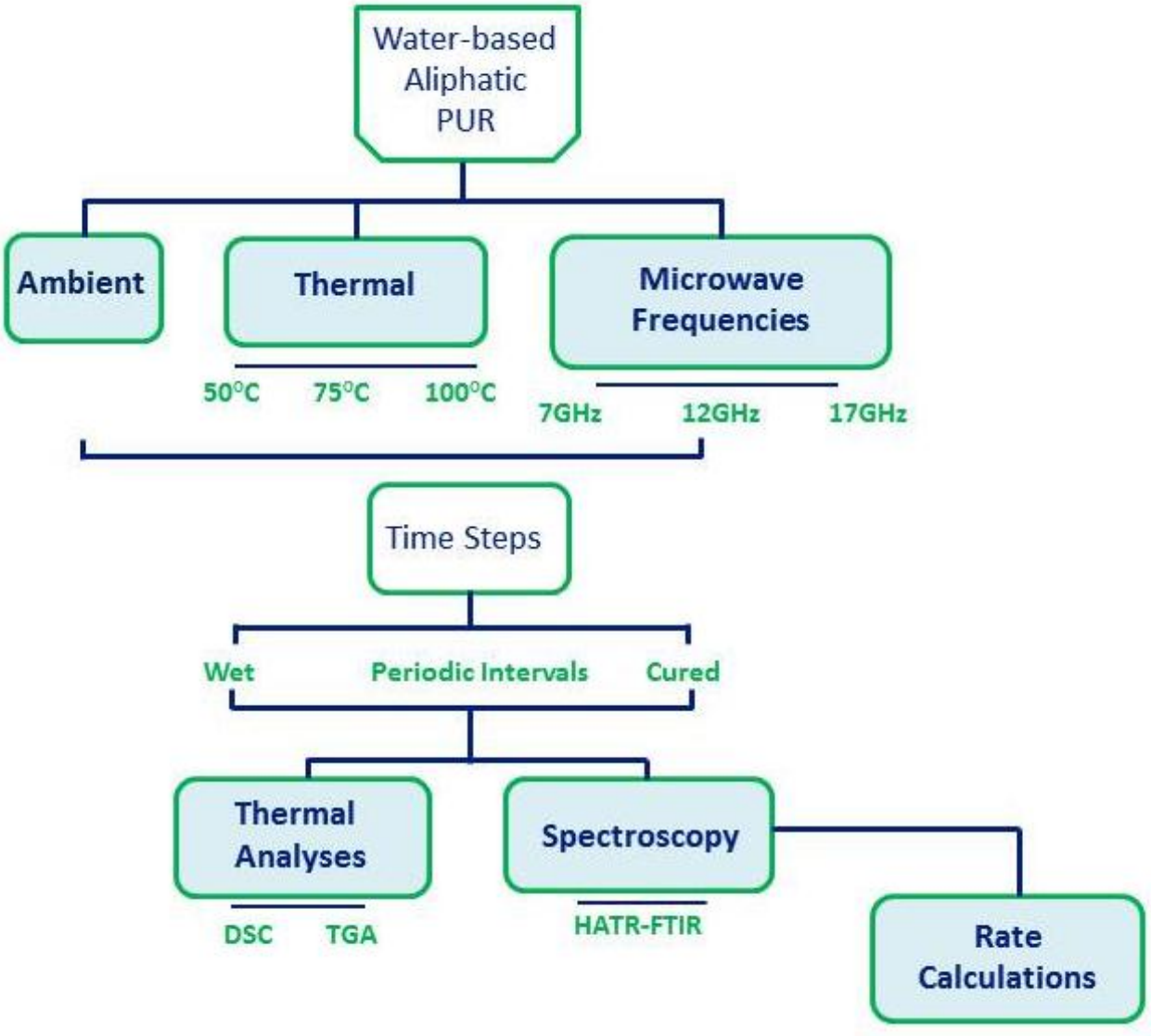

Figure 3.1: Experimental procedure for studying the effects of microwave energy and microwave frequency on the cure rate in GL-4850 water-based, aliphatic polyurethane.

3.1 Sample Preparation

Samples were prepared by measuring out 2ml of as-received GL-4850 water-based, aliphatic PUR and depositing it into a 60mm x 15mm (2.36in x 0.59in) diameter *Pyrex*® dish using a graded 3ml disposable syringe. Care was taken to avoid air in the syringe so there would be no bubbles formed in the samples. The dish was then rotated slowly to assure complete coating of the bottom surface of the dish.

3.2 Curing Regime

Prior to all sample runs, the temperature and relative humidity in the laboratory was noted. There was little variation from one day to the next. However, over the course of the experimental work, temperatures ranged from 20 to 24ºC and relative humidity ranged from 19 to 47%.

3.2.1 Process Parameters

All samples were taken from the same one-gallon container of GL-4850 water-based, aliphatic PUR manufactured by Van Technologies, Inc.[5] The PUR was ordered specifically for this study and the container was not opened until the experimental procedure was initiated.

A new syringe was used to measure each new sample set to ensure that no solids remaining in the syringe cavity would be transferred into the new sample set. Upon insertion into the PUR container, the syringe was purged three to five times to avoid the formation of air bubbles when the load was transferred to the Pyrex® dishes.

Air Curing

For many urethane-based products used as coating materials, especially in low-volume wood-coating operations, a period of exposure to the ambient environment is a typical method for achieving cure. The products become stable after a period of hours and then continue to crosslink over a period of days to weeks [Allen, 2006; Meir-Westhues, 2007; Guzzetta & Baldwin, 2007]. To establish the cure time required for this method, a sample was measured into a ZnSe sample HATR-FTIR cell[6] (stage) and left in situ while spectra were collected at regular intervals over a period of approximately four days (t_{max}= 5860 minutes). (These intervals are reflected in the plots provided in Chapter 4: Results and Discussion.)

[5] GL-4850 Water-based, aliphatic Urethane, Van Technologies, Inc., Duluth, MC.
[6] SpeculATR ZnSe liquid sample cell, Part No. 0035-603, Thermo Electron North America LLC, Madison, WI

Curing by Conventional Heating

For samples heated in the conventional oven[7], temperature was controlled using a Eurotherm controller connected to a type K thermocouple in close proximity with the sample. Additionally, temperature of the oven cavity was monitored using a thermometer inserted into an opening at the top of the oven (Figure 3.2). Immediately after 2ml liquid samples were measured, a series of 10 to 12 sample dishes was placed in the oven, which was already at the desired set point. Three soak temperatures (50, 75, and 100 ºC), were used for the conventional radiant heating experiments. At regular time steps, a sample was removed from the oven for analyses.

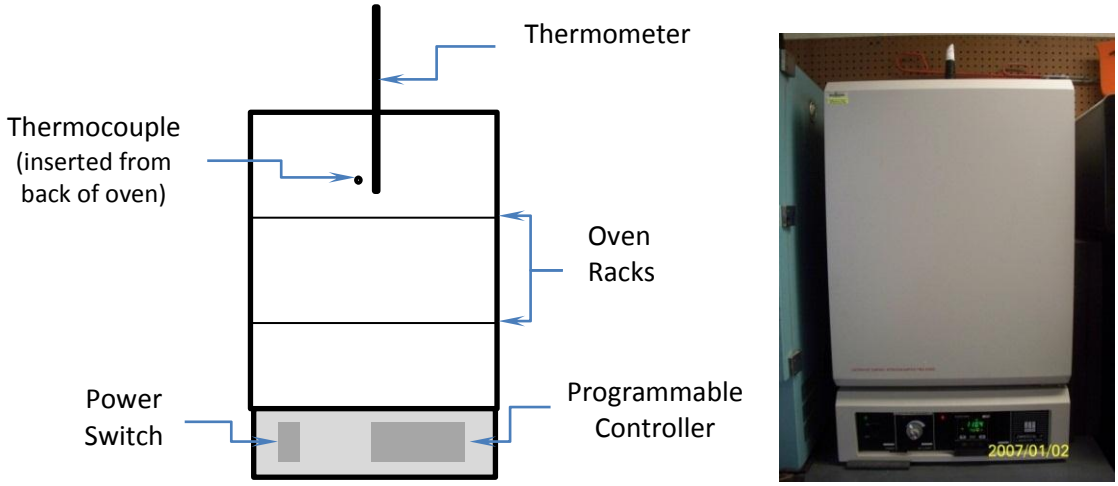

(a) (b)

Figure 3.2: Configuration of the drying oven used for conventional curing (convection via radiant heating): (a) schematic; (b) photograph.

Variable Frequency Microwave Curing

A Variwave® model 1500 Variable Frequency Microwave (VFM)[8] oven with a maximum forward power of 250W was used for microwave curing experiments. The parameters programmed for each sample run were the central frequency, the bandwidth over which the microwaves would sweep, and the sweep rate (how fast the bandwidth was covered). Three central frequencies in the microwave range (7, 12, and 17GHz) were selected that extended across the working range of the VFM (6 to 18GHz). These particular frequencies represented equal intervals across the possible bandwidth of the microwave oven, with the top frequency (17GHz) lying close to the optimal absorption frequency of water, the major component in the wet PUR

[7] LabLine Imperial V Programmable Laboratory Oven, Barnstead International, Dubuque, IA.
[8] Variwave 1500, Lambda Technologies, Inc., Morrisville, NC.

used for this study. A bandwidth of 1GHz was swept each second, making the ranges for the frequency distribution in the cavity of 6.5 to 7.5GHz, 11.5 to 12.5GHz, and 16.5 to 17.5GHz. The maximum temperature (that temperature at which, if reached, the system would shut down) was set at 100°C, with a maximum run time of 60 minutes. The Forward Power (power transmitted into the microwave cavity; FP) and Reverse Power (power not absorbed by the sample; RP) were not controlled; however, FP and RP, as well as the maximum temperature achieved for each experiment were recorded. The temperature of the microwave-cured samples was measured using an optical fiber sensor[9]. While temperature was of interest so as not to overheat and "burn" the samples, time was the dominant (thus controlled) process parameter.

Initially, 10 to 12 samples were inserted into the microwave cavity for simultaneous exposure to the microwave field. However, with so much absorbing load in the cavity, the relatively low power of the Variwave® was diluted even further and heating proved difficult. To overcome this issue, three samples at a time were placed into the VFM cavity, as shown in Figure 3.3. (Three samples did not represent too large a load for the low-power microwave used in this study. This number of samples was determined experimentally.) For the microwave studies, sample number 2 was used for analyses, as it was the one in which the optical fiber was positioned. Again, the samples for HATR-FTIR analysis were removed from the center of the sample dishes.

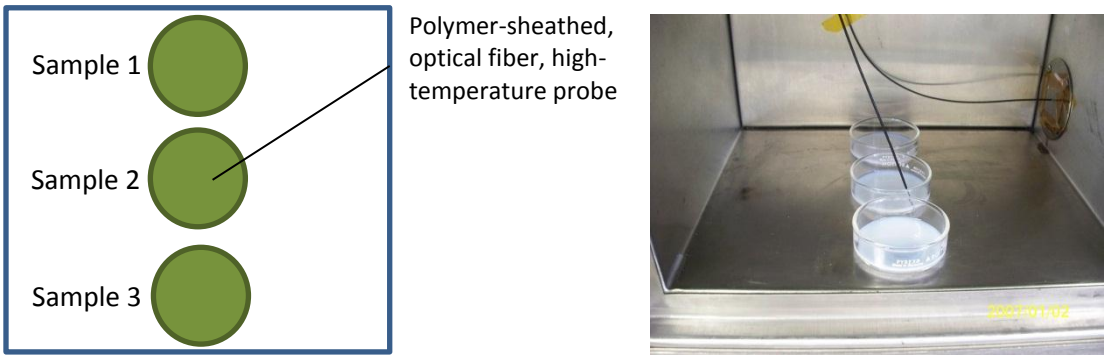

(a) (b)

Figure 3.3: Configuration of GL-4850 samples in Pyrex dishes as placed in the Variwave® variable frequency microwave oven: (a) schematic – top view; (b) photograph of samples in the VFM cavity.

[9] Luxtron optical fiber temperature probe and readout, LumaSense Technologies, Inc., Santa Clara, CA.

3.3 Fourier Transform Infrared Spectroscopy (FTIR) using a Horizontal Attenuated Total Reflectance (HATR) Technique

Due to a slight curvature of bottom of the dishes, thicknesses of the samples varied across the sample diameters. To ensure the uniformity of sample thicknesses for FTIR measurements, samples (approximately 0.5in diameter) were removed from the center of the dish, as shown schematically in Figure 3.4. They were cut from the treated PUR using a circular drill attachment to keep them as consistent as possible.

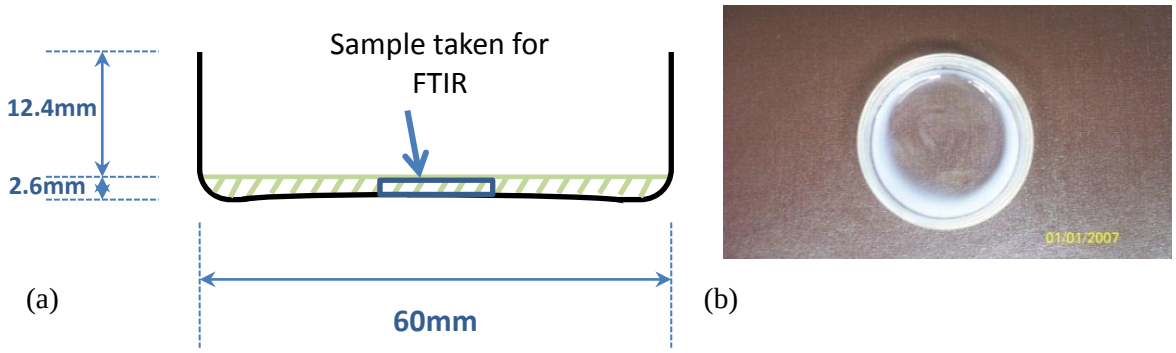

Figure 3.4: GL-4850 water-based, aliphatic PUR samples deposited in a Pyrex® petri dish: (a) cross-sectional schematic; (b) photograph - top view.

The FTIR spectrometer (Figure 3.5)[10] used for this work was equipped with a self-aligning "SMART" stage that proved very simple to operate, as opposed to IR spectrometers requiring manual mirror alignment. As indicated in Chapter 2, an internal reflection method referred to as *Horizontal Attenuated Total Reflectance* (HATR) was used to generate the spectra for all the PUR samples. This method was selected over transmission and reflection methods due primarily to the range of sample states (liquid through solid) and the need for a method requiring minimal sample preparation. Complex sample preparation would have proved difficult in a time-dependent study, where short time steps were desired.

In Figure 3.5, the ZnSe crystal stage is shown as it sits in the instrument. Figure 3.6 provides a close-up view of the top and bottom of the crystal stage.

[10] Avatar model 330 Fourier transform infrared spectrometer, Thermo Electron North America LLC, Madison, WI.

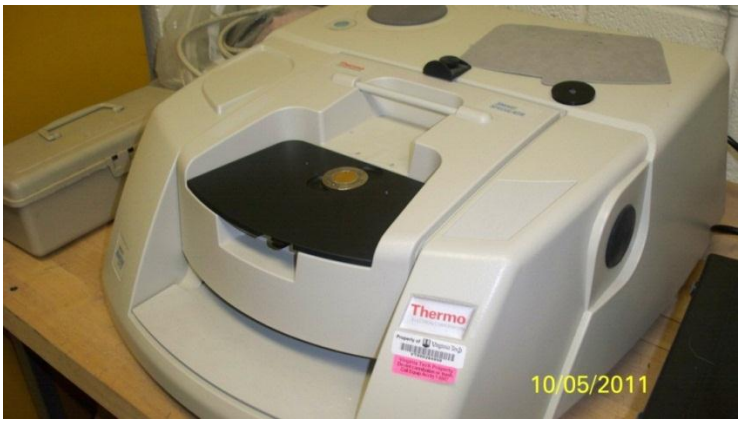

Figure 3.5: The Thermo Electron Avatar 330 FTIR with the ZnSe HATR crystal in place.

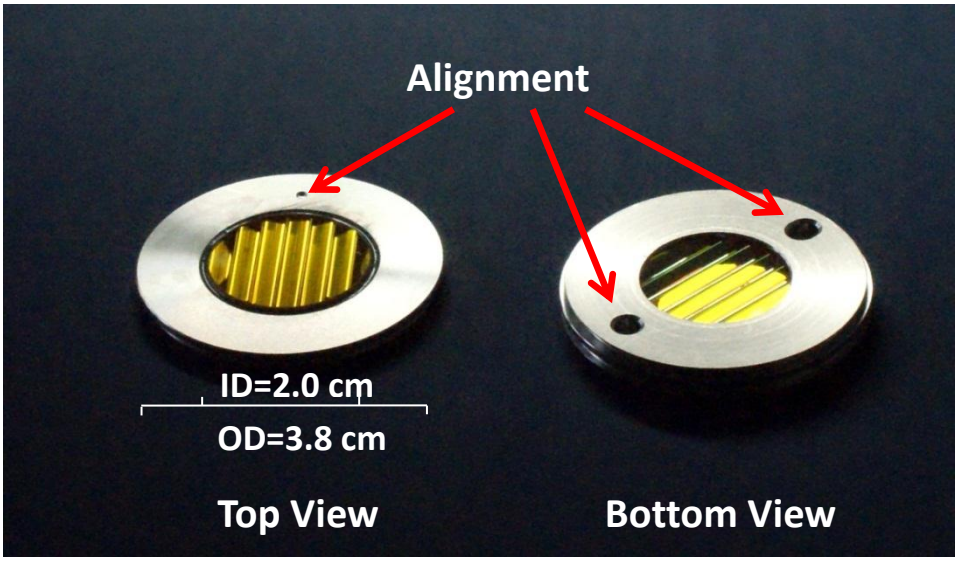

Figure 3.6: Photograph of the Avatar 330 Smart SpeculATR - ZnSe crystal[11] used to perform HATR-FTIR measurements in this work: (left) top view; (right) bottom view [photo by L. Ellis, 2011].

As can be seen in the photographs of the ZnSe stage, there are indentations in the bottom of the mounting ring that fit onto the stage housing. This configuration ensures that the crystal is placed precisely such that the angle of incidence with respected to the corrugated bottom surface is maintained at 45°. During the set-up steps for the FTIR, the opportunity to select the type of sample stage is provided by the Omnic software. When the HATR stage is selected, the instrument is programmed to send the incident beam toward mirrors that are positioned to direct

[11]Smart SpeculATR ZnSe crystal – flat configuration, part no. 0035-703; Thermo Electron North America LLC, Madison, WI.

the beam onto the facets (corrugated region) on the bottom surface of the crystal. As described in Chapter 2, the IR beams passes through the crystal, interacts with the sample surface, and exits from the faces on the opposite side of the corrugated facet, as shown in Figure 2.13. Because of this automated, SMART instrument and software design, the cumbersome mirror adjustments that were required in the older model FTIR stages (example in Figure 3.7) is not required.

Prior to running GL-4850 samples, a system calibration was conducted. This calibration consisted of a check of the interferogram (signal detection) and a bench alignment in which the instrument performed an automatic realignment of the system hardware to maximize the IR beam detection. For the sample measurements, subsequent spectra were compared to the one immediately preceding it to determine whether detectable changes in peak intensity occurred in the new samples. While weeks could be required for complete crosslinking to be accomplished, once no further changes were detected over several spectra, the samples were defined as completely cured for the purposes of this study.

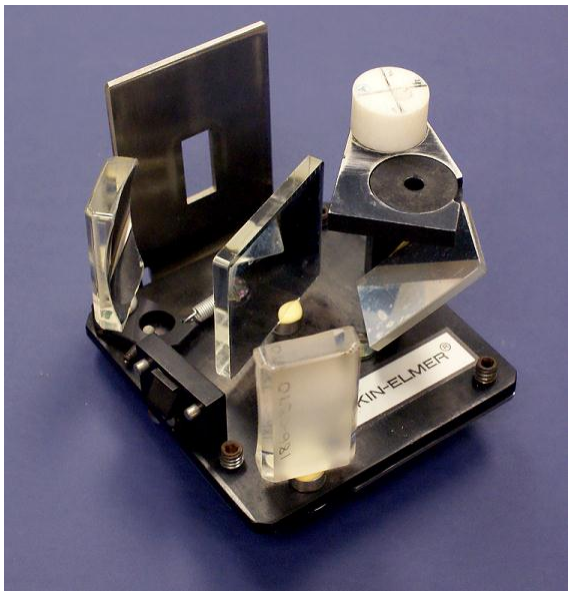

Figure 3.7: Perkin Elmer FTIR specular reflectance stage with manual adjustments required for focusing the IR beam, circa 1970s [photo by E. Ellis, 2011].

To allow for direct comparison of one spectrum to another, all spectra not already resting on the baseline were corrected using the autocorrect feature provided in the Omnic FTIR spectroscopy software [Thermo Nicolet Corporation, 2001]. An example of the autocorrected baseline is shown in Figure 3.8. Here, the blue spectrum is the actual measured data and the red represents the corrected spectrum. The original spectrum contains a small amount of noise that

has shifted the data up off of the baseline (note the area between 1900cm^{-1} and 2800cm^{-1}). This noise can be due to a number of factors, but with the HATR-FTIR techniques, is likely due to incomplete contact between the sample and the ZnSe crystal surface.

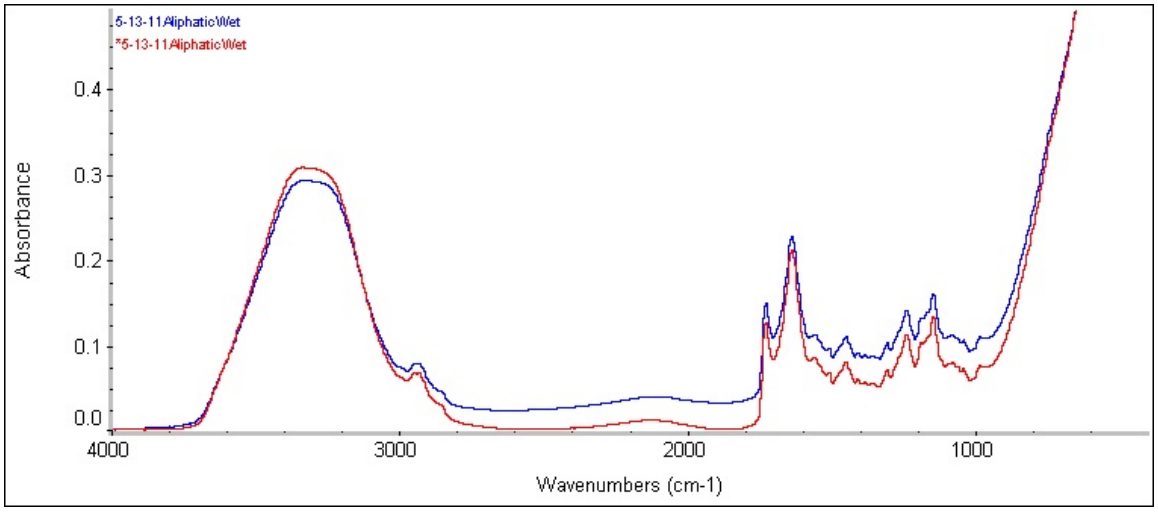

Figure 3.8: Illustration of the autocorrect feature in the Thermo Electron Omnic software. In this figure, the blue spectrum is as-measured, and the red spectrum has undergone an autocorrect step to reduce the effect of noise during the measurement.

When using the HATR-FTIR method, sample contact with the surface of the ZnSe crystal is crucial to a good measurement. To ensure good sample-crystal contact in this study, pressure was applied to the top of the sample to "squeeze" it up against the crystal surface. This step was especially important as the samples became "drier" at the later time steps as they tended to curl and leave gaps between the sample and the crystal.

The spectrum of deionized water was used to confirm that the FTIR was indeed operating within the required machine parameters. As seen in Figure 3.9, the broad peak that spans from 3200 and 3500cm^{-1} and the sharp peak at ~1650cm^{-1}, both representative of water bonds [Smith, 1996], were represented clearly.

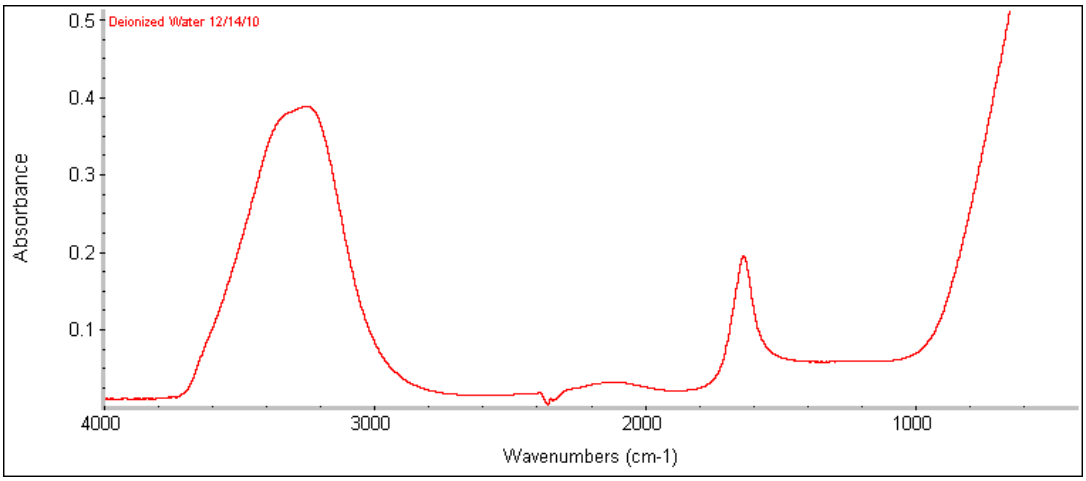

Figure 3.9: HATR-FTIR spectrum for deionized water; collected using the Thermo Electron Avatar 330 SmartSpeculATR stage with a ZnSe sample cell.

Critical Peaks to Follow in PUR

The compositions of polyurethanes are vast, with almost all except in-house manufactured samples being proprietary. The specific composition of the GL-4850 used in this study is no exception. However, most polymer compositions will exhibit sharp peaks in FTIR spectra in the range of 2000 to 600cm^{-1} [Socrates, 2001; Bauer, 1988; Smith, 1999].

The GL-4850 is a water-based, aliphatic urethane composition [Van Technologies, Inc., February 2011]. What this means is that the spectra taken of this composition should yield strong peaks due to water, aliphatic components, and isocyanates. As shown in the spectra of the as-received (wet) GL-4850 PUR (Figure 3.10), these peaks indeed are responsive to IR radiation. These main components will change significantly with cure time. The absorption bands monitored are provided in Table 3.1 [Socrates, 2001; Bauer, 1988; Smith, 1999]. In this work, the peak height versus time was used to establish the rate at which the PUR cured using each curing method.

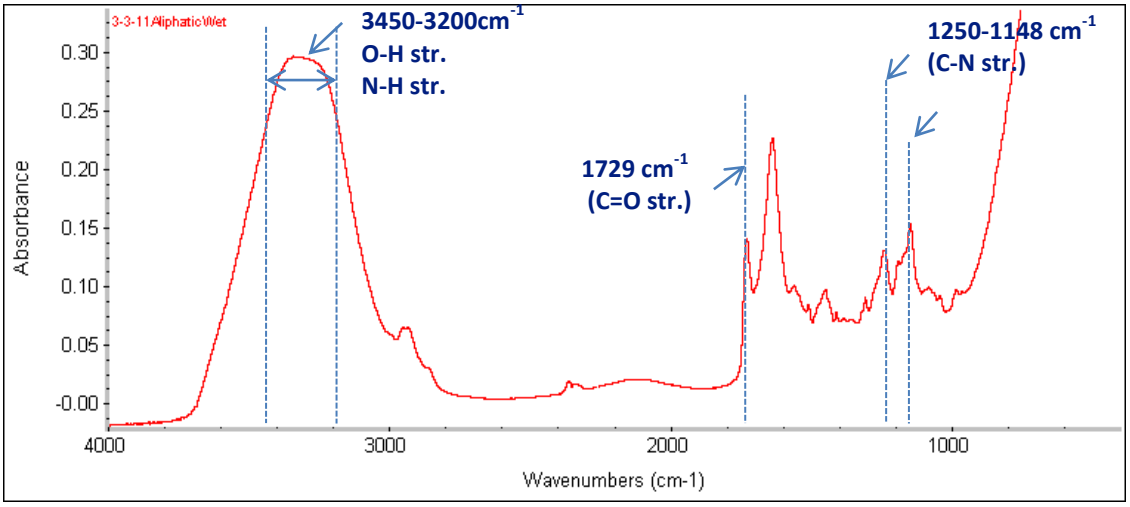

Figure 3.10: FTIR spectrum of as-received (wet) GL-4850 water-based, aliphatic urethane with major peaks identified (described in Table 3.1).

Table 3.1: Approximate wavenumber at which the peaks of interest occurred and the bonds associated with these peaks [Socrates, 2001; Bauer, 1988; Smith, 1999].

Approximate Wavenumber (cm^{-1})	**Source Component**	**Bonds Associated with Position**
3350±50 (broad peak)	Water, Alcohols, Secondary Urethanes	O-H stretching (hydrogen-bonded) N-H stretching
1729	Isocyanates, Diisocyanates	C=O stretching (carbonyls)
1241 and 1148	Aliphatic Amines	C-N stretching

The spectra generated for the GL-4850 samples were used to determine the cure rates associated with each method. A more detailed discussion of these rates is provided in Chapter 4: Results and Discussion.

3.4 Thermal Analyses

A Netzsch STA 449 Jupiter F3 Simultaneous TGA-DSC was used to perform all thermal analyses. This instrument can collect data for weight loss (TGA) and heat flow (DSC) as a function of temperature [Menczel et al, 2009].

Prior to each sample run, a baseline measurement was collected for each different thermal program, followed by the actual data run. The purpose of the baseline measurement was to calibrate the internal balance for the specific weights of the crucibles to be used in the actual data run. For the GL-4850 PUR, samples of approximately 25ml were measured out into the crucibles, each capable of holding about 50ml of the PUR. A heating rate of 10°C/min was used to reach the soak temperature. In these isothermal tests, the temperature was held constant for 60 minutes at each soak temperature used for the curing experiments (50°C, 75°C, 100°C). At the end of each run, the samples were allowed to oven cool. The measurement set-up was that of the center configuration in Figure 2.8 (b). The reference crucible was left empty and the sample loaded into the second crucible.

CHAPTER 4: RESULTS AND DISCUSSION

4.1 Air Curing

The air-cured samples were used as the standard for this study. These samples were left on the ZnSe liquid stage (liquid configuration with a deep trough) for 5560 minutes (approximately 4 days) in an ambient environment -- temperature ranged from 20 to 22°C; relative humidity ranged from 19 to 47%. Figure 4.1 shows the spectra that were collected for one of the air-cured samples and indicates the change in intensity of the absorbance peaks under investigation. As seen, the peak at 3350cm^{-1} due to water-alcohol-secondary urethane is a broad peak that generally decreases in intensity over time. However, as seen in the close-up view of these spectra in Figures 4.2 and 4.3, in some samples, there is a period of time in the first 90 minutes where this peak intensity increases before eventually exhibiting a decreasing trend. The peak intensity then decreases continually from 90 minutes until there is no further change detected in the peak intensity from 1802 to 5560 minutes. An examination of the TGA-DSC plots (Section 4.2: Thermal Curing) helps in interpreting the reason for the increase in this particular peak height prior to the substantial decrease.

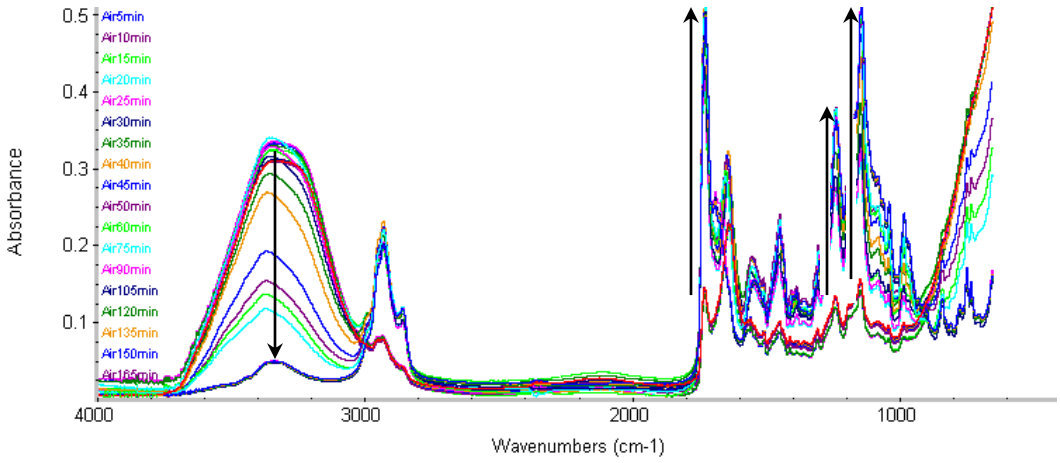

Figure 4.1: FTIR spectra for air-cured GL-4850 indicating the increase or decrease over time in the peaks of interest at approximately 3350, 1729, 1241, and 1148cm^{-1}.

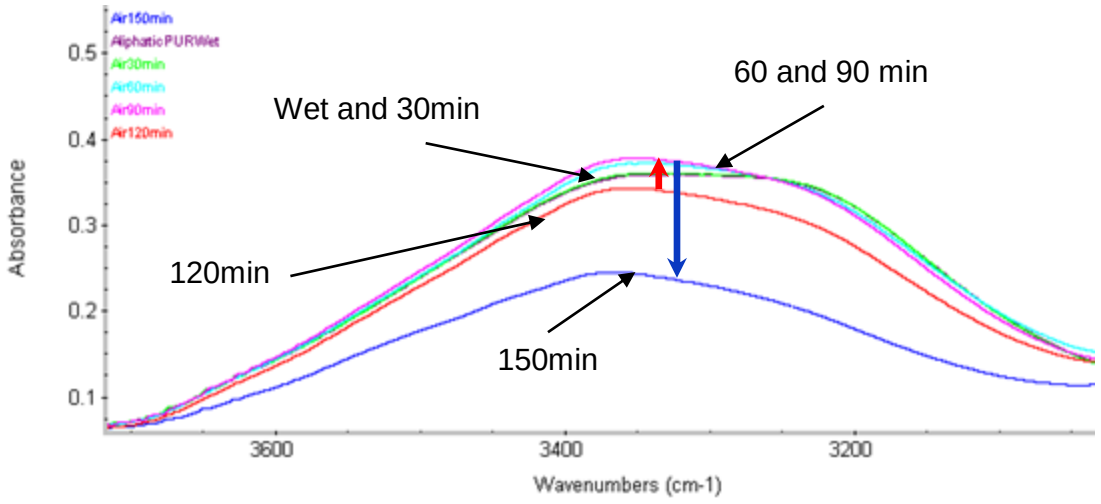

Figure 4.2: The peak for air-cured GL-4850 at 3350cm^{-1} showing an increasing intensity in the earlier time segments (wet to 90 minutes) and then a decrease from 90 to 120 minutes.

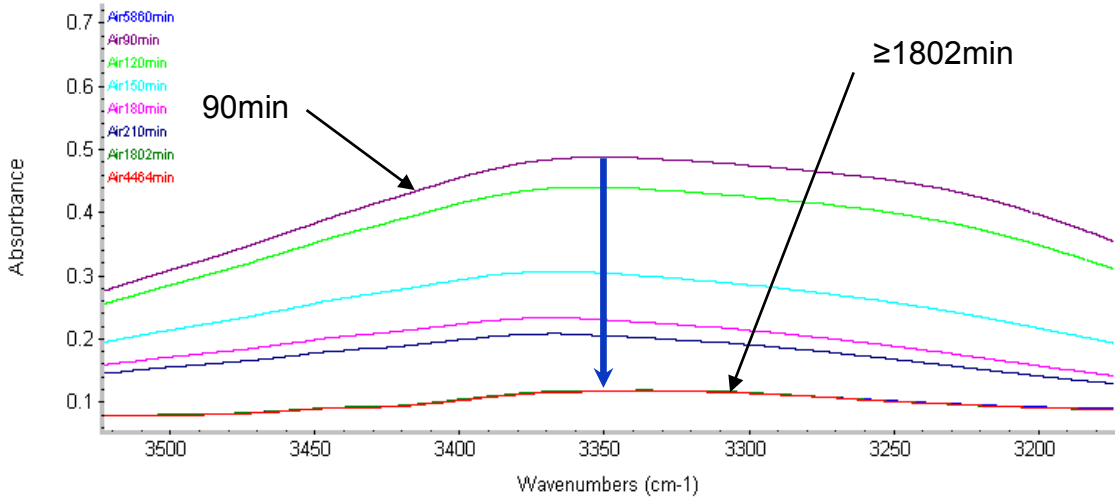

Figure 4.3: The peak for air-cured GL-4850 at 3350cm^{-1} showing a decrease in the intensity after 90 minutes and negligible change detected above 1802 minutes.

This rise is not seen in all of the air-cured samples. The reasons for this intermittent artifact could be related to the environmental conditions in the laboratory over the long period of time required for the air cure. This intermittent hump is more common in the samples processed in low humidity (19 to 22%), while the samples processed in a more humid environment (42 to 47%) did not produce a significant increase in concentration of the O-H bonds prior to the long decrease associated with the loss of the water solvent. It is possible that the high humidity slowed the removal of alcohol and water so that the transition from an alcohol-dominant stage to a water-

dominant stage was not as dramatic. In any case, the eventual result of this time-dependent cure under ambient conditions results in the air-cured samples is a decrease in the peak centered around 3350cm^{-1} and increases in those associated with the 1729, 1241, and 1148cm^{-1} peaks.

4.2 Thermal Curing

TGA-DSC Data

As discussed in Chapter 2, it is common to perform thermal analyses of samples to determine the expected behavior of the material as a function of temperature and time. In this study, a TGA-DSC technique was used to indicate the anticipated phase changes in the GL-4850 PUR. Using this method, a small sample (~25mg) was heated at a rapid ramp rate (10°C/min) to the desired soak temperature. The maximum time over which data was collected was 60 minutes.

The TGA plot for the as-received wet GL-4850 PUR is shown in Figure 4.4. In this figure, the dotted lines represent the thermal profile (temperature versus time plots) for each of the isothermal runs at 50, 75, and 100°C. The dashed lines represent the actual TGA data, which is plotting the weight loss as a function of time. The solid, numbered lines are inserted for the sake of discussing the plots.

At times under 10 minutes, the samples undergo initial heating and there is not good control of the thermal profiles, as can be seen in the temperature plots. In this stage, it is likely that the initial drop in weight is due to the loss of the alcohols that can be very volatile, even at low temperatures. At the intersection of lines 1 and 2 at approximately 9 minutes and 7% weight loss, the 100°C plot has begun to decrease at a fairly quick rate so that, between lines 2 and 3, it has achieved a rate of approximately 2.1 %/min. The 50 and 75°C plots have a much slower weight loss of approximately 1.4 %/min and 0.23 %/min, respectively, from the point at which weight loss begins.

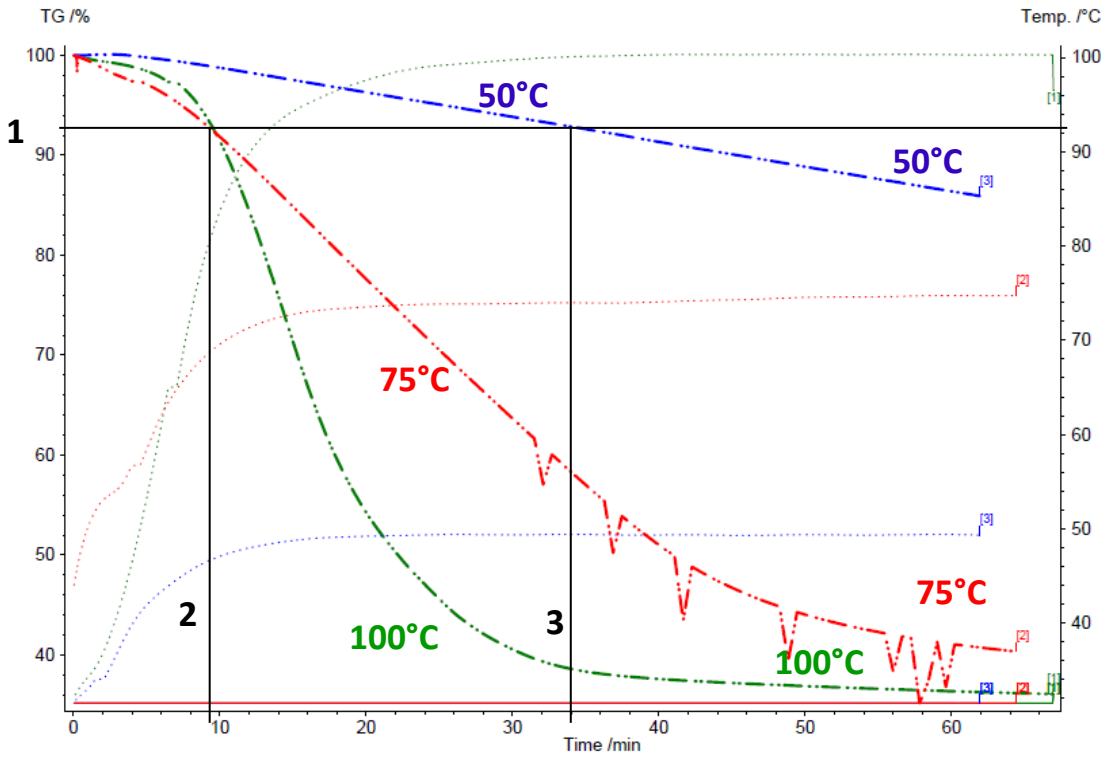

Figure 4.4: Isothermal thermogravimetric analyzer plots for wet GL-4850 PUR run at 50, 75, and 100°C. A heating rate of 10°C/min was used in all cases.

By 34 minutes into the 100°C run, the sample has achieved most of the weight loss due to water. This behavior is expected, as the sample reached 100°C by the 20 minute mark where the water would begin to boil off. In the 75°C run, the sample takes much longer to release the water and does not begin to level off until approximately 50 minutes. In this case, the water is changing phase and evolving out of the sample more slowly, never reaching the boiling point. Over the course of the 60 minute TGA runs, the 50°C sample does not reach the point where a rate increase is observed that would mark the transition from alcohol to water removal. Instead, the slope of the plot remains fairly constant and the alcohol and water are removed very slowly from the sample.

The DSC plot is shown in Figure 4.5. Again, the dotted lines represent the thermal profiles and the dashed lines, the actual DSC data for each of the isothermal runs. Recall that DSC data is presented in terms of the amount of energy absorbed to maintain a temperature in the sample that is equal to that of the cavity in the instrument. Therefore, a decreasing trend (dip in the curve) is observed for endothermic reactions (heat flow is directed toward the sample, as opposed to heat flow from the sample to the surrounding cavity in the case of exothermic reactions).

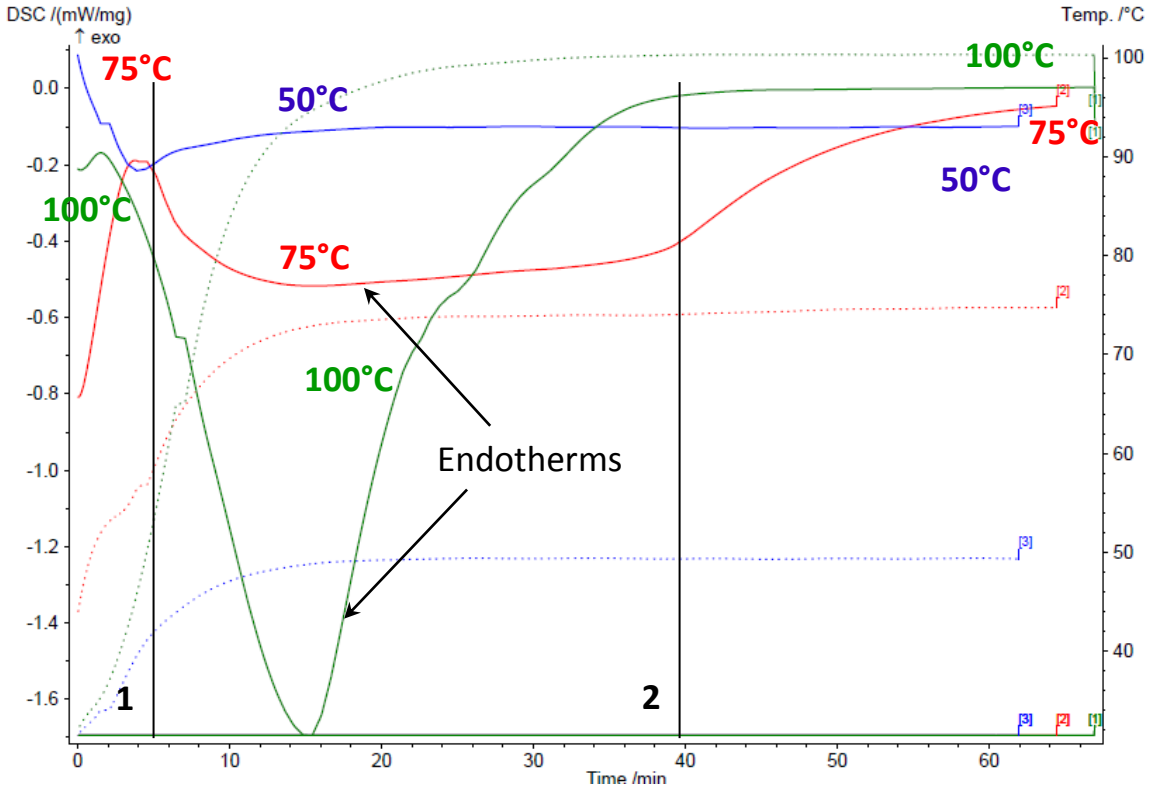

Figure 4.5: Isothermal differential scanning analyzer plots for wet GL-4850 PUR run at 50, 75, and 100°C. A heating rate of 10°C/min was used in all cases.

The most prominent features in the DSC plot occur at times between about 5 and 40 minutes. Here, the 75°C and 100°C samples exhibit endotherms, indicating that they are absorbing heat. The alcohols are gone from the PUR in this stage and all of the energy being absorbed is used to break the bonds in the water. The endotherm associated with this loss of water in the 75°C data is broad and less intense, as the water never comes to a boil. In other words, the transition from the liquid state to the gaseous state is slower and less violent than that exhibited by the 100°C sample.

The 50°C plot does not show the endotherm due to water loss, but rather exhibits a very long plateau that can be attributed primarily to alcohol loss and some water loss. The water at 50°C and 75°C is accomplished through an 'enhanced evaporation' rate, rather than boiling or a noticeably sharp phase change. Looking back at Figures 4.2 and 4.3 and the air-cured sample, the process is even slower. It takes approximately 90 minutes to lose the alcohols and to begin the evaporation of the water; a process that does not show a steady state until about 1800 minutes.

HATR-FTIR Spectroscopy Data

For each of the temperatures studied, spectra were collected for each of the targeted absorbance peaks. This data is presented in Figures 4.6 through 4.9. Figure 4.6 presents the time-progression for the recorded spectra at each temperature (50°C, 75°C, 100°C), ranging from 600 to 4000 cm^{-1}. Based on these spectra, it is clear that there was a temperature effect on the rate of change in absorbance peak intensities. As the soak temperature increases, so does the rate of change in the spectra. However, it also is evident that the peaks increase or decrease at different rates. In other words, this difference indicates that the bonds associated with each wavenumber are affected to varying degrees by the change in soak temperature. Figures 4.7 through 4.9 provide an enhanced view of the peak positions for each soak temperature.

For the broad alcohol-water-secondary urethane peak at $3350cm^{-1}$, associated primarily with the O-H and N-H stretching bonds, the peak intensity is lower at a shorter soak time for the 100°C samples than for those soaked at 50°C and 75°C (45 minutes versus 55 minutes, respectively). An analogous behavior is observed for the carbonyl peak at $1729cm^{-1}$ (C=O stretching bond; a double bond) and for the peaks associated with the aliphatic amines (C-H stretching bonds) at 1241 and $1148cm^{-1}$. The primary difference between the broad peak at $3350cm^{-1}$ and the peaks for the carbonyls and aliphatic amines is that the first is a decreasing peak due to alcohol and water loss, and the latter peaks are increasing as curing progresses and these characteristic PUR peaks emerge.

There are some anomalies in the spectra with regards to the each of the peaks at the higher soak times. As discussed for the peak at $3350cm^{-1}$ in the air-cured samples, the highest peaks were not always associated with the longest soak times. The air-cured samples were prepared in the ZnSe sample stage and the experiments were conducted on each sample in place (not removed from a dish and placed on the crystal); therefore, some conclusions could be drawn about the increase in the peak prior to the eventual decrease associated with the O-H bonds being broken as water was lost. For the thermally cured samples, each was prepared in a dish and removed from that dish for placement on the ZnSe stage to collect the spectra. For the samples that were removed from the dishes at the higher soak times, damage sometimes occured in the PUR solid, preventing them from making close contact with the stage. Steps were taken to ensure good contact by applying pressure to the sample to 'squeeze' it against the ZnSe; however, it is possible that some error persisted. Recall that the penetration of the evanescent wave into the sample surface could have been as short as 0.5μm, leaving the possibility of error with only a very small gap at the sample-crystal interface. For the shorter soak times, the samples contained a good deal of liquid that could wet the crystal surface, providing good contact and a lower

possibility of error. Even for the 100°C samples that experienced rapid loss of the liquid phase, they were more pliable at the short soak times and could be easily pressed onto the stage.

Based on an evaluation of the spectra obtained for the thermally cured samples, it is possible to conclude that the higher the soak temperatures and the longer soak time led to accelerated curing and increased extent of cure in the GL-4850 PUR samples over those cured in air.

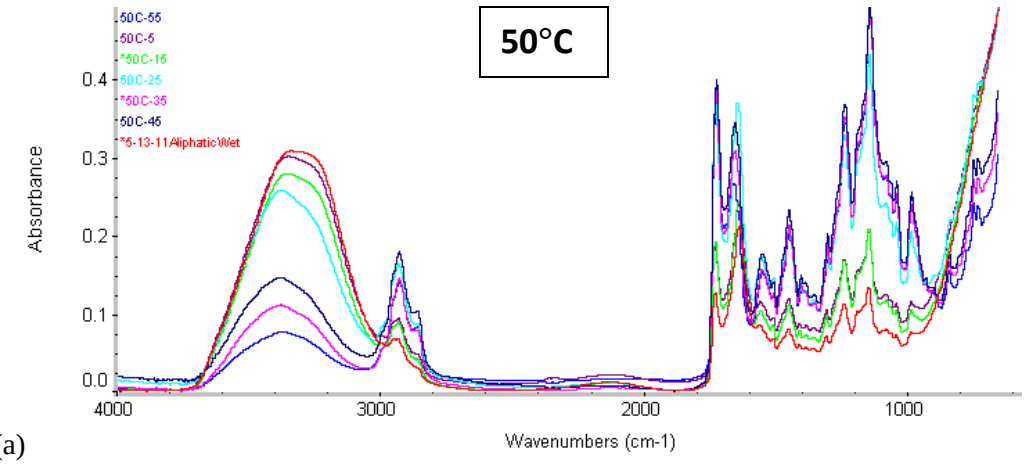

(a(a)

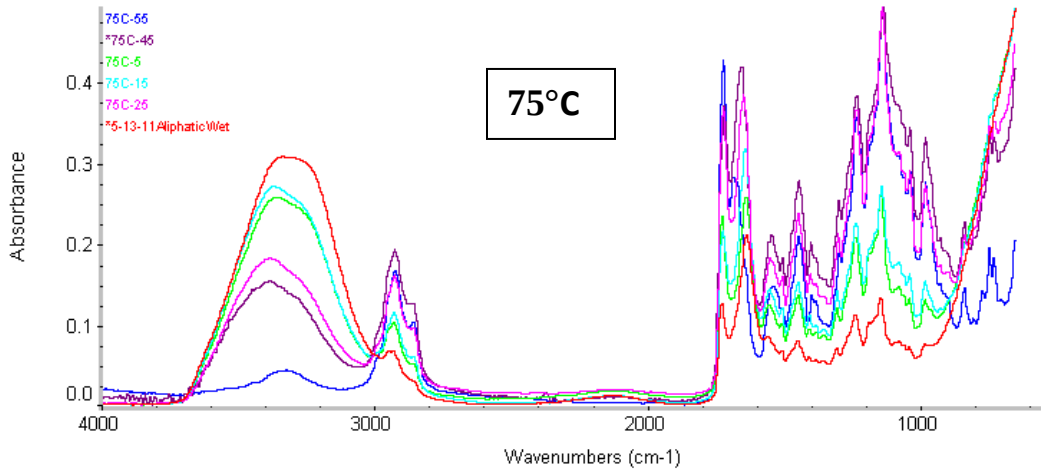

(b)

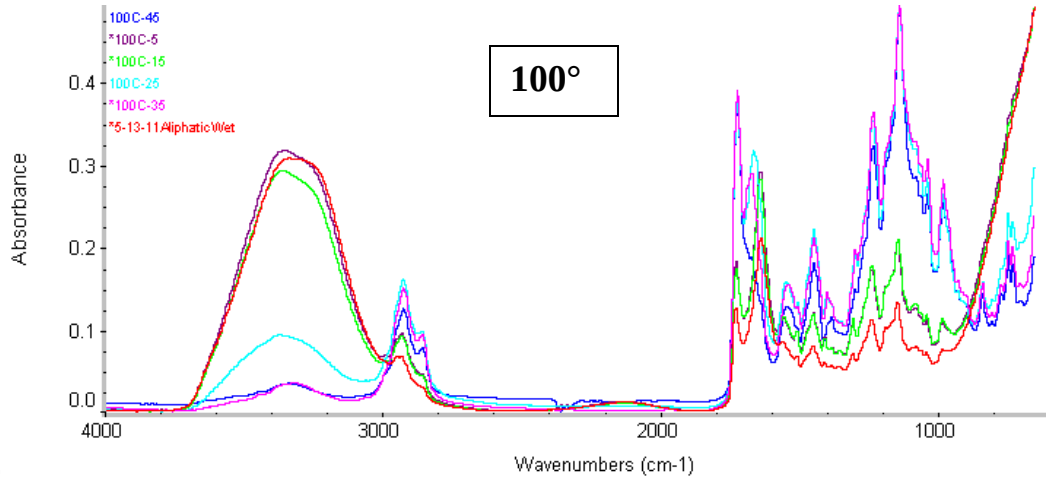

(c)

Figure 4.6: FTIR spectra for GL-4850 indicating the increase or decrease over time in the peaks of interest at approximately 3350, 1729, 1241, and 1148cm^{-1} for samples thermally cured at (a) 50 ºC , (b) 75 ºC, (c) 100 ºC.

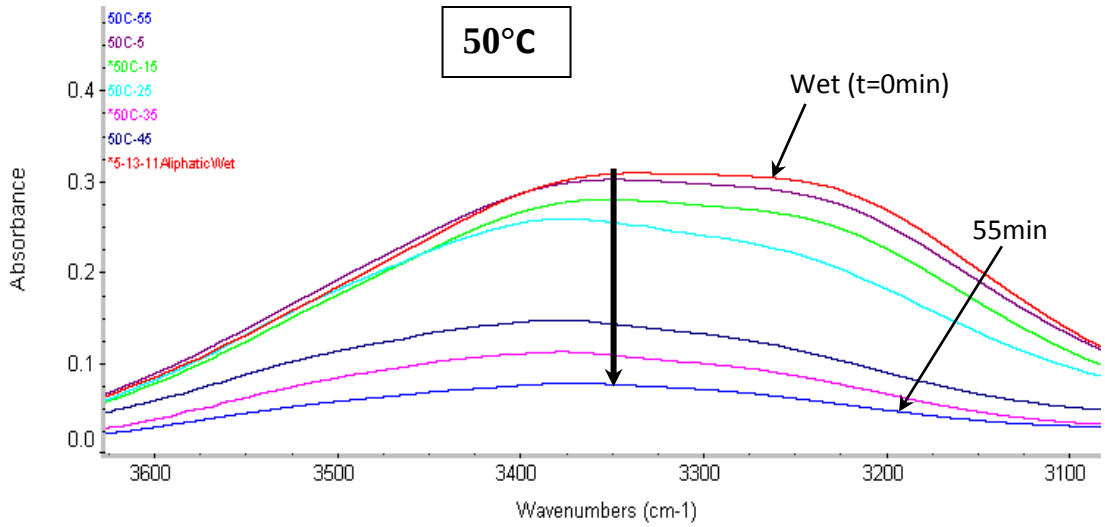

(a)

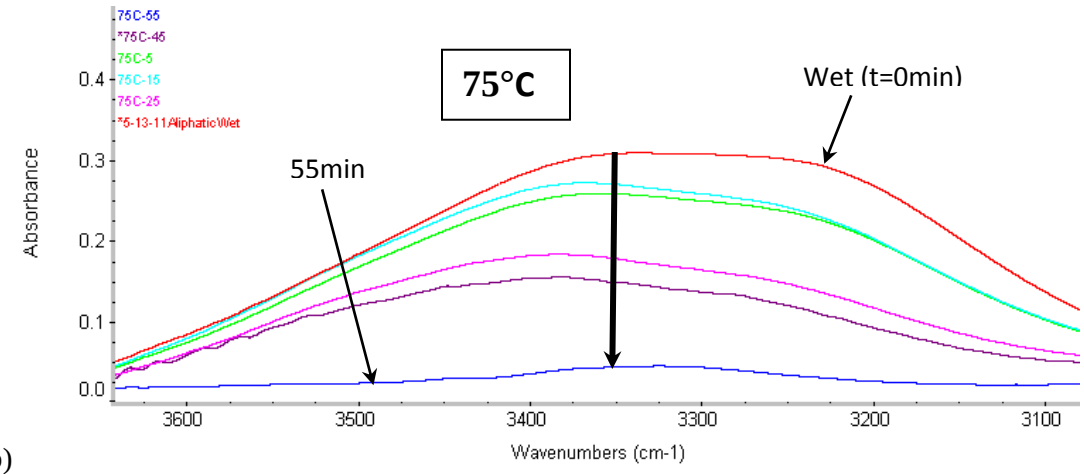

(b)

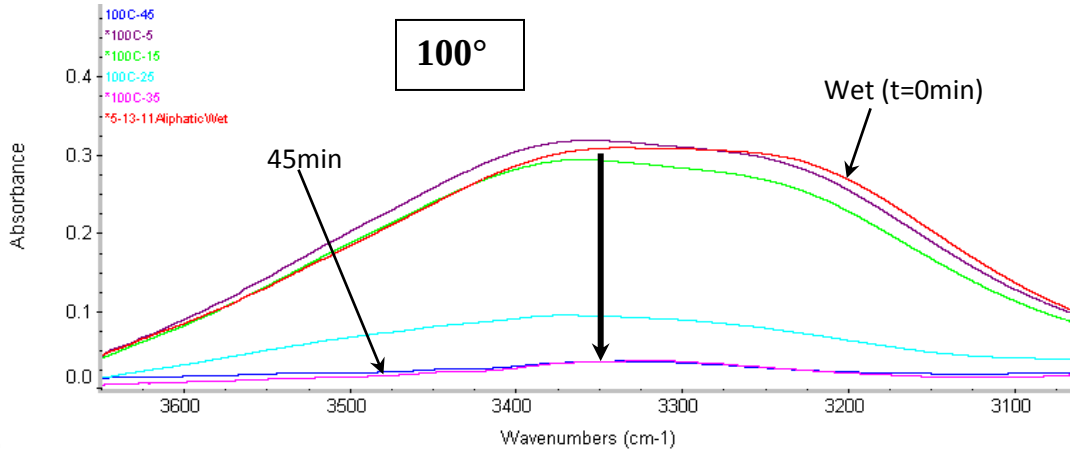

(c)

Figure 4.7: The peak at 3350cm^{-1} (alcohol-water-secondary urethanes) for thermally cured GL-4850 showing a decrease in the peak intensity over time at a constant temperature of (a) 50ºC, (b) 75 ºC, (c) 100 ºC.

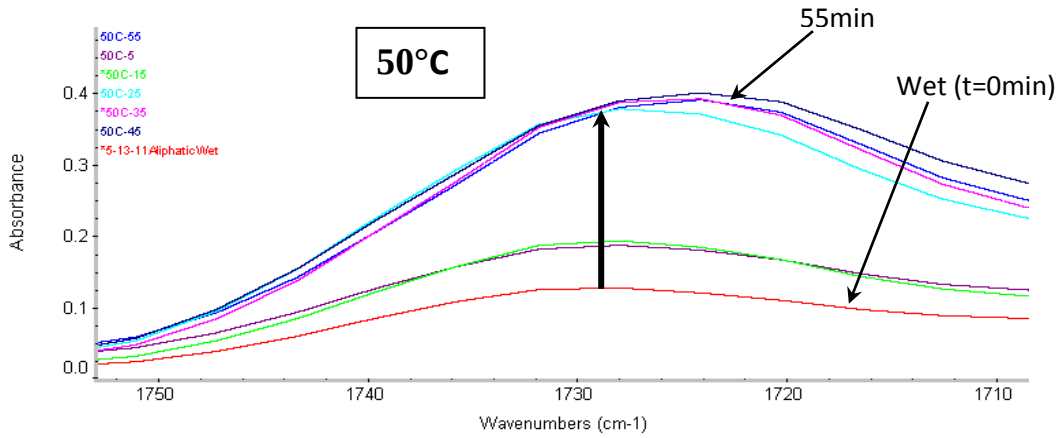

(a)

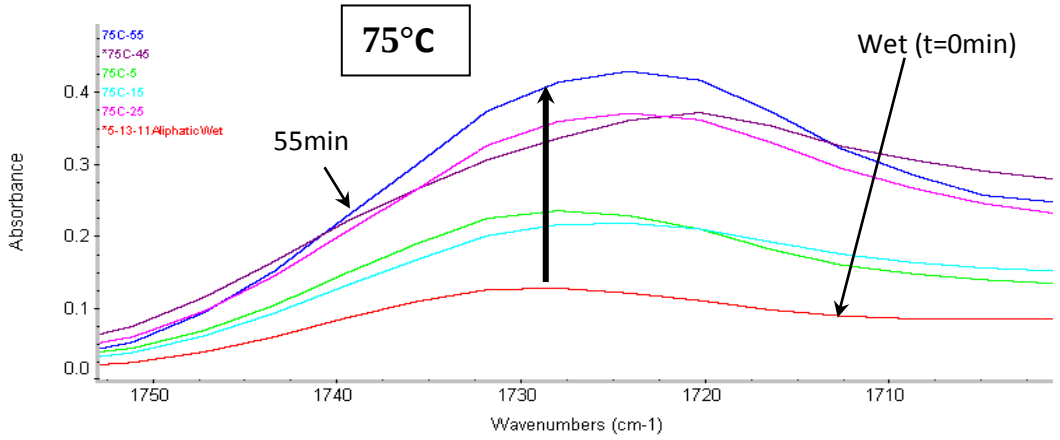

(b)

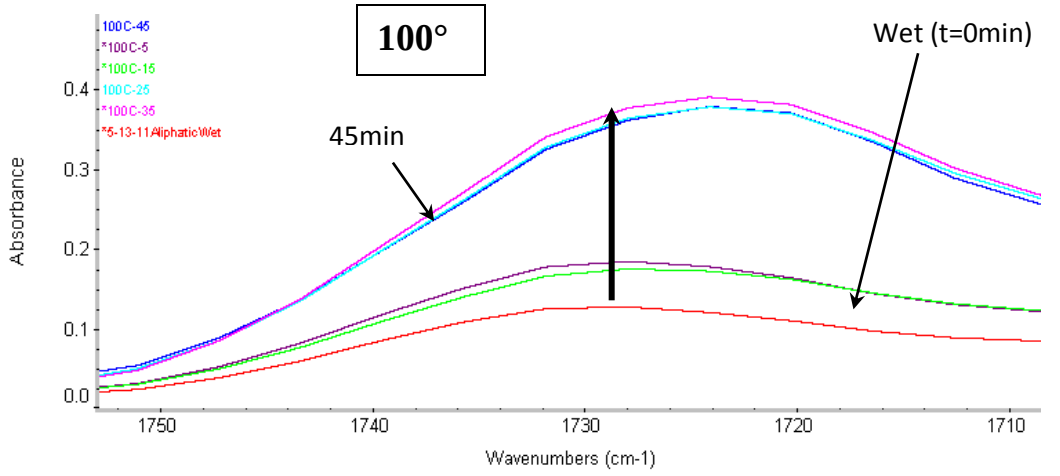

(c)

Figure 4.8: The peak at 1729cm^{-1} (carbonyl) for thermally cured GL-4850 showing an increase in the peak intensity from over time at a constant temperature of (a) 50ºC, (b) 75 ºC, (c) 100 ºC.

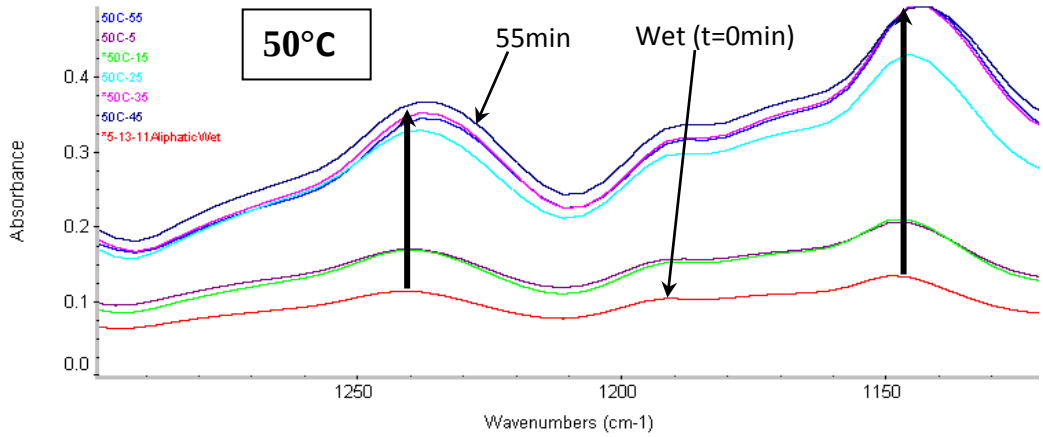

(a)

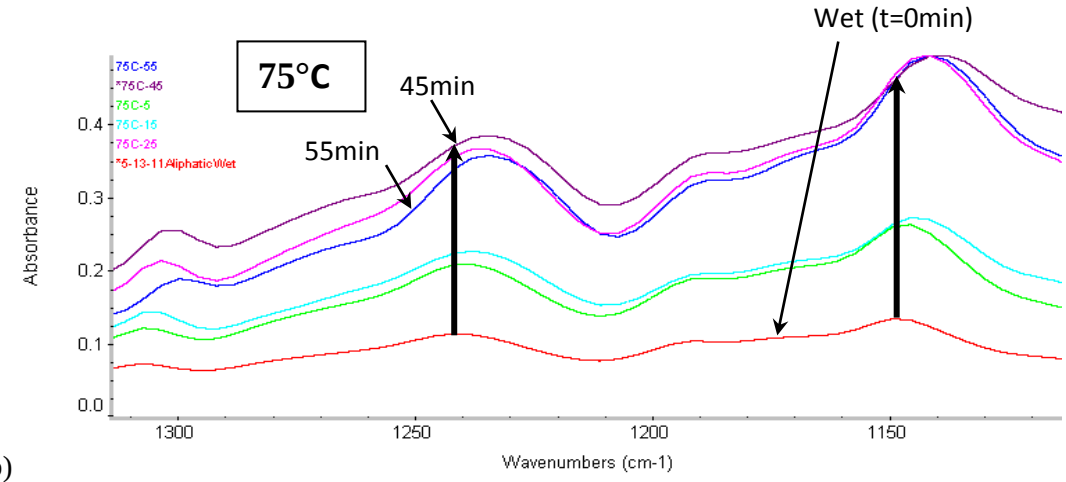

(b)

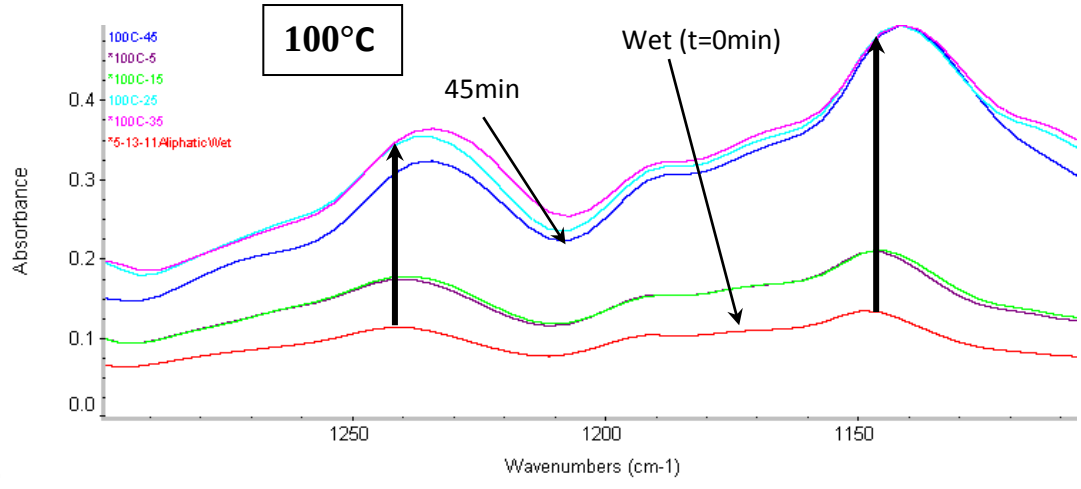

(c)

Figure 4.9: The peaks at 1241 and 1148cm^{-1} (aliphatic amines) for thermally cured GL-4850 showing an increase in the peak intensity over time at a constant temperature of (a) 50ºC, (b) 75 ºC, (c) 100 ºC.

4.3 Microwave Curing

The FTIR spectra for the microwave-cured samples (Figures 4.10 through 4.13) appear to have the same general behavior as that of the thermally cured samples for all of the peaks studied. As in the thermally cured sample spectra, the broad alcohol-water-secondary urethane peak drops with no observable increase in the intensity that would mimic behavior exhibited by some of the air-cured samples. The absence of this rise in the O-H bond intensity could be due to the decreased time for cure (over air curing). (The increase in intensity observed in the 3350cm^{-1} peak of the air-cured sample peak may occur in the first 5 minutes in the thermally cured and microwave-cured samples.) The carbonyl and aliphatic amine peaks in the thermally cured samples generally increase over time of exposure to microwave energy.

These spectra also have shown some of the same inconsistencies as those observed in the thermally cured samples in the order of the times to achieve the cured state; the longest times do not always reflect the most cured state at each wavenumber. Since there is no TGA-DSC available that uses a microwave generator in place of the conventional radiant heating method, thermal analyses cannot be conducted in the presence of a microwave field. Therefore, it is not possible to confirm the times or temperatures for the phase changes that take place in the samples at different frequencies.

Recall that the microwave experiments were designed to determine (1) whether microwave energy had an effect on the cure rate in the GL-4850 PUR, and (2) if the microwave energy did affect the cure rate, if there was an observable effect of frequency. Therefore, data was collected at three central frequencies that spanned the range of the Variwave® VFM oven with a sweep time of 1 second and a 1GHz bandwidth. While the power was not controlled in these experiments, both the forward and reverse power (FP and RP) were monitored (Table 4.1). Additionally, the temperature of the sample in position 2 (Figure 3.4) was monitored, but not controlled. The spectra were generated at 5-minute intervals.

Table 4.1: Values for forward and reverse power, as well as maximum temperature achieved for each VFM central frequency.

Central Frequency (CF; GHz)	**Forward Power (FP; W)**	**Reverse Power (RP; W)**	**Max. Temp. (T_{max}; ºC)**
7	54-71	5-9	96
12	24-26	2-5	81
17	40-85	3-19	91

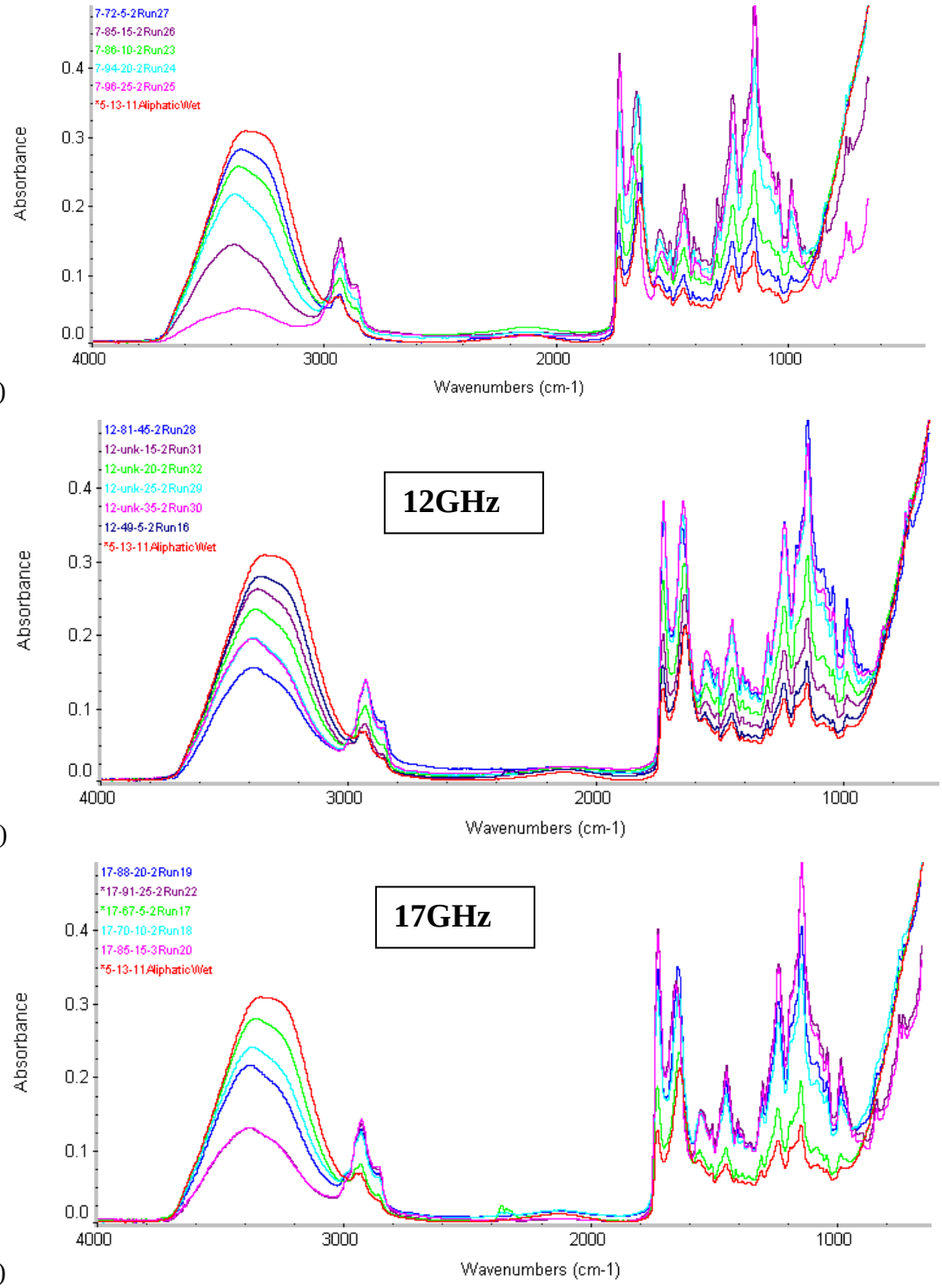

Figure 4.10: FTIR spectra for GL-4850 indicating the increase or decrease over time in the peaks of interest at approximately 3350, 1729, 1241, and 1148cm^{-1} for samples microwaved-cured at central frequencies of (a) 7GHz, (b) 12GHz, (c) 17GHz.

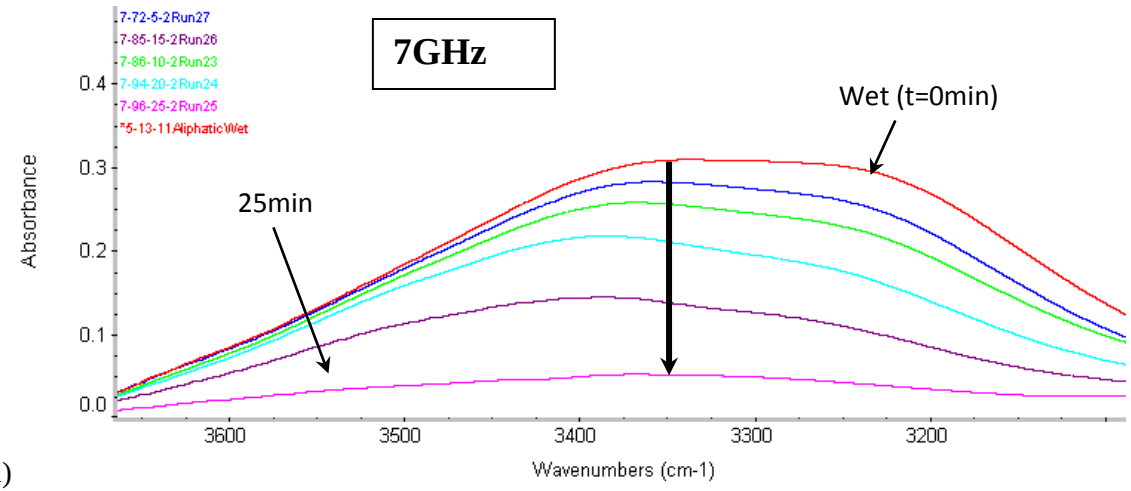

(a)

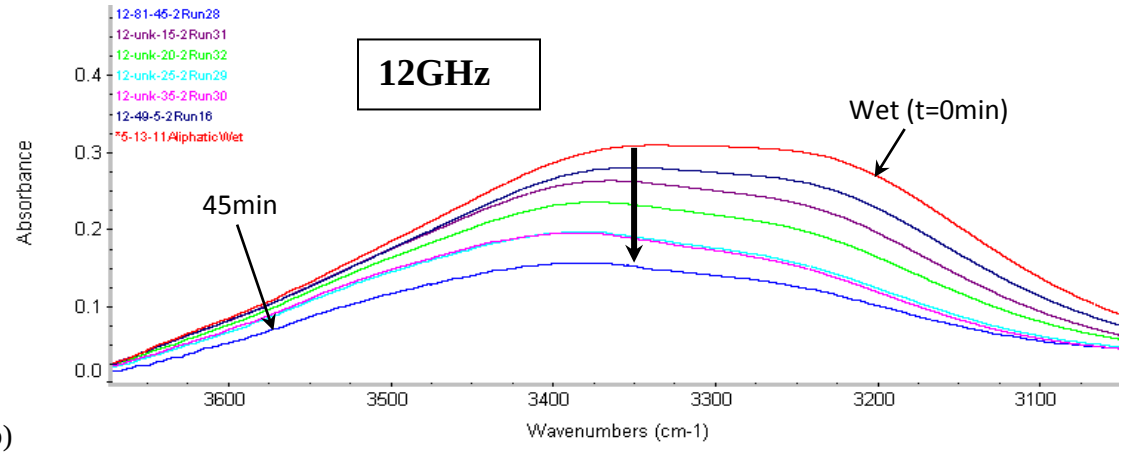

(b)

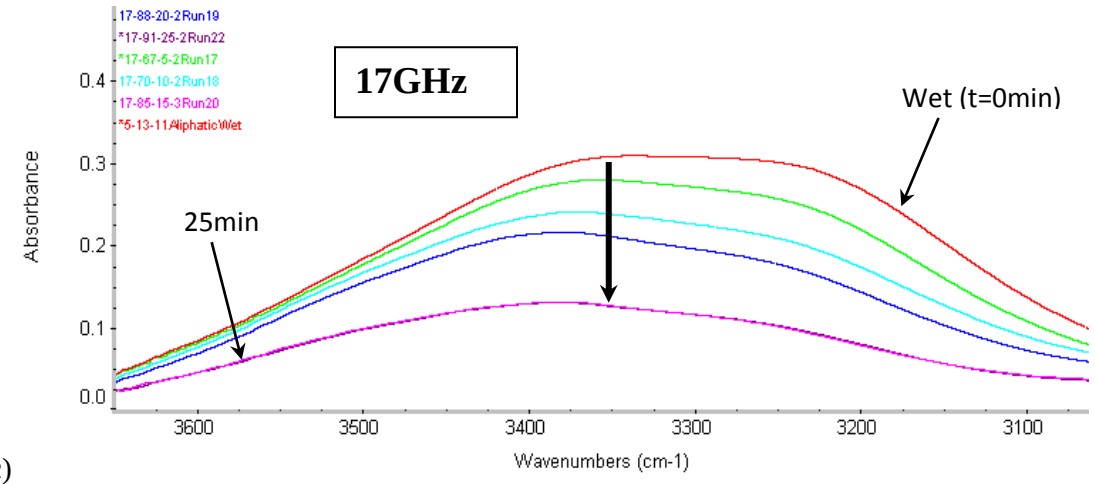

(c)

Figure 4.11: The peak at 3350cm^{-1} (alcohol-water-secondary urethanes) for microwave-cured GL-4850 showing a decrease in the peak intensity over time at central frequencies of (a) 7GHz, (b) 12GHz, (c) 17GHz.

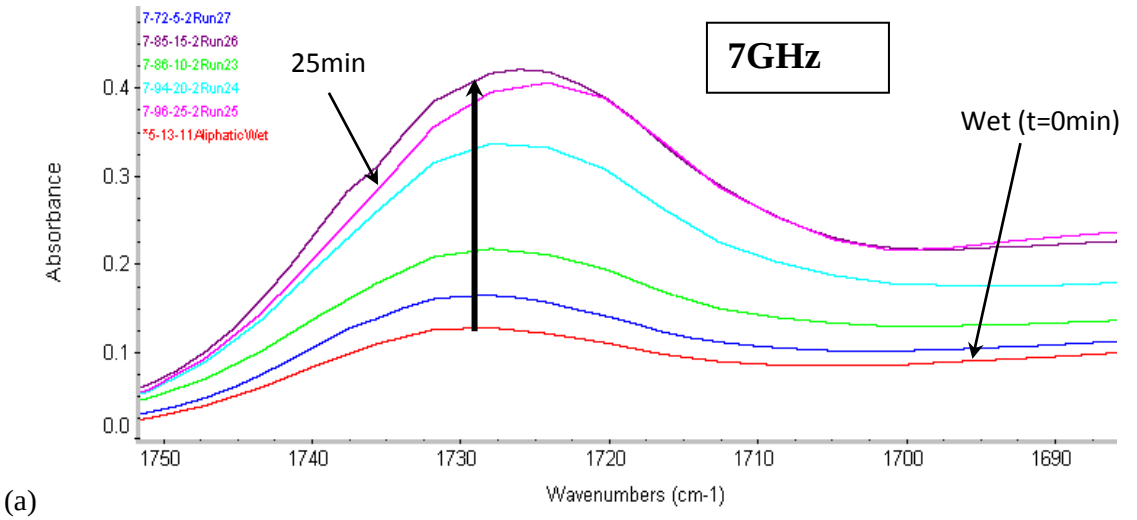

(a)

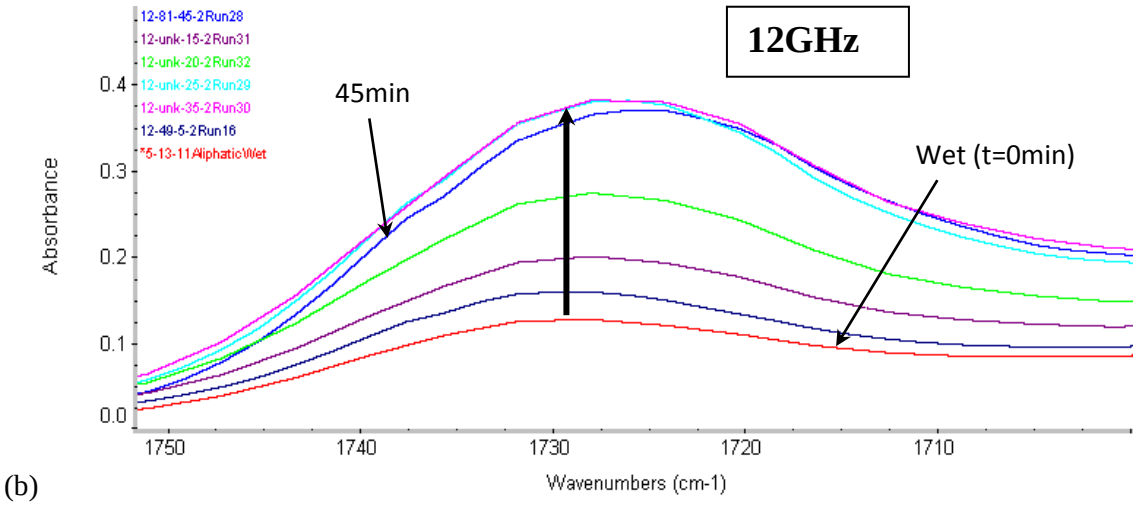

(b)

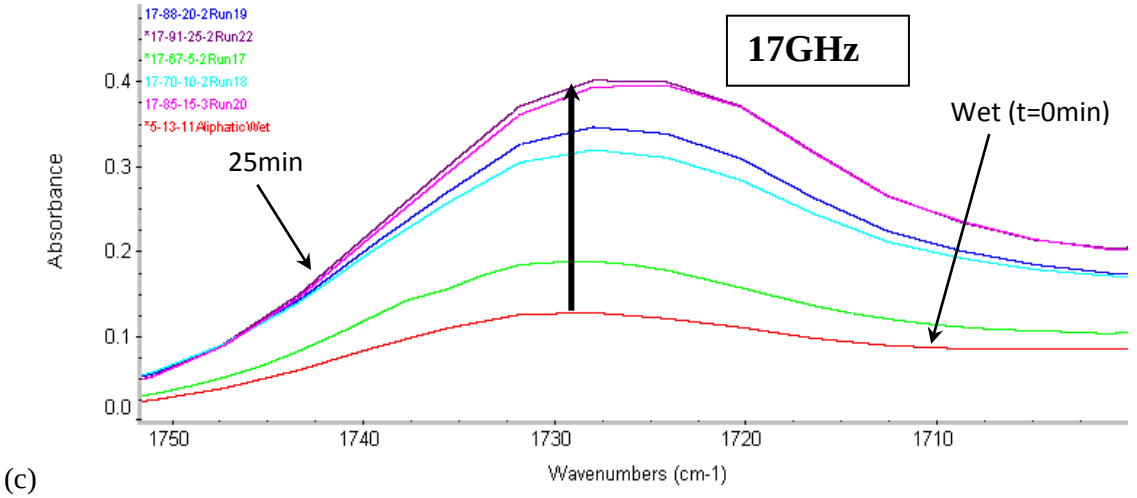

(c)

Figure 4.12: The peak at 1729cm^{-1} (carbonyl) for microwave-cured GL-4850 showing an increase in the peak intensity over time at central frequencies of (a) 7GHz, (b) 12GHz, (c) 17GHz.

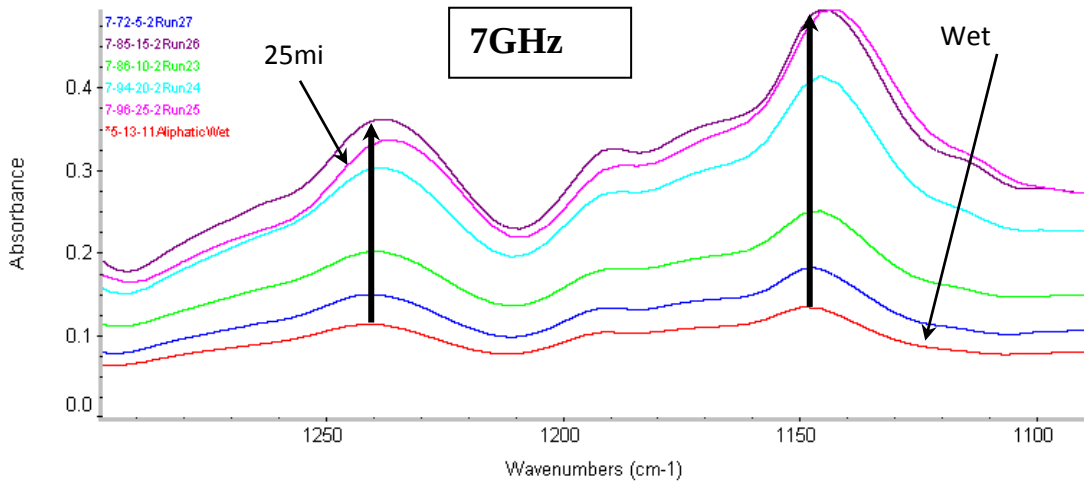

(a)

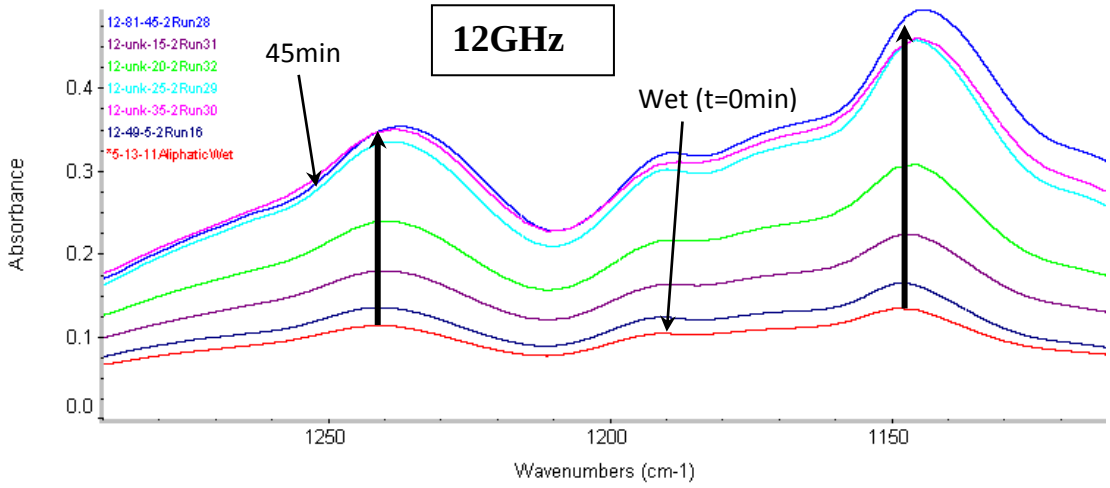

(b)

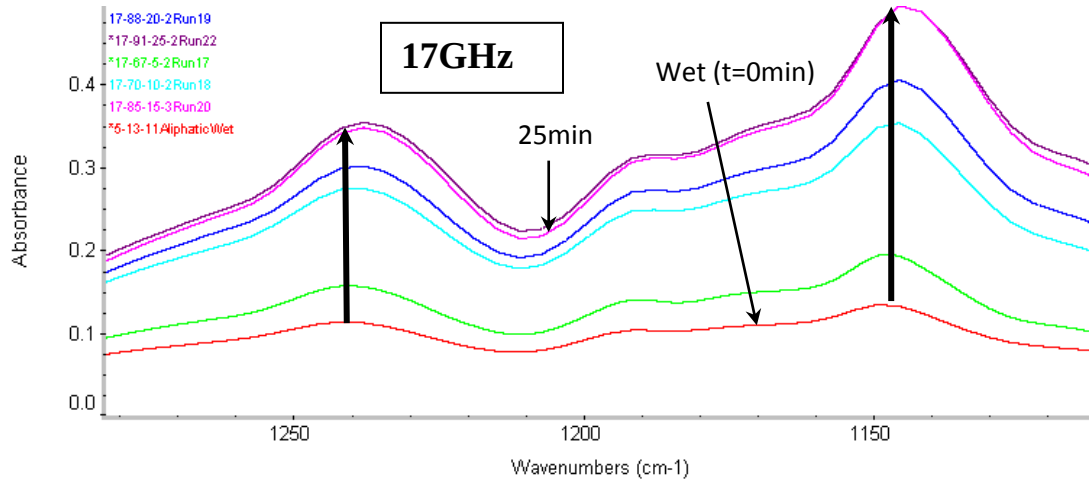

(c)

Figure 4.13: The peaks at 1241 and 1148cm^{-1} (aliphatic amines) for microwave-cured GL-4850 showing an increase in the peak intensity over time at central frequencies of (a) 7GHz, (b) 12GHz, (c) 17GHz.

4.4 Rate Plots

Rate plots were constructed using the peak absorbance intensities associated with each of the bonds as a function of time. For the thermally cured sample plots, each data point was associated with a different sample. For the microwave-cured sample plots, all the data were generated using only sample number 2 for each time step (Figure 3.4). Each point represents a different sample. Samples 1 and 3 were control samples; their spectra were recorded to insure that the behavior of sample 2 was representative of the particular time step for the central frequencies studied.

Curves that follow a polynomial function are inserted for each of the data sets, with the exception of the air-cured plots in which the data points simply are connected to make the progressions easier to follow (Figure 4.14). There is an interesting trend that is observed in the plots of the air-cured samples. It appears as though there is a plateau at the beginning of the air-cured samples, after which the peaks experience significant rates of change. In the sample reported in Figure 4.14, the plateau exists for about 50 minutes. What magical event is taking place at 50 minutes that causes such a dramatic change in the data? For the answer, it is necessary to return to the HATR-FTIR characterization set-up (Figure 4.15).

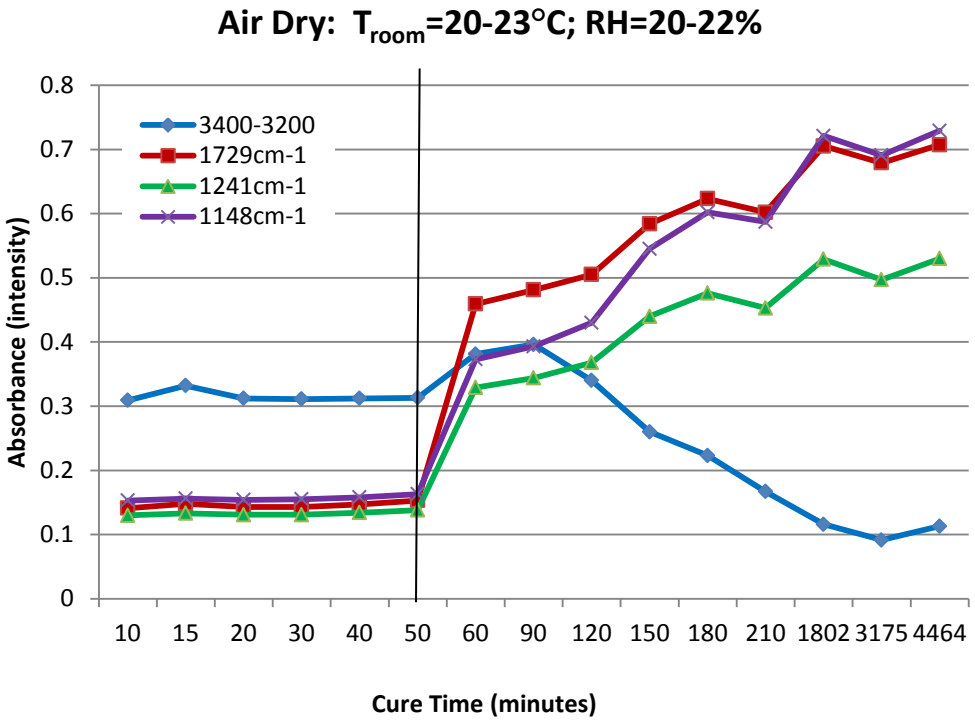

Figure 4.14: Absorbance vs. cure time for GL-4850 PUR cured in air at ambient temperature, pressure, and relative humidity.

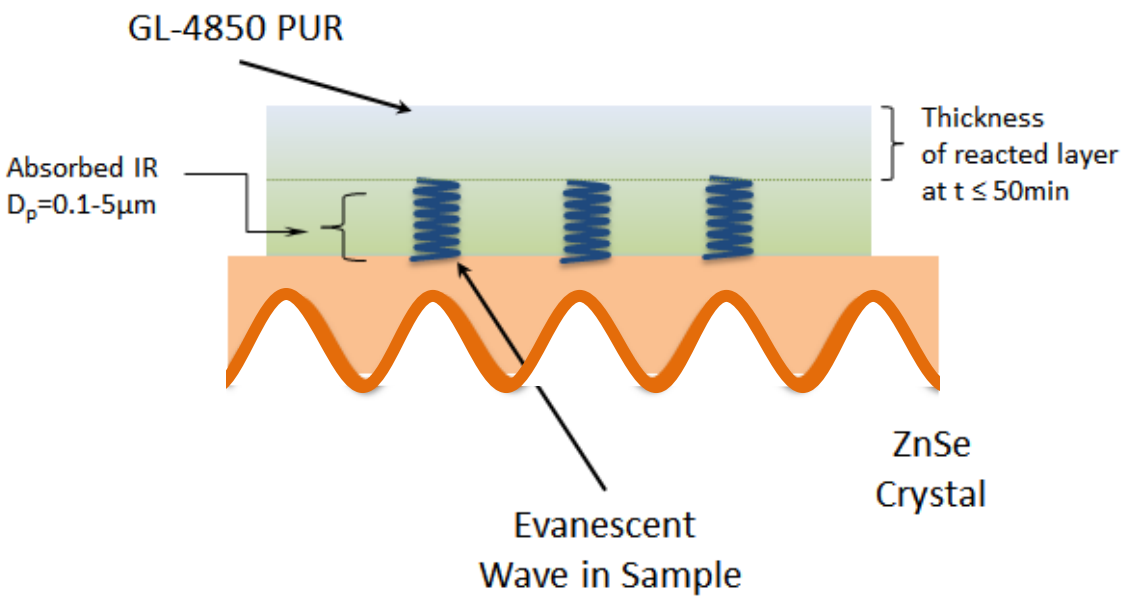

Figure 4.15: GL-4850 PUR sample resting on a ZnSe HATR crystal.

In the samples left in ambient conditions, curing is taking place essentially from the top surface of the sample and progressing downwards, toward the sample/ZnSe interface. Recall that the evanescent wave (attenuated beam) generated in the sample (due to close contact of the sample with the ZnSe HATR crystal) reaches a depth of penetration of no more than about 5.0µm into the bottom of the sample surface. However, the sample thickness in this study is approximately 2.0mm. For the reaction wavefront to reach the evanescent wave, a sufficiently thick reacted layer much be achieved. At the point where the evanescent wave is reached by this wavefront, the spectra begin to show changes due to the continued reaction (curing) of the sample at this depth. Because of this delay in detectable change in the sample due to the limitations of the HATR configuration, the air-cured samples exhibit a plateau at the beginning of the runs before the absorbance spectra is registered. Three additional air-cure runs are plotted in Figures 4.16 through 4.19. The plateau is eliminated from each of these plots so the rate of change in intensity can be compared from the time where the reaction wavefront reaches the evanescent wave. (The ambient conditions for these runs: T=24-25°C and RH=40-47%.) Note that the samples behave almost identically for all the runs. Appendix 2 provides the approach for generating these plots and the error associated with each.

The other interesting feature in Figure 4.14 is the apparent hump in the intensity plot for the 3350cm^{-1} curve. This hump was not present in all of the samples and the reason for its appearance in some of the plots is unknown. This feature could be addressed in future work.

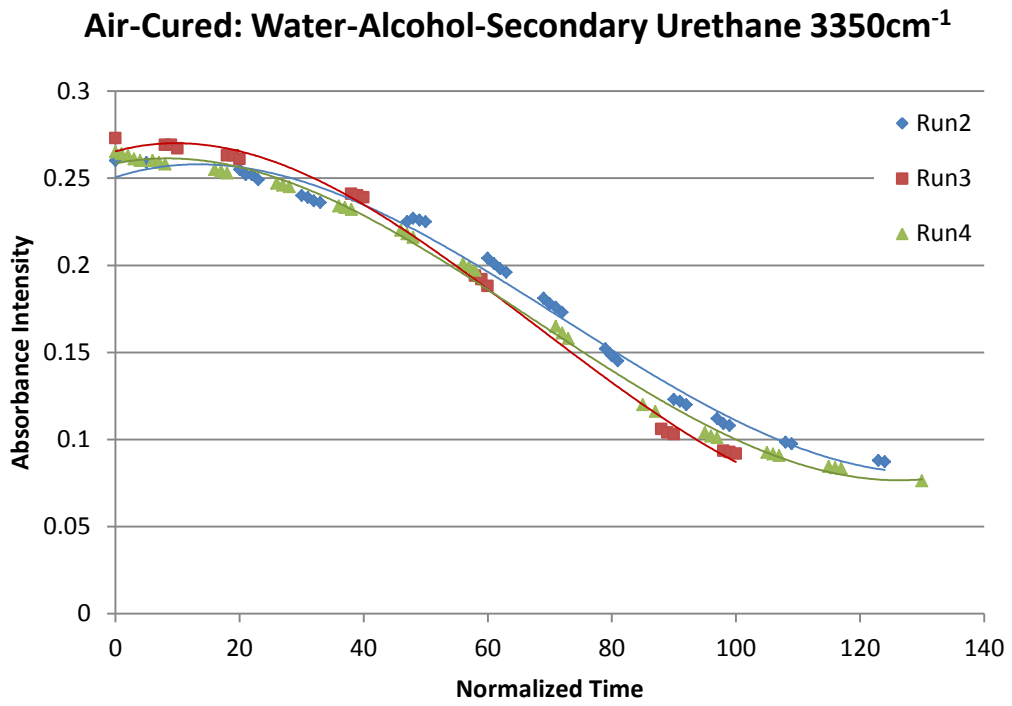

Figure 4.16: Change in absorbance vs. normalized time for the water-alcohol-secondary urethane peak at 3350cm^{-1} in air-cured GL-4850 PUR.

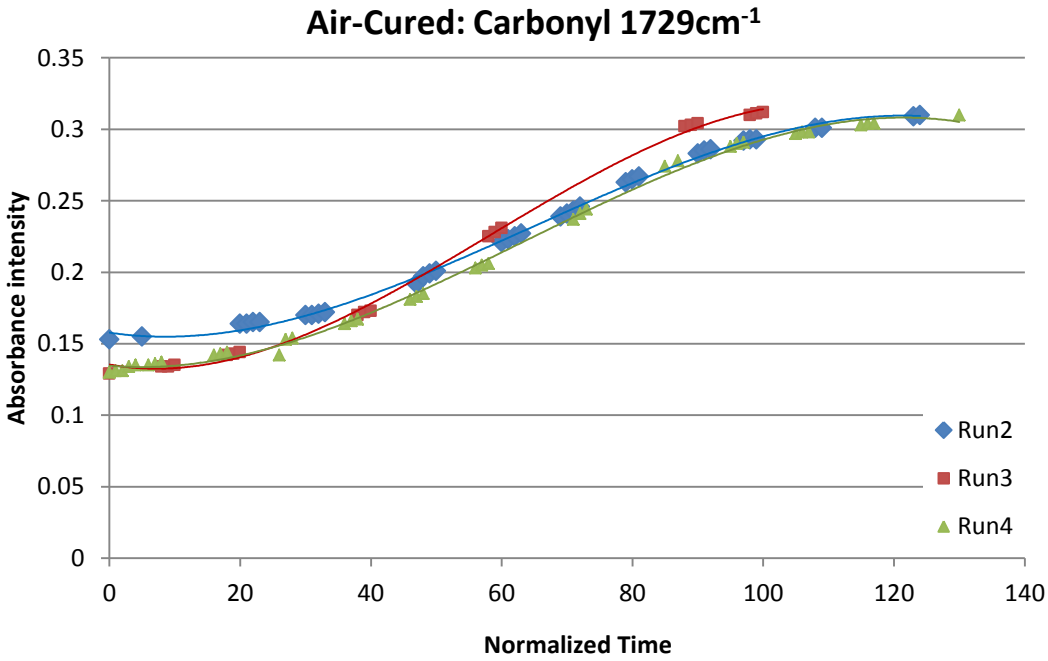

Figure 4.17: Change in absorbance vs. normalized time for the carbonyl peak at 1729cm^{-1} in air-cured GL-4850 PUR.

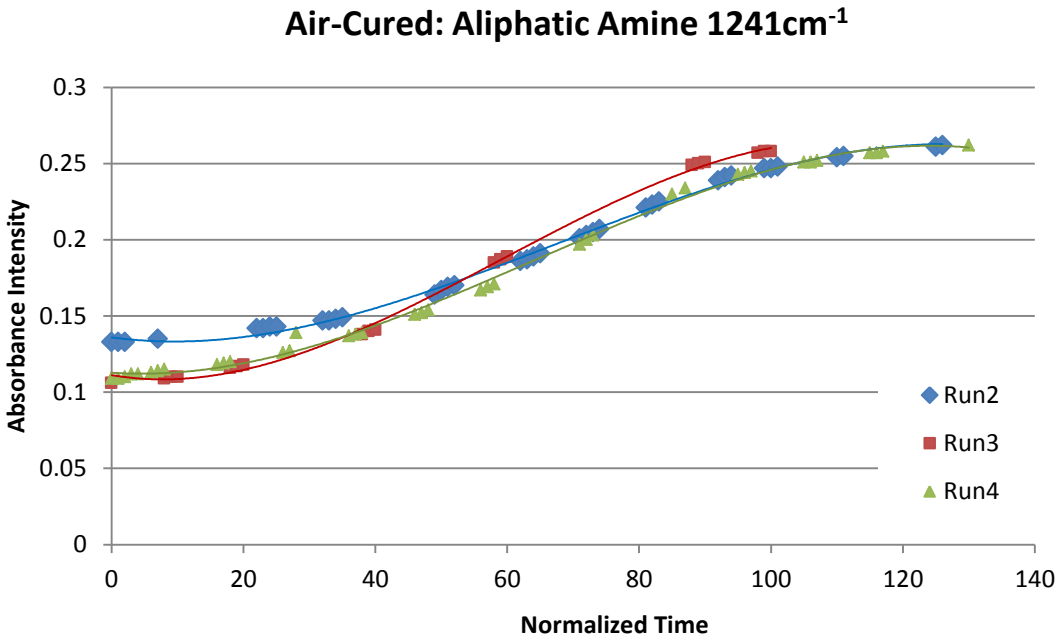

Figure 4.18: Change in absorbance vs. normalized time for the aliphatic amine peak at 1241cm^{-1} in air-cured GL-4850 PUR.

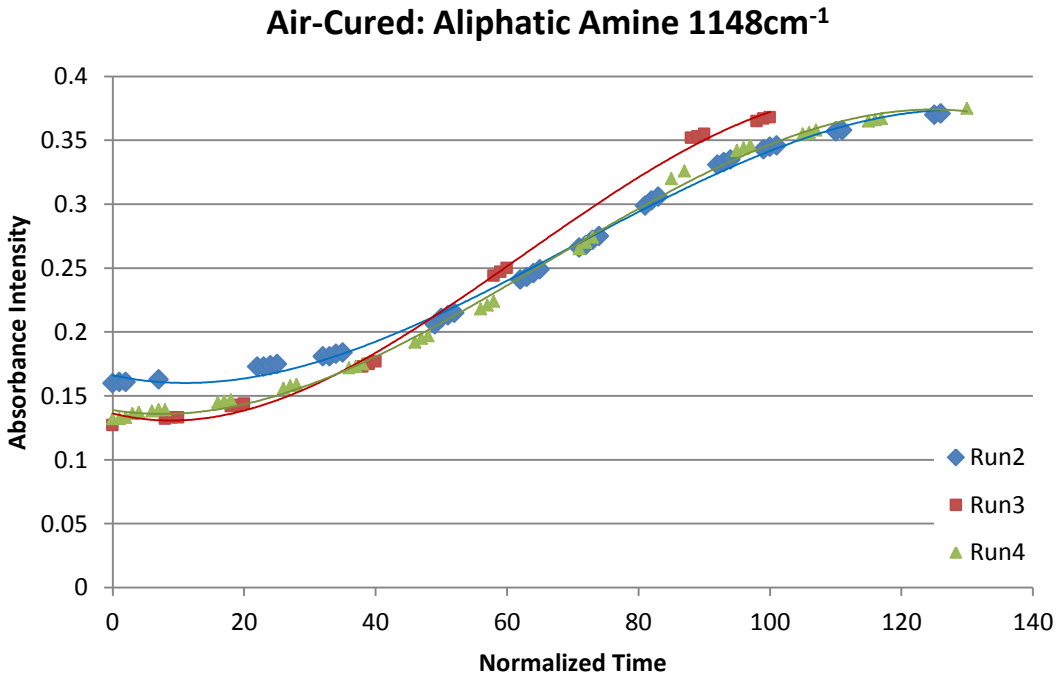

Figure 4.19: Change in absorbance vs. normalized time for the aliphatic amine peak at 1148cm^{-1} in air-cured GL-4850 PUR.

Those samples exposed to conventional heating or microwave energy show change almost immediately. This difference is believed to be due to curing occurring more uniformly over the whole sample, rather than from the top down, as in the samples processed in air. Also, the ambient environment is changed for the samples cured thermally or with microwave energy. In a true comparison of the thermal-cure and microwave-cure methods with the air-cure method, one would have to start the clock at the point where the reaction is initiated (beyond the plateau). As the length of the plateau also could be changing because of differences in thickness of the samples, tight control of the sample thicknesses may be crucial to obtaining a cured product in uniform times.

Figures 4.20 through 4.22 show the plots for absorbance versus cure time for the thermally cured samples. Note that, as the soak temperature increases, the absorbance intensities decrease for the alcohol-water-secondary urethane curves, with the 100°C reaching the lowest intensity (most cured).

The plots of the absorbance as a function of time for the samples cured with microwave energy are presented in Figures 4.23 through 4.25.

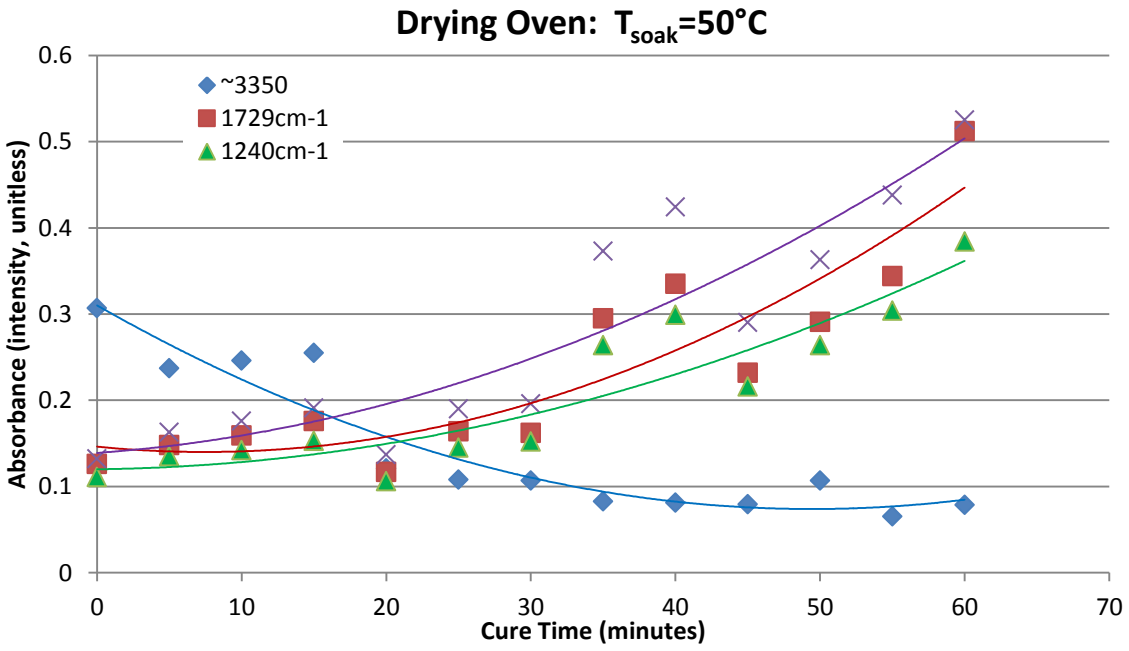

Figure 4.20: Absorbance vs. cure time for GL-4850 PUR cured at 50°C.

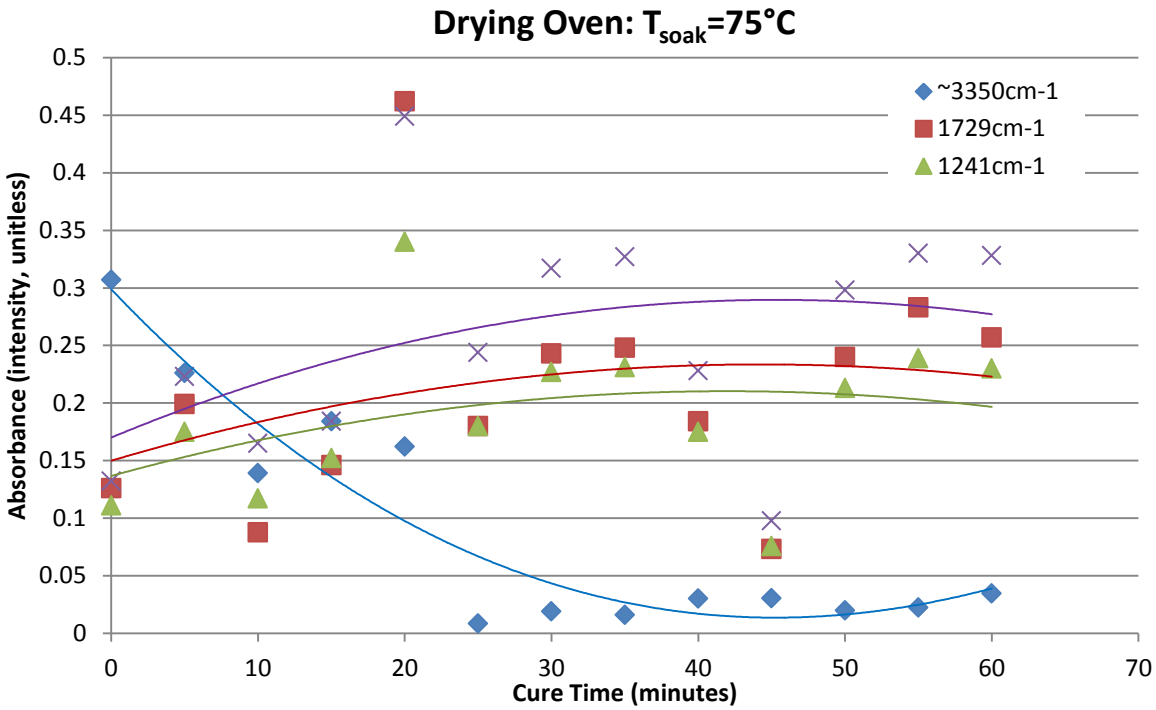

Figure 4.21: Absorbance vs. cure time for GL-4850 PUR cured at 75°C.

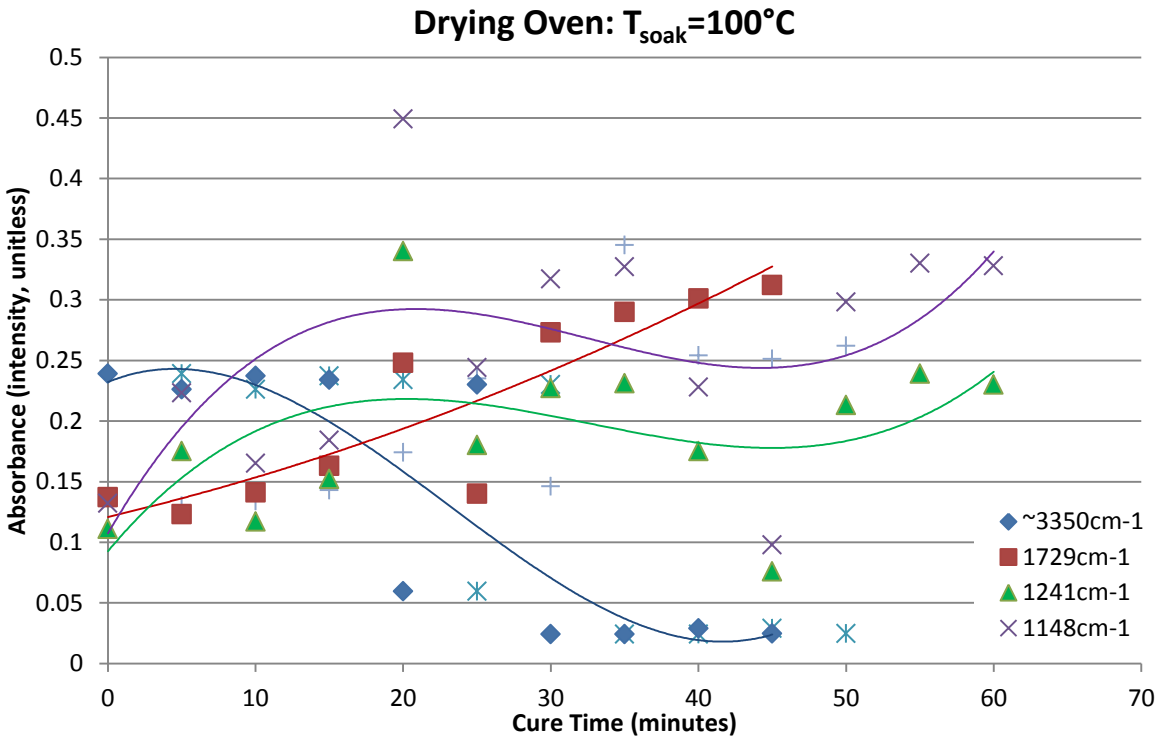

Figure 4.22: Absorbance vs. cure time for GL-4850 PUR cured at 100°C.

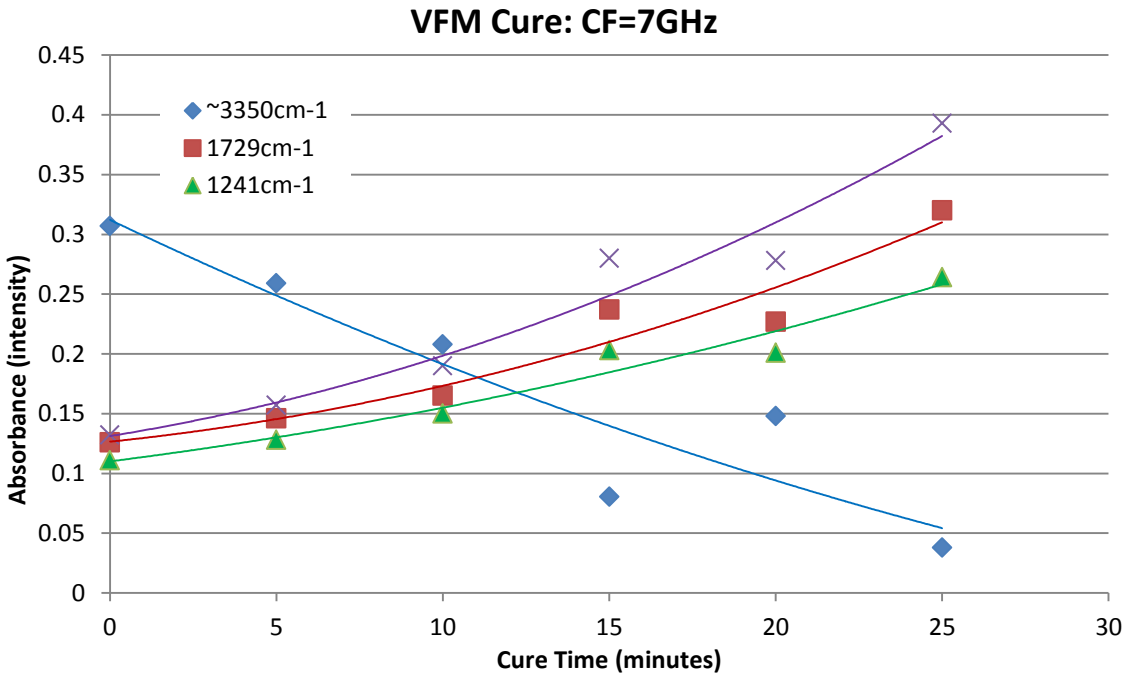

Figure 4.23: Absorbance vs. cure time for GL-4850 PUR cured at a central frequency of 7GHz with a sweep rate of 1GHz/sec.

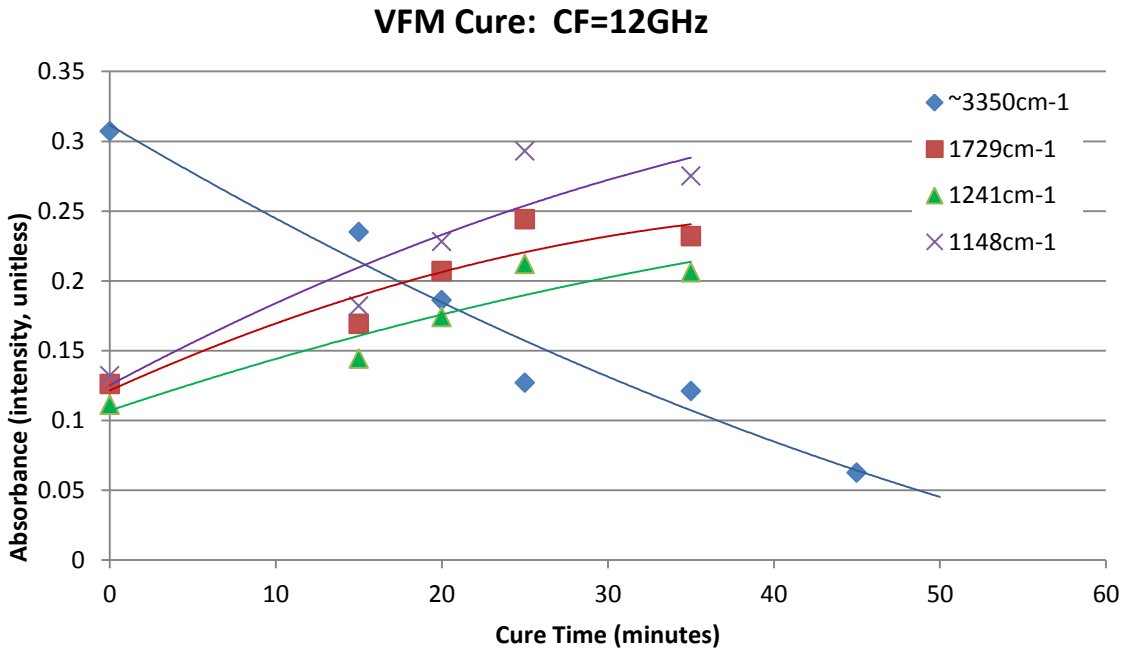

Figure 4.24: Absorbance vs. cure time for GL-4850 PUR cured at a central frequency of 12GHz with a sweep rate of 1GHz/sec.

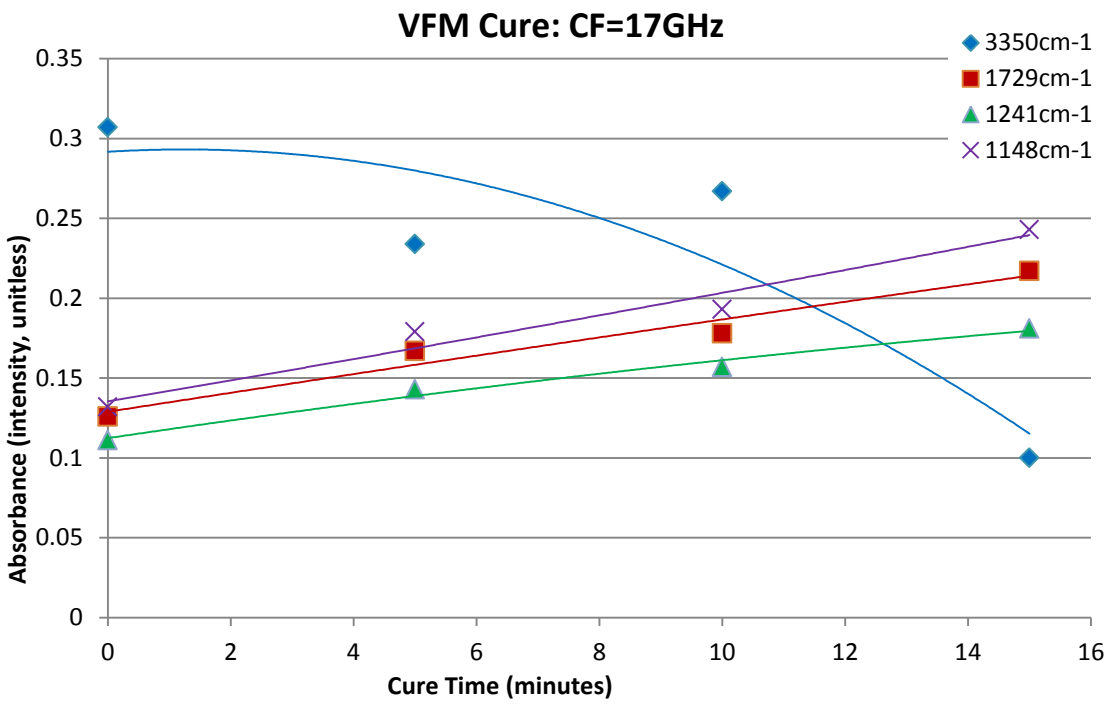

Figure 4.25: Absorbance vs. cure time for GL-4850 PUR cured at a central frequency of 17GHz with a sweep rate of 1GHz/sec.

In order to address the two goals stated in Chapter 1, the absorbance peak intensity data from the air-cured, thermally cured, and microwave-cured samples were used to generate normalized rate plots. The values for the air-cured sample intensities at 4464 minutes were used as the cured intensities (I_c) for each of the peaks. The normalized ratios (measured intensity at each peak, I_m, over I_c) were plotted as a function of time (Figures 4.26 through 4.29). The samples were considered to be cured when the ratio was equal to 1.

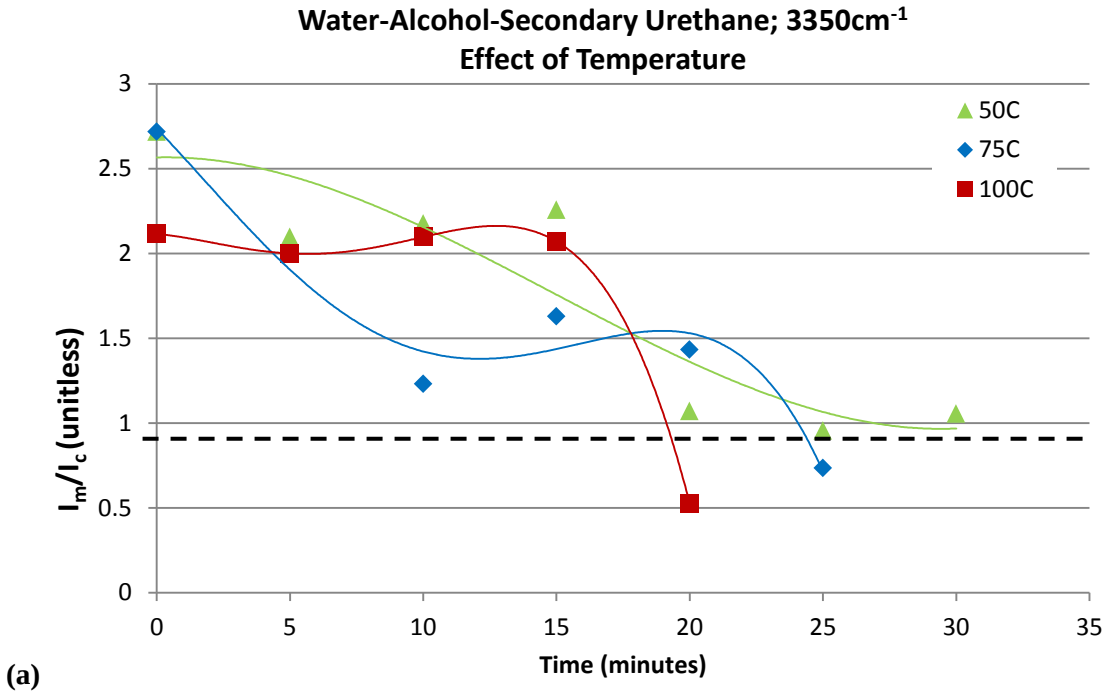

(a)

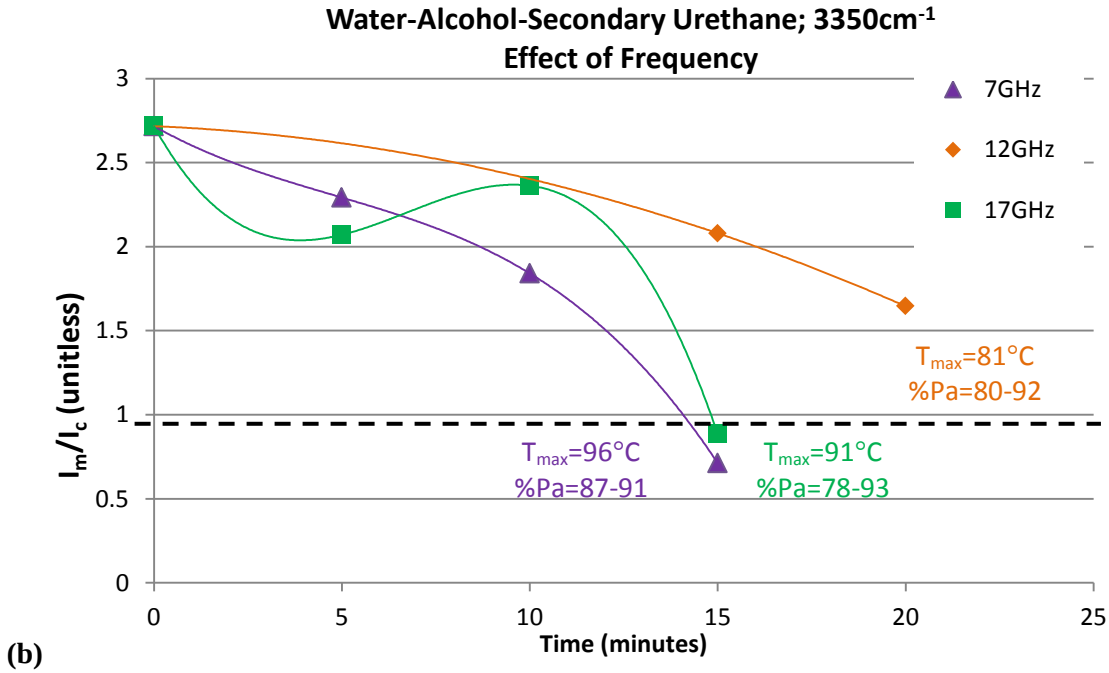

(b)

Figure 4.26: The ratio of measured absorbance intensity to intensity of cured GL-4850 PUR samples at a function of time for the broad alcohol-water-secondary urethane peak at 3350cm^{-1}: (a) effect of temperature; (b) effect of frequency.

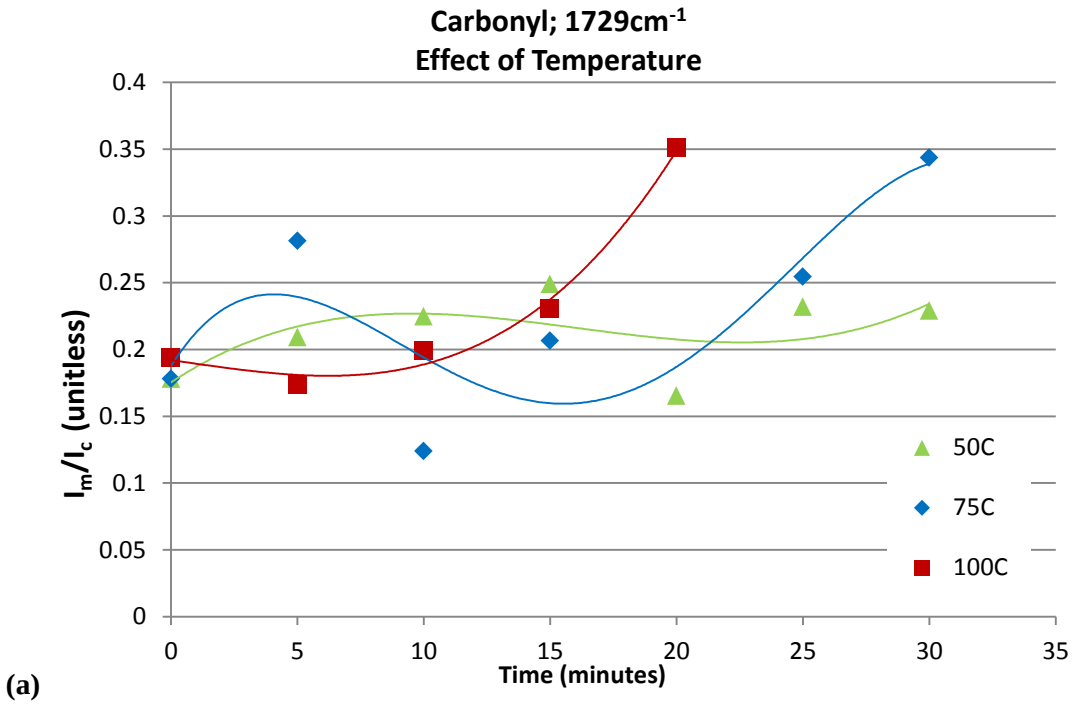

(a)

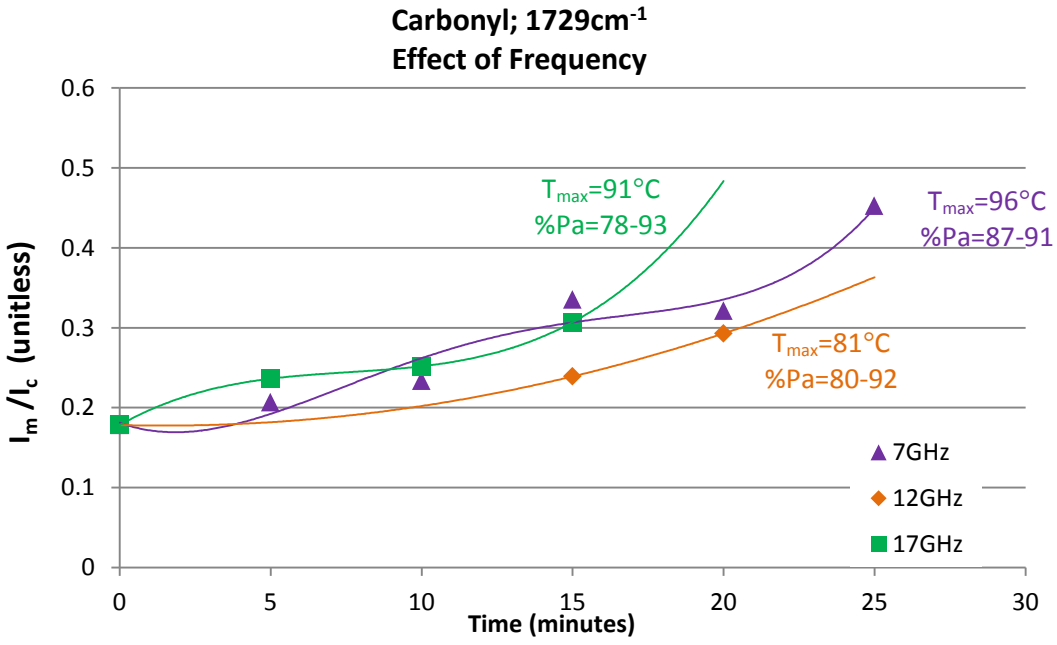

(b)

Figure 4.27: The ratio of measured absorbance intensity to intensity of cured GL-4850 PUR samples at a function of time for the carbonyl peak at 1729cm^{-1}: (a) effect of temperature; (b) effect of frequency.

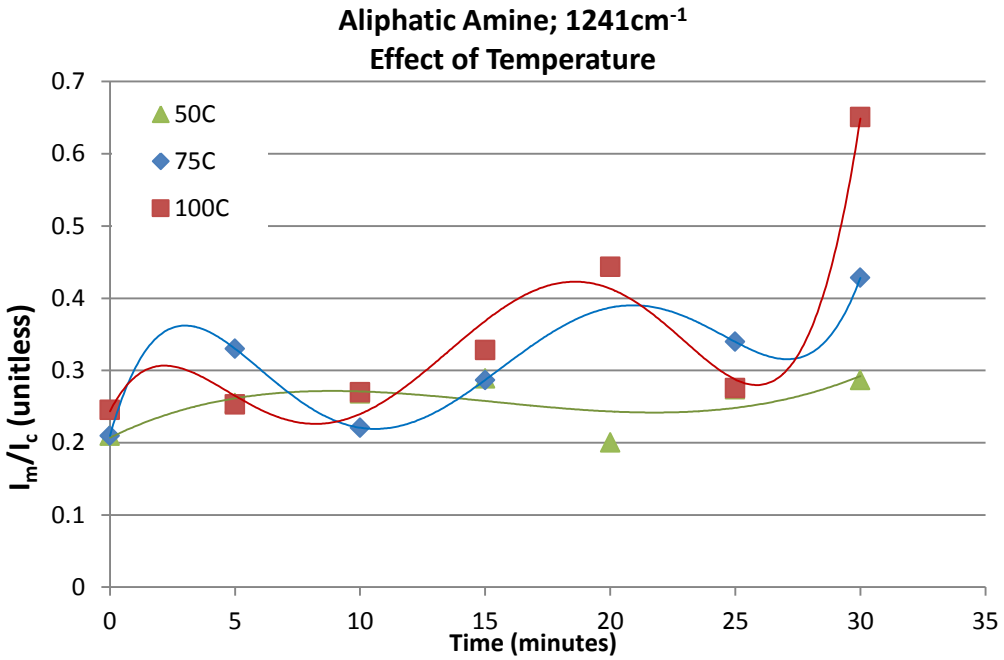

(a)

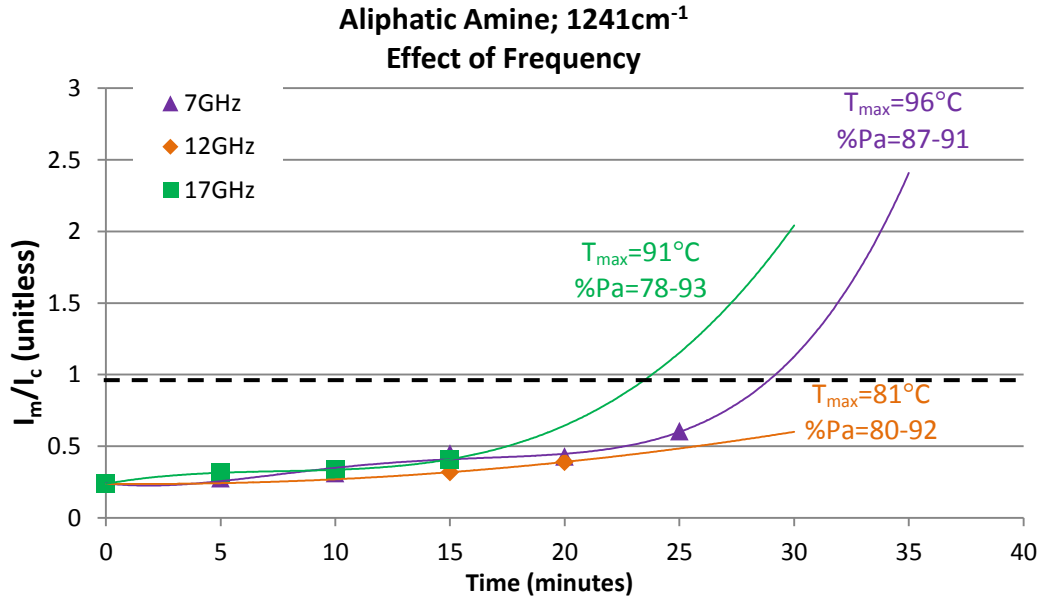

(b)

Figure 4.28: The ratio of measured absorbance intensity to intensity of cured GL-4850 PUR samples at a function of time for the aliphatic amine peak at 1241cm^{-1}: (a) effect of temperature; (b) effect of frequency.

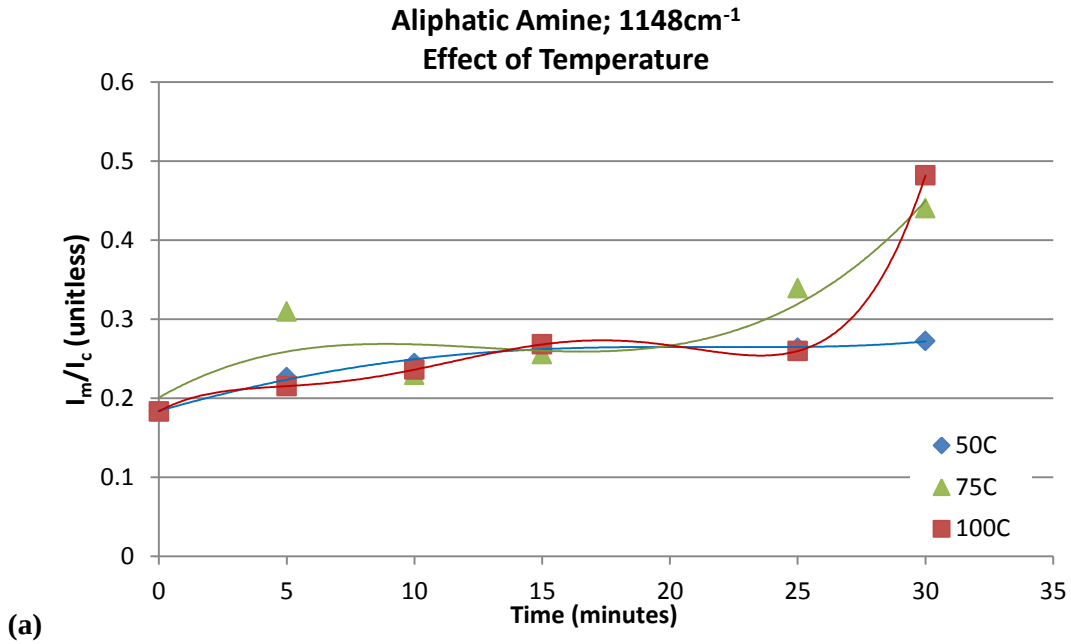

(a)

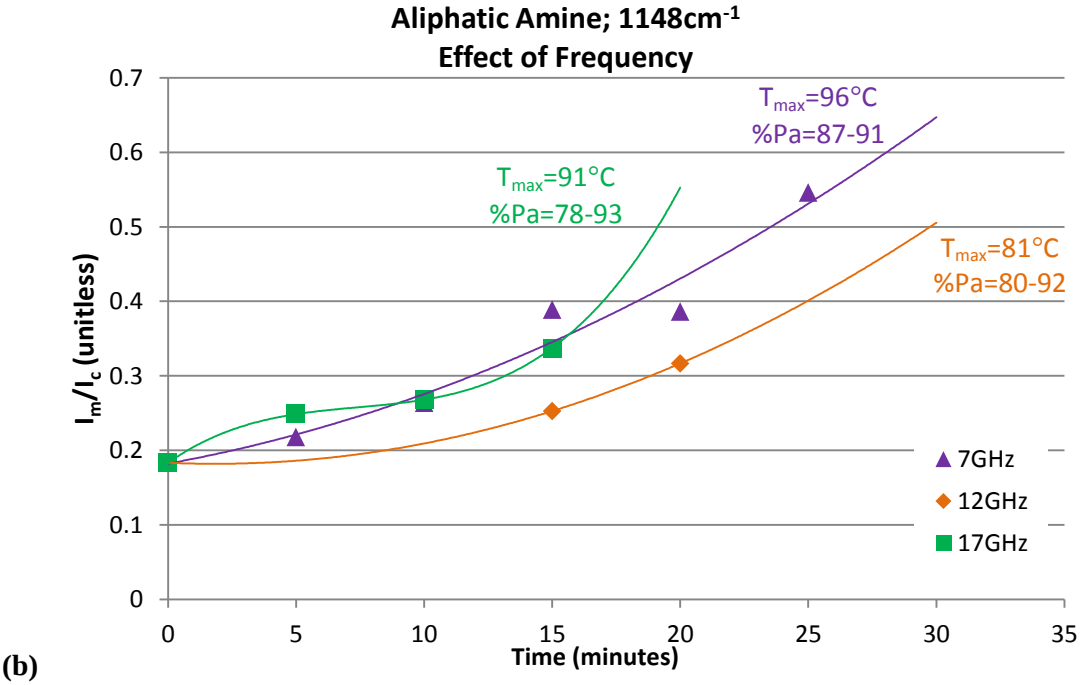

(b)

Figure 4.29: The ratio of measured absorbance intensity to intensity of cured GL-4850 PUR samples at a function of time for the aliphatic amine peak at 1148cm^{-1}: (a) effect of temperature; (b) effect of frequency.

The data presented in Table 4.2 summarizes the cure times (peak-specific) for the different process conditions, based on the plots of the intensity ratios presented in Figures 4.26 through 4.29. **Based on this data, it is possible to conclude that microwave energy, independent of temperature, did affect the cure rate in the GL-4850 PUR and that there was a microwave frequency effect on the cure rate.**

Table 4.2: Approximate cure time for each process condition (temperature, T, and frequency, *f*). Results are listed for each individual absorbance peak as the ratio of time for measured intensity to cured intensity is equal to 1, $t_{Im/Ic} = 1$.

Cure Process T (°C); f (GHz)	Approximate Cure Time (min) ($\sim t_{Im/Ic} = 1$) for Each Peak Wavenumber (cm^{-1}) and Associated Bond				Range of Cure Times per Process (min)	Cure Rate Coefficient (min^{-1})
	3350 $O\text{-}H_{str}$;$N\text{-}H_{str}$	1729 $C{=}O_{str}$	1241 $C\text{-}N_{str}$	1148 $C\text{-}N_{str}$		
50; 0*	27	88	67	>200	27- >200	0.005
75; 0	24	72	33	43	24-72	0.014
100; 0	19	38	31	35	19-38	0.026
81; 12	25	56	47	50	25-56	0.018
91; 17	15	27	23	25	15-27	0.037
96; 7	14	33	28	41	14-41	0.024

*As the TGA-DSC data showed, the 50°C samples did not cure.

With the exception of a 1 minute difference at $3350cm^{-1}$ for 7GHz, it is evident that the samples associated with the central frequency of 17GHz (91°C) resulted in the shortest cure time, as defined by $t_{Im/Ic} = 1$, and the highest cure rate at 3.4°C/min. At 17GHz, water is near its highest dielectric loss (actually highest in the range from 18 to 23GHz) [Calculator, 2009; Kaatze, 1989]. Being the primary solvent in the particular urethane composition under study, it is logical that this frequency would lead to a rapid rate in the decrease of the peak at $3350cm^{-1}$. However, it appears that this frequency also led to the fastest increase in intensity for the remaining characteristic PUR peaks at 1729, 1241, and $1148cm^{-1}$, in some cases, significantly. This result indicates that there is a frequency dependent effect on the breaking of some of the bonds present

in the wet PUR and on forming the crosslinks that lead to the cured PUR. To enable a complete study of these phenomena, the exact composition of the PUR would be required.

As expected, the samples at 100°C were cured in the shortest time of those treated thermally. In fact, it can be seen that the cure time for the thermally cured samples increased for each peak as a function of the soak temperature.

The 7 and 17GHz process conditions led to a faster cure than those at the 12GHz central frequency, and the cure times for each peak did not change consistently with frequency. Overall, the 17GHz central frequency led to the shortest cure time of all the process conditions. The 7GHz central frequency behaved almost identically for the peak at 3350cm^{-1}; however, for the remaining peaks, it was not consistent; it was close to the 17GHZ central frequencies at 1729 and 1241cm^{-1}, but closer to the 12GHz central frequency for the 1148cm^{-1} peak.

The major component of the GL-4850 was believed to have been water, so it was expected that the dielectric loss of water would be the dominant factor in the microwave-PUR interaction. This expectation is supported by the increase in dielectric loss of water with frequency at room temperature and the soak temperature for each central frequency studied (Table 4.3) [Meissner et al, 2004]. This data, combined with the data from this study that is summarized in Table 4.2, indicates that the microwave-water interaction is not the dominant reaction in the cure rate for the GL-4850 PUR.

Table 4.3: The loss tangent (a measure of the ability to absorb energy) for water at room temperature and soak temperature for each central frequency [Meissner et al, 2004].

Temperature (°C)	Central Frequency (GHz)	Loss Tangent for Water
25	7	0.34
25	12	0.57
25	17	0.78
96	7	0.17
81	12	0.29
91	17	0.41

That all of the microwave-cured samples reached temperatures that fell between 75°C and 100°C leads to a number of questions. For example, why do the 7 and 17GHz samples that reached maximum temperatures of 96 and 91°C, respectively, exhibit shorter cure times than the samples cured at 100°C? Is there an unidentified non-thermal microwave effect causing this behavior, or is there an error in the temperature measurements? Additionally, the thermally cured samples were inserted into an oven where the set-point was already achieved, while the microwave-cured samples reached the maximum temperatures recorded over the period of the sample runs. How long were these samples actually at the maximum temperatures? If they did not spend a significant portion of the experiment at the maximum temperatures, then the question of a non-thermal effect is even more relevant.

CHAPTER 5: SUMMARY AND CONCLUSIONS

The primary goals of this work were to (1) determine whether microwave energy affected the cure rate in water-based, aliphatic polyurethane when compared with conventional curing techniques, and (2) to determine whether different microwave frequencies had different effects on the cure rate.

5.1 Objectives

There were three primary objectives established as crucial to achieving the project goals. Each objective is presented below with the associated conclusion.

5.1.1 Objective 1: Establish the definition of cure for the specific polyurethane under study

For the study of GL-4850 water-based aliphatic polyurethane, **cure was established experimentally based on infrared spectroscopy data** of a sample left at ambient temperature, pressure, and relative humidity over a period of four days. Based on this method, the absorbance peak intensity for cured GL-4850 PUR was determined to be those values presented in Table 5.1. Though not all sample conditions were maintained until the samples were fully cured, the normalized rate plots allowed for an extrapolation of the curves to provide an estimate of the time to reach the cured state.

Table 5.1: Associated bonds for absorbance peaks for FTIR spectroscopy measurements, and the intensity of each peak associated with the air-cured GL-4850 PUR at a cure time of 4464 minutes.

Wavenumber of Absorbance Peak (cm^{-1})	**Associated Bonds**	**Intensity of the Peak at t=4464min (I_c, unitless)**
3350	$O\text{-}H_{str}$; $N\text{-}H_{str}$ Alcohol-water-secondary urethanes	0.113
1729	$C{=}O_{str}$ Carbonyl	0.707
1241	$C\text{-}N_{str}$	0.530
1148	$C\text{-}N_{str}$	0.730

5.1.2 Objective 2: Establish the microwave processing method and parameters and conduct processing experiments

Since the primary interest in using microwave energy for curing this specific polyurethane was for use in curing the coatings on wood products, specifically musical instruments, it was determined that multimode microwave techniques should be used for all experimental work. This decision was based on the fact that single-mode microwave cavities are very small (decreasing in size considerably as the frequency is increased) and impractical for the application of interest. Additionally, while the single-mode technique offers an excellent method for researching the interaction of microwave energy with materials, it does not allow for rapid transfer of samples from the cavity to the characterization instrument. Since this study was to determine rates, the timing of transferring the samples from the microwave cavity to the FTIR spectrometer was critical. Furthermore, since most multimode microwave ovens make use of magnetrons, a fixed frequency microwave generator, **a Variwave® Variable Frequency Microwave oven using a traveling wave tube as the generator was selected to enable a study of the effects of frequency on the cure rate.**

The Variwave® offered a frequency range from 6 to 18GHz, as well as the potential for sweeping a desired bandwidth in the frequency range in order to maximize the uniformity of the microwave field distribution in the cavity. **Central frequencies of 7, 12, and 17GHz were selected** so that the effects of frequencies on cure rate across the entire range of the oven could be evaluated. **A bandwidth of 1GHz was swept each second**, making the ranges for the frequency distribution in the cavity of 6.5 to 7.5GHz, 11.5 to 12.5GHz, and 16.5 to17.5GHz.

In order to determine whether microwaves had an effect on the cure rate over other methods of cure, additional experiments were conducted using air curing and thermal curing methods. Curing in air was performed over a time of approximately four days at ambient temperature, pressure, and relative humidity. Thermal curing was conducted at 50, 75, and 100°C for soak periods of 60 minutes.

5.1.3 Objective 3: Identify the characterization and/or testing technique(s) to evaluate the effect of microwave irradiation on the cure rate of polyurethane

To identify the anticipated phase changes that could occur in the polyurethane as it cured, thermal analyses was conducted using thermogravimetric analysis (TGA) and differential scanning calorimetry (DSC). Using these methods, the weight loss and heat flow as a function of temperature could be followed in the sample material, and the data compared to that obtained in thermal curing experiments. Isometric studies at cure temperatures of 50, 75, and

100°C were carried out using these thermal analysis methods. However, TGA and DSC studies could not be performed using microwave curing as these instruments are not available commercially.

Fourier transform infrared (FITR) spectroscopy, in conjunction with Horizontal Attenuated Total Reflectance (HATR), was used to follow three peaks identified as characteristic of water-based, aliphatic polyurethanes: the broad water peak at approximately 3450cm^{-1} [Barnes, 2002]**; the carbonyl peak at 1729cm^{-1}** [Smith, 1990]**; the aliphatic amine peaks at 1241cm^{-1} and 1148cm^{-1}** [Smith, 1990]**.**

Since the HATR-FTIR was selected as the primary characterization tool for these experiments, considerable time was dedicated to understanding the system and in developing the procedures for using it to determine the extent and rate of cure. The versatility, simplicity of sample preparation, and amount of information that was possible was understood generally, but this research led to a much better working knowledge of the FTIR spectrometer.

The HATR-FTIR method is very robust, capable of generating FTIR spectra for a wide range of sample types, including powder compacts, films, and liquids. By understanding the need for good sample/crystal contact, a strong signal-to-noise ratio can be maintained and errant measurements can be avoided. For different types of materials, the crystal composition can be altered to one with a different index of refraction. For example, if a germanium (Ge) crystal is substituted for the ZnSe, the refractive index is increased (4 versus 2.4, respectively) and the depth of penetration of the evanescent wave into the sample material is decreased. This change in the depth of penetration decreases the pathlength of the wave, translating into a decrease in the magnitude of the transmitted beam. There are other reasons for choosing one crystal composition over another, such as the reactivity of the particular composition with the sample material and the index of refraction of the sample material.

5.2 Primary Goals/Conclusions

5.2.1 Goal 1: Determine whether microwave energy affected the cure rate in water-based, aliphatic polyurethane when compared with conventional curing techniques

The normalized rate plots indicate that the microwave energy can cause an increase in the cure rate at lower temperature and time for some frequencies, as compared to thermal curing. As shown in Table 4.2, the samples microwave-cured at 17GHz, followed by those cured at 7GHz, achieved higher cure rates than those cured using any of the process conditions, based on the time required to reach a ratio of the measured intensity to the cured intensity equal to one (achieved for

air curing at 4464 minutes; I_m/I_c=1). Therefore, **the results of this study indicate that microwave energy does affect the cure rate in the samples.**

5.2.2 Goal 2: Determine whether different microwave frequencies had different effects on the cure rate.

The results in Table 5.2 show **significantly different results for cure time based on the VFM central frequency**. The cure times for the 12GHz central frequency were quite long; they were relatively close to the 75°C thermal cure, even though the temperature achieved at 12GHz was higher (81°C vs. 75°C). The 17GHz cure time was faster than all the other conditions and, while the cure time at 7GHz was faster for the peak at 3350cm^{-1}, the very small difference of 1 minute could have resulted from error in the FTIR data.

The power ranges for the different frequencies also indicate some differences in the efficiency of the processes based on VFM curing (Table 5.2). Although the cure time was shortest for the 17GHz central frequency, the percent of power absorbed (%P_a) varied significantly throughout the experiment (15%), with the temperature reaching as high as 91°C. The maximum temperature for the central frequency of 7GHz was 96°C, with a variation in %P_a of only 4%. This result is quite interesting, given that the variation in the cure times versus wavenumber was significantly higher for the 7GHz frequency than for 17GHz. The 12GHz central frequency resulted in a 12% variation in the %P_a and a maximum temperature of only 81°C, indicating a much less efficient process condition, especially for cure times of about twice those of the 17GHz samples.

Table 5.2: Power absorption and maximum temperature achieved for each central frequency.

Central Frequency (CF; GHz)	**Power Absorbed (P_a*; W)**	**Average P_a* (W)**	**%P_a**	**Max. Temp. (T_{max}; °C)**	**Cure Time (min)**
7	49-62	55.5	87-91	96	25-56
12	21-22	21.5	80-92	81	15-25
17	37-66	51.5	78-93	91	14-41

*The power absorbed in this table does not incorporate the volume of the sample material. These values are based on the forward power minus the reverse power (values provided in Table 4.1).

Graphical representations of the data in Table 5.2 are provided in Figures 5.1 and 5.2. Equation (2.6) says that the rate of temperature increase is proportional to the power

absorbed. Figure 5.1 shows that the maximum temperature and the average power absorbed per unit area follow the same trend - higher for 7 and 17GHz and lower for 12GHz. Given the variation in the data for 7 and 17GHz, the data behaves according to that predicted by the equation.

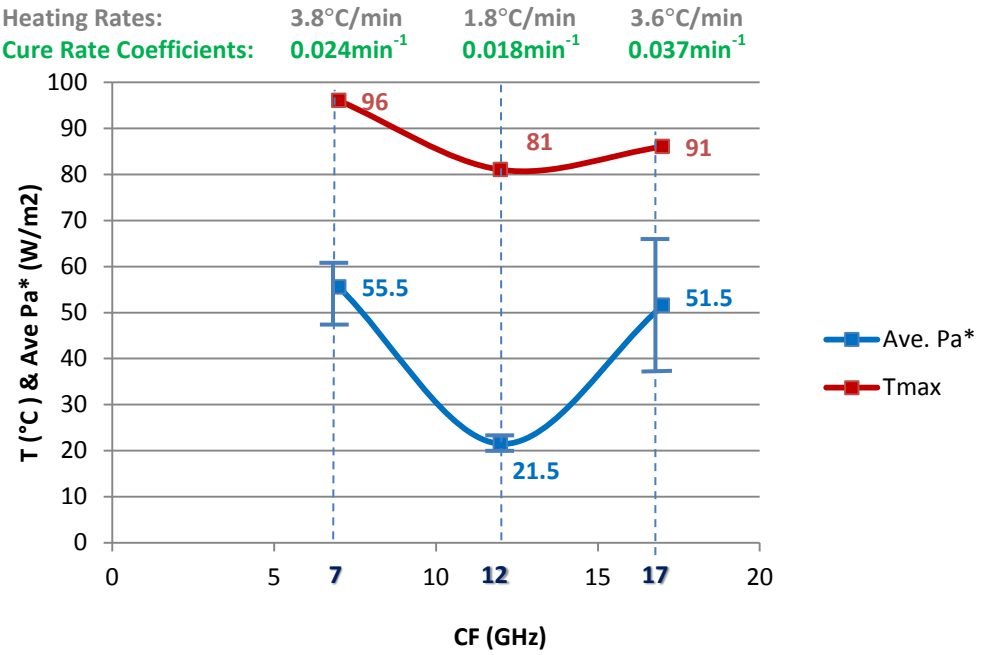

Figure 5.1: Average value for Pa* and maximum temperature, both as functions of central frequency.

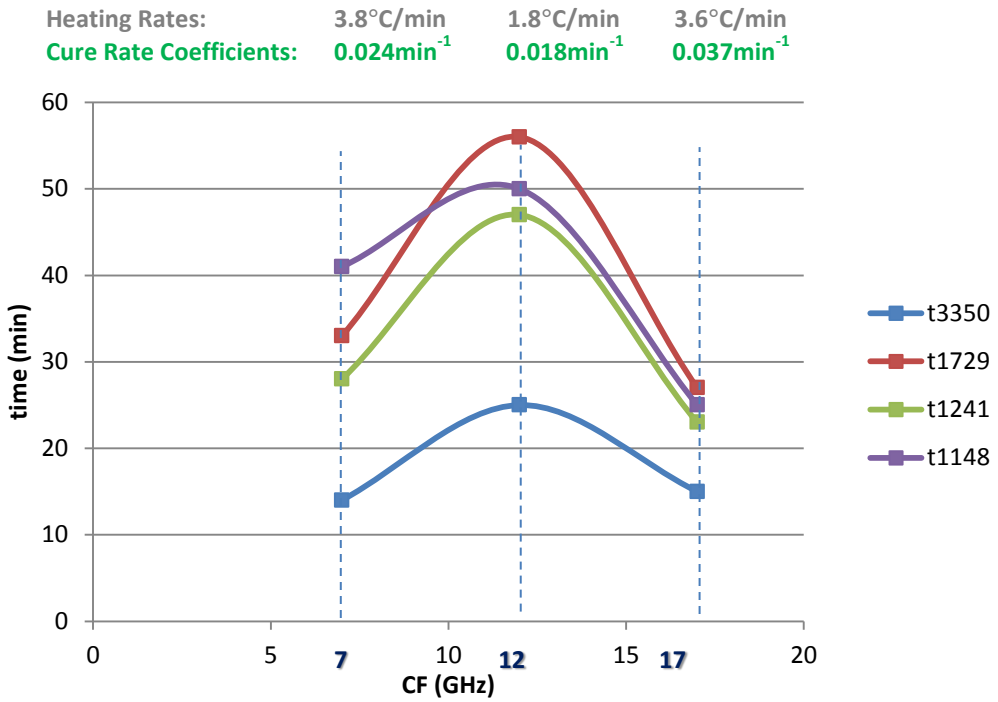

Figure 5.2: Cure time for each peak as a function of central frequency.

The plot in Figure 5.2 shows the relationship in the time required to achieve cure in each of the peaks studied. The peaks show the same order of cure for the peaks for all the central frequencies, with the notable exeption of the peak for 1148cm^{-1} at 7GHz. Here, the cure requires a longer time than either the carbonyl peak at 1729cm^{-1} or the associated aliphatic peak at 1241cm^{-1}. The data in Figure 5.2 indicates that (1) the frequency does have an effect on the cure rate, and (2) that the microwave frequency-molecular bond interactions are not the same for each of the frequencies studied.

In summary, all of the goals and objectives of this Master's study have been achieved:

Goals:

1. **Microwave energy has been shown to effect the cure rate in GL-4850 water-based, aliphatic polyurethane.**
2. **Different microwave frequencies have been shown to have different effects on the cure rate in GL-4850 water-based, aliphatic polyurethane.**

Objectives:

1. **A water-based, aliphatic polyurethane was selected for the study and characteristic peaks were identified for the composition.**
2. **Thermal and microwave cure parameters were established and an experimental procedure developed to address the goals for the project.**
3. **Fourier transform infrared spectroscopy (FTIR) was selected as the primary tool for evaluating the cure rates associated with each processing parameter. An in-depth study was performed on FTIR methods, especially attenuated total reflectance (ATR) techniques, for determining cure rates in an infrared-absorbing polymer.**

5.3 Future Work

While the goals of this study were met, as with most research projects, more questions are asked than were answered! Therefore, some recommendations for future work that would enhance the body of knowledge are provided below.

Coating Composition

There are a couple of recommendations with respect to the composition of the PUR. First, there are thousands of compositions of polyurethane available commercially. The GL-4850 represents only one of these. It would be helpful to study the cure rates in different classes of PURs (i.e. aromatic versus aliphatic, solvent-based versus water-based) to determine whether the microwave energy has different effects on the components that serve as the basis for these various compositions. The experiments also should be taken out to longer times to determine more accurately the time for complete cure for each process condition.

In addition to studying the effects of the components, it would be a natural extension of this work to conduct a materials design experiment in which the optimum composition for a microwave-curable wood coating is the major goal.

Characterization

In situ Characterization

Investigating the polymer coating is the first step to understanding and controlling the microwave curing process; however, by studying the effects of microwave curing of the coating as applied to the intended substrate may yield additional vital information regarding the

feasibility of using the process industrially. The effects of the microwave energy can be altered by the addition of a substrate, based on how the substrate material interacts with the microwaves.

Microwave Thermal Analyses

The study of cure rates in polymer materials could be enhanced if methods for conducting thermal analyses under the influence of a microwave field could be conducted. As the results of this study show, the frequency also affects the cure rate, so it would be beneficial for this method to be useful over a range of frequencies.

Dielectric Properties

The relationship between microwave absorption and dielectric properties is fundamental to microwave processing of materials. Measuring the dielectric loss of the coating material across a range of frequencies and temperatures is crucial if the coating composition is to be optimized for microwave curing. The results of these experiments show that the cure rate does not appear to increase or decrease with frequency. A study of the dielectric properties of a known composition of the PUR may be able to address this result. Also, by understanding the relationship between the various components of the composition and the dielectric loss of the resulting coating material, the microwave absorption could be tailored to absorb more or less than the substrate on which it is applied.

Mechanical and Physical Properties

No matter what the application for the coating, its performance over its expected/desired service life will be a key to commercialization of the material and/or the process. For the application as a coating on instrument-grade woods, properties including stiffness, scratch resistance, glossiness must be measured to determine whether the microwave process can improve the coating performance. In future work, these properties should be prioritized and measurements made to determine the effects of the microwave process.

Investigate Green Engineering Issues

As described in Chapter 1, motivations for moving toward the use of water-based, aliphatic urethanes include cost and environmental factors. Recall that the particular application for which this urethane is being investigated is that of a coating material for high-grade woods for musical instruments. Taylor Guitar Company has led the way in developing new coatings and coating processes for this application; however, they always are in search of the next new improvement

that can be made to their product and production operations [Guzzetta and Baldwin, 2008]. As a continuation of this research study, an evaluation is underway of some of the advantages and disadvantages associated with water-based, aliphatic polyurethane versus a polyester resin and with changing from an ultraviolet curing method to one that uses microwave energy.

The Coating Material

The current material used by the guitar company participating in this study is a UV-curable polyester resin [Guzzetta and Baldwin, 2011]. For many UV-cured wood coatings, the advantage of a 100% solids composition is the ability to recover over-spray and re-introduce, what would once have been waste, back into the process front-end for re-use. However, the particular polyester resin used by Taylor Guitars contains about 20% materials that irreversibly change phase once exposed to UV radiation. Although the remaining solids could be re-used, by putting them back into the coating feed, the composition would be altered significantly and the coating would no longer be optimal, aesthetically or acoustically, for application for which it was designed.

All that said, it is no small task to change the coating materials! Candidate compositions for a replacement coating must meet or exceed the aesthetic, acoustic, cost, and environmental criteria established for the products. Also, the new coatings ideally could be applied using the current robotic coating method in which the company has invested heavily.

The Curing Process

The first question one might ask when considering at all the possible methods for curing the coatings is, "Why not just use an air cure?" While at first thought this might seem like a reasonable suggestion, one only need look at the costs associated with leaving large volumes of product in an environmentally controlled building for weeks while the curing process is complete to know that it is not a viable option. The current manufacturing and storage buildings cost approximately $100K/month each to maintain. With anywhere from 200 to 500 instruments produced each day, the costs would be prohibitive for a large manufacture.

Over the course of the investigation, the value associated with a complete on-site cure via microwave energy, the financial costs associated with refitting the manufacturing operation and training employees, and other issues associated with changing from UV to microwave processing will be considered.

BIBLIOGRAPHY

Acierno, D., M. Frigione, V. Fiumara, D. Napoli, I.M. Pinto, M. Ricciardi, "Thermal and Dielectric Properties of Thermal and Microwave Cured Thermoset Polymers," in *Materials Research Innovations* (1998) **2,** pp. 28-32.

Alger, M., *POLYMER SCIENCE DICTIONARY*, 2nd ed. (1997) Chapman & Hall, London, UK, [ISBN: 0 412 60870 7].

Allen, M., *THE COMPLETE GUIDE TO WOOD FINISHES*, 2nd ed. (2006) Quarto Publishing, Inc., New York, NY [ISBN: 0 7432 8487 5].

Andor Technology, "Absorption / Transmission / Reflectance (ATR) Spectroscopy," Learning Center Documents, http://www.andor.com/learning/applications/ATR_Spectroscopy/, (accessed July 2011).

Ayres, E., W.L., Vasconcelos, R.L. Oréfice, "Attachment of inorganic moieties onto aliphatic polyurethanes," *Materials Research* (2007) **10** [2] 119-125.

Barnes, M., "Fourier Transform Infrared Spectroscopy," Technical Notes, *Machinery Lubrication Magazine*, March 2002, http://www.machinerylubrication.com/Read/305/fourier-transform-infrared-spectroscopy, (accessed May 2011).

Bauer, D.R., "Network Formation and Degradation in Urethane and Melamine-Formaldehyde Cross-linked Coatings," in *American Chemical Society Symposium Series* (1988) **367** pp. 77-92.

Brundle, C.R., C.A. Evans, Jr., S. Wilson, *ENCYLOPEDIA OF MATERIALS CHARACTERIZATION* (2002) Butterworth-Heinemann (Elsevier), Oxford, UK [ISBN: 13: 978 7506 9168 0].

Campbell, D., R.A. Pethrick, J.R. White, *POLYMER CHARACTERIZATION: Physical Techniques*, 2nd ed. (2000) Stanley Thornes Ltd., Glos. UK [ISBN: 0 7487 4005 8].

Carlson, G.M., C.M. Neag, C. Kuo, T. Provder, "FT-IR and Thermo-mechanical Cure Characerization of Blocked Isocyanate Containing Coatings," in *Polymer Science and Technology* (1984) **36**, pp. 197-212.

Chan, T.V.C.T., H.C. Reader, *UNDERSTANDING MICROWAVE HEATING CAVITIES*, (2000) Artech House, Norwood, MA [ISBN: 1 58053 094 X].

Clark, D.E., D.C. Folz, "What is Microwave Processing?" in *MICROWAVE SOLUTIONS FOR CERAMIC ENGINEERS* (2005) pp. 1-32 [ISBN: 1 57898 224 9].

Clark, D.E., W.H. Sutton, "Microwave Processing of Materials," *Annual Review of Materials Science* (1996) 26, pp. 299-331.

Calculator for the Complex Dielectric Constant of Water, http://www.random-science-tools.com/electronics/water_dielectric.htm, (accessed June 2011), based on "The Complex Dielectric Constant of Pure and Sea Water from Microwave Satellite Observations," T. Meissner, F. Wentz, IEEE Transactions on Geoscience and Remote Sensing (2004) 42 [9] pp. 1836-1849.

Cox, J.N., "Fourier Transform Infrared Spectroscopy," in *ENCYCLOPEDIA OF MATERIALS CHARACTERIZATION* (1992) pp. 416-427 [ISBN: 0 7506 9168 9].

Dias, R.C.M., A.M. Goes, R. Serakides, E. Ayres, R.L. Oréfice, "Porous, biodegradable polyurethane nanocomposites: preparation, characterization, and biocompatibility tests," *Materials Research* (2010) **13** [2] 211-218.

Dictionary.com, on-line dictionary, http://dictionary.reference.com, (accessed June 2011).

Fathi, Z. *SURFACE MODIFICATION OF SODIUM ALUMINOSILICATE GLASSES USING MICROWAVE ENERGY* (1994), dissertation submitted to the University of Florida.

Fathi, Z., R.S. Garard, J. Clemmons, G. Saltiel, R.M. Hutcheon, M.T. DeMeuse, "Processing and Characterization of a Polymer Matrix Composite Using Variable Frequency Microwave Heating," *Ceramic Transactions* (1995) **59**, pp. 441-456.

Flinn, R.A, P.K. Trojan, *ENGINEERING MATERIALS AND THEIR APPLICATIONS*, 2nd ed. (1981) Houghton Mifflin Co., Boston, MA [ISBN: 0 395 29645 5].

Folgar, C.E., *STRUCTURAL EVOLUTION OF SILICA AEROGEL UNDER A MICROWAVE FIELD* (2010), dissertation submitted to Virginia Polytechnic Institute and State University.

Fried, J.R., *POLYMER SCIENCE AND TECHNOLOGY* (1995) Prentice-Hall, Inc., Englewood Cliffs, NJ [ISBN: 0 13 685561 X].

Garard, R.S., Z. Fathi, J.B. Wei, "Materials Processing via Variable Frequency Microwave Irradiation," *Ceramic Transactions* (1995) **59**, pp. 117-124.

George, C.E., G.R. Lightsey, A.G. Wehr, "Microwave Processing of Polymers and Biomass Materials," *Materials Research Society Symposia Proceedings* (1988) **124**, pp. 189-194.

Guzzetta, M., S. Baldwin, Taylor Guitar Company, direct communication - technical meetings and site visit, January 2008.

Guzzetta, M., S. Baldwin, Taylor Guitar Company, direct communication - technical meetings and site visit, June 2011.

Hench, L., J. West, *PRINCIPLES OF ELECTRONIC CERAMICS* (1990) John Wiley & Sons, Inc., New York, NY [ISBN: 0 471 16182 17].

Hudson, A., R. Nelson, *UNIVERSITY PHYSICS* (1982) Harcourt Brace Jovanovich, Inc., New York, NY [ISBN: 0 15 59260 7].

Kaatze, U., "Complex Permittivity of Water as a Function of Frequency and Temperature," *Journal of Chemical Engineering* (1989) **34** pp. 371-374.

Kirchhoff, G., "On the relationship between the radiation and absorbing powers of different bodies for light and heat," *Philosophical Magazine and Journal of Science*, Series 4, July 1860.

Lambda Technologies, Inc., www.microcure.com (accessed May 2011).

Li, S., R. Vatanparast, H. Lemmetyinen, "Cross-linking kinetics and swelling behavior of aliphatic polyurethanes," *Polymer* (2000) 41 pp. 5571-5576.

Martin Guitar Company, Plant Tour, June 2007.

Meier-Westhues, U., *POLYURETHANES – Coatings, Adhesives and Sealants* (2007) Vincentz Network GmbH & Co. KG, Hannover, Germany [ISBN: 3 87870 334 1].

Meissner, T., F.J. Wentz, "The Complex Dielectric Constant of Pure and Sea Water from Microwave Satellite Observations," IEEE Transaction on Geoscience and Remote Sensing (2004) **42**[9] pp. 1836-1849.

Menczel, J.D., R.B. Prime, *THERMAL ANALYSIS OF POLYMERS: FUNDAMENTALS AND APPLICATIONS* (2009) John Wiley & Sons, Inc., New York, NY [ISBN: 978 0 471 76917 0].

MERRIAM-WEBSTER'S COLLEGIATE DICTIONARY, 11th ed. (2003) Merriam-Webster, Inc., Springfield, MA.

Metaxas, A.C., R.J. Meredith, *INDUSTRIAL MICROWAVE HEATING* (1993) Peter Peregrinus Ltd., London, UK [ISBN: 0 906048 89 3].

Mirabella, F.M., *INTERNAL REFLECTION SPECTROSCOPY: THEORY AND APPLICATIONS* (1993) Marcel Dekker, Inc., New York, NY [ISBN: 0 8247 8730 7].

Mirabella, F.M., *MODERN TECHNIQUES IN APPLIED MOLECULAR SPECTROSCOPY*, (1998) John Wiley & Sons, Inc., New York, NY [ISBN: 0 471 12359 5].

Moore, G.R., D.E. Kline, *PROPERTIES AND PROCESSING OF POLYMERS FOR ENGINEERS* (1984) Prentice-Hall, Inc., Englewood Cliffs, NJ [ISBN: 0 13 731125 7].

Netzsch Corporation, STA 449 F3 Jupiter® - product brochure, http://www.netzsch-thermal-analysis.com/en/products/detail/pid,43,t,6.html (accessed April 2011).

Newport Corporation Technical Notes, www.newport.com (accessed May 2011).

New World Encyclopedia, http://www.newworldencyclopedia.org/ (accessed July 2011).

Pozar, D.M., *MICROWAVE ENGINEERING*, 3rd ed. (2005) John Wiley & Sons, Inc., Danvers, MA [ISBN: 0 471 44878 8].

Rabek, J.F., *EXPERIMENTAL METHODS IN POLYMER CHEMISTRY – Physical Principles and Applications* (1980) John Wiley & Sons Ltd., New York, NY [ISBN: 0 471 27604 9].

Rains, R.C., "Structural Adhesive Curing for Bonding Composites, Thermosets and Thermoplastics," *Materials Research Society Symposia Proceedings* (1988) **124** pp. 323-328. John Wiley & Sons Ltd, New York, NY [ISBN: 0 470 85041 8].

Radice, S., S. Solexis, M. Bradley, "Time-based FT-IR Analysis of Curing of Polyurethanes," *Thermo Fisher Application Note*: 51255, www.thermoscientific.com, (accessed November 2010).

Randall, D., S. Lee, *THE POLYURETHANES BOOK* (2002) John Wiley & Sons Ltd. [ISBN: 0 470 85041 8].

Schiffmann, R., "Principles of Industrial Microwave and RF Heating," *Ceramic Transactions*, **80**:41-60 (1997).

Simonis, J., Thermo Electron Corporation LLC, electronic communication (July 11, 2011).

Smith, B. *INFRARED SPECTRAL INTERPRETATION: A Systematic Approach* (1990) CRC Press, New York, NY [ISBN: 0 8493 2463 7].

Smith, B. *FUNDAMENTALS OF FOURIER TRANSFORM INFRARED SPECTROSCOPY* (1996) CRC Press, New York, NY [ISBN: 0 8493 2461 0]

Socrates, G., *INFRARED AND RAMAN CHARACTERISTIC GROUP FREQUENCIES: Tables and Charts*, 3rd ed. (2001) John Wiley & Sons Ltd., West Sussex, U.K. [ISBN: 0 471 85298 8].

Storm, S.L., A. Springsteen, T.M. Ricker, "A Discussion of Center Mount Sample Holder Designs and Applications," Labsphere Application Note 02, January 1998.

Stuart, B., *POLYMER ANALYSIS* (2002) John Wiley & Sons, Inc., New York, NY [ISBN: 0 471 89926 7].

Sutton, W.H, "Microwave Processing of Ceramic Materials," *Ceramic Bulletin*, **68[**2]:376-386, (1989).

Szulga, K., *HISTORY OF PAINT AND COATINGS: EVOLUTION OF EMULSIONS* (2003), Master's Thesis, submitted to the School of the Art Institute of Chicago, Chicago, IL.

Szycher, M., *SZYCHER'S HANDBOOK OF POLYURETHANES* (1990) CRC Press, New York NY [ISBN: 0 8493 0602 7].

Thermo Nicolet Corporation, "Introduction to Fourier Transform Infrared Spectrometry," *Thermoelectron Technical Notes* (2001) www.thermoelectron.com (accessed March 2011).

Thermo Nicolet Corporation, "ATR Theory," *Thermoelectron Technical Notes* (2001) www.thermoelectron.com (accessed July 2011).

Thuery, J., *MICROWAVES: INDUSTRIAL, SCIENTIFIC AND MEDICAL APPLICATIONS*, (1992) Artech House, Inc., Norwood, MA [ISBN: 0 89006 448 2].

Twente, "Methods of Infrared Spectroscopy," University of Twente, The Netherlands http://physics.schooltool.nl/irspectroscopy/method.php (accessed May 2011).

Urban, M.W., *ATTENUATED TOTAL REFLECTANCE OF POLYMERS: THEORY AND PRACTICE* (1996) American Chemical Society, Washington, D.C. [ISBN: 0 8412 3348 9].

Van Iseghem, L.C., "Wood Finishing with UV-curable Coatings," *Radtech Report*, May/June 2006.

Van Technologies, Inc., company website, http://www.vtcoatings.com/ (accessed February 2011).

APPENDICES

Appendix A

DICTIONARY OF TERMS

absorbance: In FTIR spectroscopy, "the amount of infrared radiation absorbed by the sample material;" "defined by Beer's Law;" " linearly proportional to concentration." [Newport, 2011]

aliphatic: "Of, relating to, or being an organic compound having an open-chain structure." [Merriam-Webster, 2003]

alkyd: "A synthetic resin derived from a reaction between alcohol and certain acids, used as a base for many laminates, paints and coatings." [Dictionary.com, June, 2011]

amine: Amines are organic compounds and functional groups that contain a basic nitrogen atom with a lone pair. Amines are derivatives of ammonia, where in one or more hydrogen atoms have been replaced by a substituent such as an alkyl or aryl group. [Dictionary.com, June, 2011]

anisotropy: "The dependence of the properties of a material on the direction in which they are being observed." [Alger, 1997]

aromatic: "Definition 2: *Of an organic compound*: characterized by increased chemical stability resulting from the delocalization of electrons in a ring system (as benzene) containing usually multiple conjugated double bonds." [Merriam-Webster, 2003]

Attenuated Total Reflectance (ATR): A spectroscopic sampling technique in which infrared radiation is incident on a crystal composted of infrared-transparent material with a high refractive index. An evanescent wave is formed in a sample in contact with the surface of the crystal and an infrared spectrum is generated for the sample material.[Smith, 1996]

background spectrum: single beam spectrum with no sample in the beam; a measure of the instrument and environment contribution to the spectrum; "these effects are removed from a sample spectrum by ratioing the sample single beam spectrum to the background spectrum." [Newport, 2011]

catalyst: "A substance that causes or accelerates a chemical reaction without itself being affected." [Dictionary.com, June 2011]

centerburst: In FTIR spectroscopy, a sharp, intense part of an interferogram whose "size is directly proportional to the amount of infrared radiation striking the detector." [Newport, 2011]

constructive interference: In FTIR spectroscopy, "a phenomenon that occurs when two waves occupy the same space and are in phase with each other." [Newport, 2011]

crosslink: "A covalent bond or relatively short sequence of chemical bonds joining two polymer chains together, thus forming a crosslinked polymer." [Alger, 1997]

cure: "The process of deliberately crosslinking a polymer to improve its properties, especially mechanical properties such as stiffness." [Alger, 1997] Note that the solubility and swelling will decrease with increased cure.

"Definition 3: To prepare or alter especially by chemical or physical processing for keeping our use; to undergo a curing process." [Merriam-Webster, 2003]

curing agent: "An additive used with a polymer in order to bring about, or increase the rate of, cure (crosslinking). [Alger, 1997]

Debye equation: "A relationship for the relative permittivity (ε) of a dielectric material as a function of the electronic and atomic polarizability (α_a) and the orientation polarizability terms." [Alger, 1997]

degradation: Refers to "chemical changes occurring in a polymer (often chain scission) which causes a deterioration of its useful properties." [Alger, 1997]

destructive interference: In FTIR spectroscopy, as with constructive interference, a phenomenon in which two waves occupy the same space; however, in this case, they are out of phase with each other. [Newport, 2011]

dielectric constant: (ε′; also known as relative permittivity) Measure of a material's ability to store electric charge through polarization mechanisms under an electric field. [Alger, 1997]

dielectric loss factor: (ε″) The imaginary part of the complex relative permittivity that is equal to the product of the dielectric constant and the dielectric loss; $\varepsilon'' = \varepsilon' \tan\delta$. [Alger, 1995]

dielectric properties: "Those electrical properties of a material relating to its behavior as a dielectric. They comprise the relative permittivity and the dielectric loss properties. The latter are most commonly characterized by the loss factor." [Alger, 1997]

dielectric thermal analysis: "A technique for the measurement of the dielectric loss, loss and storage components of the dielectric constant as they vary with temperature." Also known as dielectric relaxation spectroscopy. [Alger, 1997]

differential scanning calorimetry: (DSC) "A thermal analysis technique that measures the energy required to maintain the temperature of the sample the same as that of an inert reference material." [Alger, 1997]

differential thermal analysis: (DTA) "A thermal analysis technique that measure the temperature difference between the sample and an inert reference material." [Alger, 1997]

diffuse reflectance: The phenomenon that takes place light incident on a rough surface is transmitted, absorbed, scattered and reflected in all directions by that surface. [Smith, 1996]

diisocyanate: "A compound containing two isocyanate groups, i.e. one of the type OCN – R – NCO, where R is an alkyl, cycloalkyl or aromatic group." [Alger, 1997]

dilatometry: "The measure of the changes in the volume of a substance by filling a small containing vessel, usually a cylindrical glass bulb, with the substance and following the change in level of the substance (of liquid) or of a liquid in which the substance is immersed (if solid), in an attached capillary tube." [Alger, 1997]

diol: "A compound containing two hydroxyl groups." [Merriam-Webster, 2003]

dispersive instruments: "Infrared spectrometers using a grating or prism to disperse the infrared radiation into component wavenumbers before detecting the radiation." [Newport, 2011]

dynamic mechanical analyzer (DMA): An instrument for determining the "dynamic mechanical behavior over a range of frequency or temperature." Results of the measurements usually are expressed in terms of the storage modulus or loss modulus as a function of frequency or temperature. [Alger, 1997]

endothermic: "Noting or pertaining to a chemical change that is accompanied by an absorption of heat." [Dictionary.com; June 2011]

evanescent wave: A standing wave generated in an ATR crystal so that, when a sample is put into close contact with the surface of an ATR crystal, a portion of the energy is absorbed into the sample to generate an FTIR spectrum. [Smith, 1996]

exothermic: "Noting or pertaining to a chemical change that is accompanied by a liberation of heat." [Dictionary.com, June 2011]

Felgett Advantage (Multiplex Advantage): An advantage of FTIR over dispersive spectroscopy methods; based on the fact that, in FTIR, all wavenumbers of light are detected simultaneously. [Newport, 2011]

free radicals: "An atom or molecule that bears an unpaired electron and is extremely reactive, capable of engaging in rapid chain reactions that destabilize other molecules and generate many more free radicals: in the body, deactivated by antioxidants, uric acid, and certain enzyme activities." [Dictionary.com, June 2011]

Fourier transform: "A mathematical widely used in science and engineering that coverts a signal which is intensity vs. time into a spectrum which is amplitude vs. frequency, and the latter is actually a complex spectrum where for each frequency both the phase and amplitude is specified. There is an associated inverse Fourier transform that coverts the complex spectrum back into a time dependent signal." [Alger, 1997]

Fourier transform infrared spectroscopy (FTIR): "A method of obtaining infrared spectry by first measuring the interferogram of the sample using an interferometer, then performing a Fourier transform on the interferogram to obtain the spectrum." [Smith, 1996]

functional groups: "A group of atoms responsible for the characteristic behavior of the class of compounds in which the group occurs, as the hydroxyl group in alcohols." [Dictionary.com, June 2011]

infrared spectroscopy: "A technique that measures a material's absorption of infrared (IR) radiation over a range of IR in the electromagnetic spectrum, usually in the range of ~4000-250 cm^{-1}." [Alger, 1997]

interferogram: "A plot of infrared detector response vs. optical path difference; fundamental measurement by an FTIR; Fourier transformed to give infrared spectrum." [Newport, 2011]

isocyanate: "A compound containing the group, -N = C = O, abbreviated as –NCO." [Alger, 1997]

isothermal: "Noting or pertaining to a chemical change that is accompanied by a liberation of heat." [Dictionary.com, June 2011]

Horizontal Attenuated Total Reflectance: An FTIR technique in which the ATR crystal is seated in a stage in a horizontal orientation, making sample preparation and handling simpler for performing FTIR spectroscopy. [Thermo Electron Corporation, 2001]

Jacquinot Advantage: "A throughput advantage of FTIRs over spectrometers with a slit aperature; varies as wavenumber and depends on resolution; also depends on source dimensions." [Newport, 2011]

klystron: "A brand name for a vacuum tube containing an electron gun, a resonator that changes the velocity of the electron beam in accordance with a signal, a drift tube in which the electron velocity does not change, another resonator that abstracts energy from the electron beam, and an electrode that collects the electrons. It has several ultra-high-frequency applications." [Dictionary.com, June 2011]

lacquer: "A coating composition consisting of a polymer solution which, after application as a liquid film on a substrate, drives rapidly to a solid film by evaporation of the solvent. The term often refers specifically, especially in the older literature, to cellulose nitrate or other cellulose based, film forming compositions." [Alger, 1997]

linear polymer: "A polymer in which the molecules consist of single unbranched chains of atoms." [Alger, 1997]

loss tangent: ($\tan\delta$) "Ratio between the real dielectric constant of the sample (ε') and the dielectric loss factor (ε'')." [Rabek, 1980]

Michelson interferometer: The most common configuration for optical spectroscopy in which an interference pattern is produced by splitting a beam of light into two paths and then recombining them. If the paths are different, a spectrum can be generated that is specific to a particular chemical composition. [Smith, 1996; Wikipedia, June 2011]

microwave: "Definition 1: A comparatively short electromagnetic wave, especially one between about 1 millimeter and one meter in wavelength." [Merriam-Webster, 2003]

mirror displacement: The distance that a mirror in an FTIR spectrometer moves from the zero path difference. [Newport, 2011]

optical path difference: In FTIR spectroscopy, "the distance in an optical path distance that two light beams travel in an interferometer." [Newport, 2011]

polarization: "The displacement of the component charges of a dielectric by an applied electric field, causing the material to behave as an electric dipole." [Alger, 1997]

polymerization: "The chemical reaction by which a monomer is converted to polymer." [Alger, 1997]

polyol: "A molecule containing two or more hydroxyl groups. The term is used to describe both the low molecular mass hydroxyl compounds with two hydroxyls (diols or glycols) and polymeric molecules with hydroxyl end groups." [Alger, 1997]

The polyols are major contributors to the final properties of polyurethanes. The wide range of polyols directly leads to the very diverse and wide ranging polyurethanes, making them the most versatile classification of plastic materials. [Randall et al, 2002].

polyurethane: (PUR) "A polymer which contains urethane groups in the polymer chain." [Alger, 1997]

Pyrex®: Introduced by Corning Inc. in 1915, this glass originally was made of a borosilicate glass. The composition was later changed to a tempered soda-lime-silicate glass improve mechanical strength. [Wikipedia, June 2011]

reflectance: "The ratio of the intensity of reflected radiation to that of the radiation incident on a surface." [Dictionary.com, June 2011]

rheometry: "The experimental determination of the rheological property of materials, particularly fluid materials." [Alger, 1997]

resin: This term originally referred to polymer extrudates from plants and trees after they had hardened in air or long-term burial. It also was used to describe natural polymers, such as lacquers and varnishes. It is used more often now to refer to liquid pre-polymers that develop into thermosets upon processing. [Alger, 1997]

resolution: In FTIR spectroscopy, the measure of ability of a spectrometer to distinguish spectral features that lie close to one another. [Newport, 2011]

shellac: "Definition 1: Purified lac usually prepared in thin orange or yellow flakes by heating and filtering and often bleached white; 2. A preparation of lac dissolved usually in alcohol and used chiefly as a wood filler and finish." [Merriam-Webster, 2003]

specular reflectance: "The type of reflectance that takes place off smooth, shiny surfaces, such as that of mirrors. By definition, in specular reflectance, the angle of incidence of light equals the angle of reflectance of light." [Smith, 1996]

strike-in: A phenomenon associated with the inability of a range of wavelengths to penetrate deeply enough into a material to initiate curing. [Van Iseghem, 2006]

thermogravimetric analysis: (TGA) A thermal analysis technique often used in polymer degradation studies in which the sample weight is recorded continuously while being heated in a thermobalance. [Alger, 1997]

thermoplastic: "A plastic material existing below the Tg value (if amorphous) or between the Tg and Tm values (if crystalline), in which the polymer is a linear polymer. [Alger, 1997]

thermoset: "A polymer that is so extensively crosslinked that on heating it does not significantly soften." [Alger, 1997]

transmittance: "The ratio of the radiant flux transmitted through and emerging from a body to the total flux incident on it: equivalent to one minus the absorptance." [Dictionary.com, June 2011]

traveling wave tube: "An electron tube used in microwave communications systems, having an electron beam directed coaxially through a wire helix to produce amplification." [Dictionary.com, June 2011]

urethane: "A reaction of the type, R-O-CONH-R′." Urethanes normally are formed by the reaction between isocyante and hydroxyl groups. [Alger; Meier-Westhues]

viscosity: The ability of a fluid to resist flow. [Alger, 1997]

waveguide: "A conduit, as a metal tube, coaxial cable, or strand of glass fibers, used as a conductor or directional transmitter for various kinds of electromagnetic waves." [Dictionary.com, June 2011]

wavenumber: $1/\lambda$; used most often for the x-axis in spectra with absorbance, percent transmittance, or percent reflectance plotted on the y-axis. [Smith, 1996]

zero path difference (zero path optical difference): In FTIR spectroscopy, "the mirror displacement at which the optical path difference for the two beams in an interferometer is zero." [Newport, 2011]

Appendix B

NORMALIZING TIME AND ERROR ANALYSIS IN RATE PLOTS FOR AIR-CURED SAMPLES

Figures 4.16 through 4.19 represent runs 2 through 4 under ambient conditions in the laboratory. Run 1 is plotted in Figure 4.14. These figures represent the absorbance intensity from the sample spectra at random time steps throughout the experiments. In these figures, all of the data taken in each run is plotted.

The data provided in Figures B2.1 through B2.4 was generated using averages calculated for groups of data taken over the course of the air-cure experiments at 1-minute intervals. Each of the points on the following figures represents one of these average values. The error bars have been generated using a standard error calculation in Excel, and are plotted for each of the averages. As the time between measurements was one minute, the measurements that were averaged were considered to be at approximately the same time; therefore, the error bars represent instrument error, rather than error due to differences in the samples. By looking at the upper and lower bounds of the error bars for the plotted runs (runs 2 through 4), the error due to differences in sample and the environmental conditions can be estimated.

In Figures B2.1 (a) through B2.4(a), the full time scale is presented for each of the peaks in runs 2 through 4. Note that each of the runs contained plateaus over which the change in peak intensity was minimal. Also note that each of these runs had plateaus that existed for different times. The differences in the plateaus could have been attributed to varying sample thickness. Although care was taken to ensure that the sample volume (thus thickness) was consistent from one run to the next, due to the accuracy of the calipers used to measure the thickness of the "wet" samples in the ZnSe trough, there could have been differences as large as a tenth of a millimeter. Another source of error could have been the changing relative humidity in the laboratory. The conditions varied between 20% and 47% relative humidity for runs 1 through 4 in the air-cured samples.

In order to evaluate the curves for each peak once changes have begun, the time is normalized to remove the plateaus from each of the plots. In other words, t = 0min in Figures B2.1(b) through B2.4(b) represents the point at which the samples begin to experience change. This step allows for a comparison of the cure behavior without the influence of the sample thickness. Table B2.1 provides the time of each plateau.

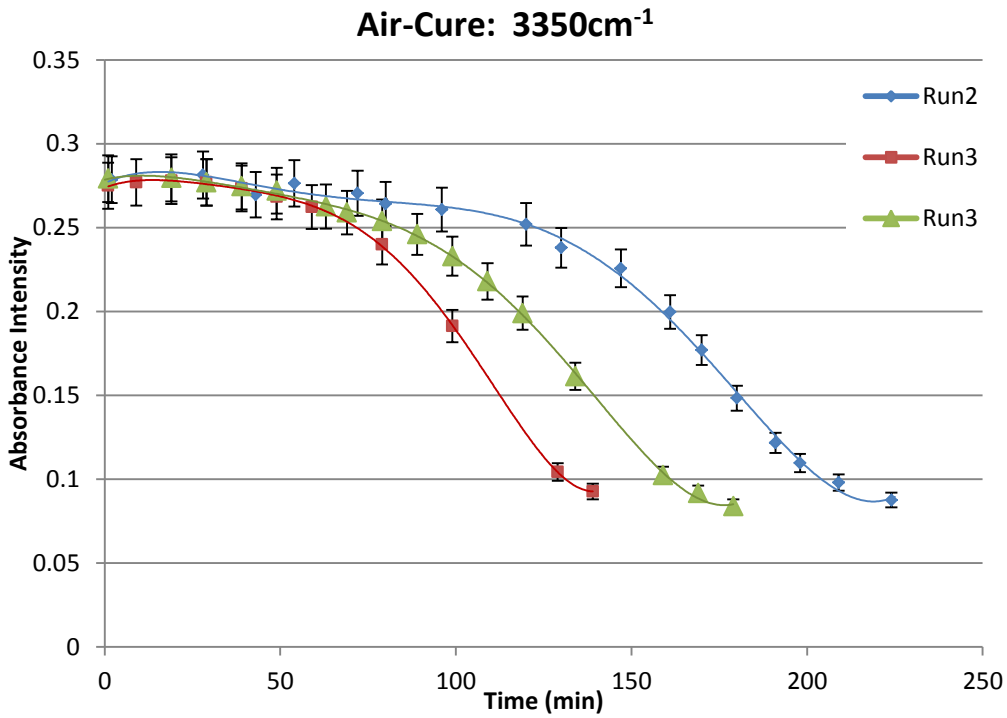

(a)

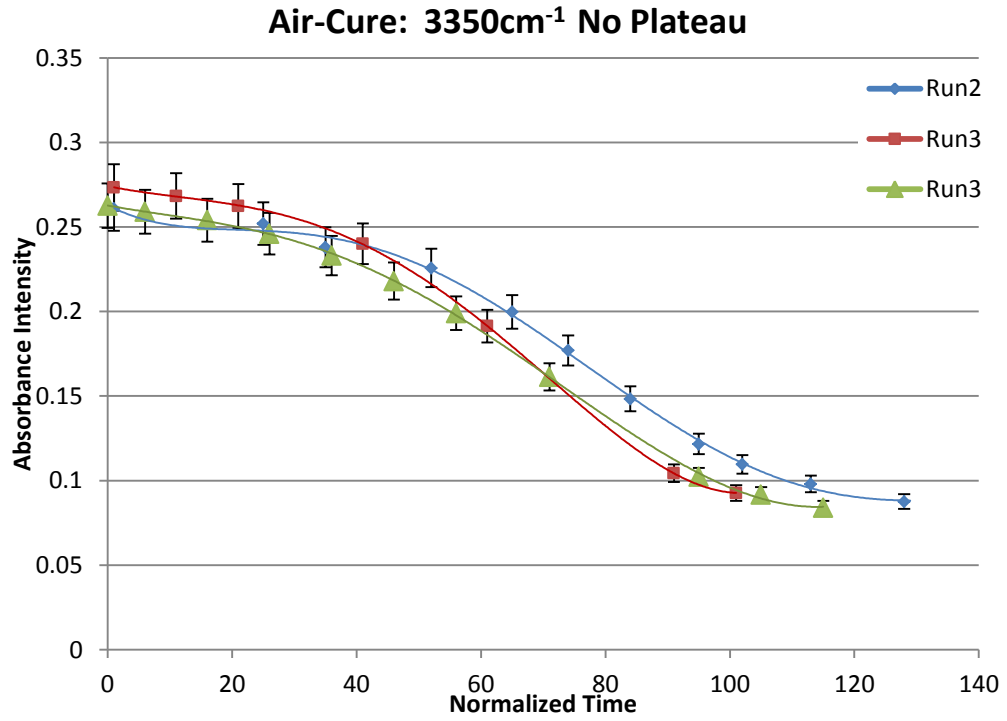

(b)

Figure B2.1: Change in absorbance vs. time for the aliphatic amine at 3350cm^{-1} in air-cured GL-4850 polyurethane: (a) all data; (b) normalized time steps after eliminating plateaus.

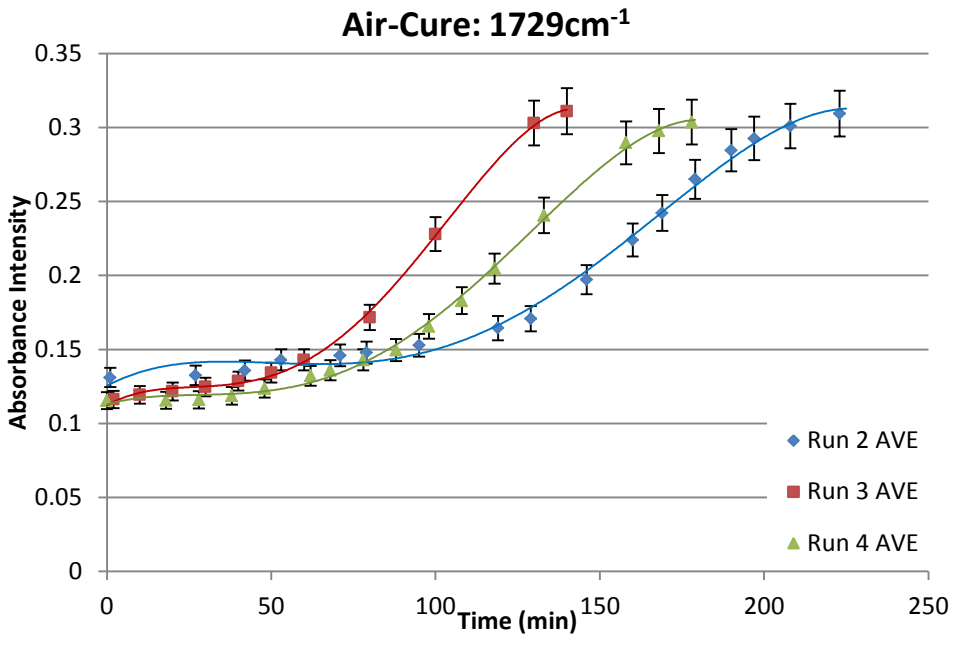

(a)

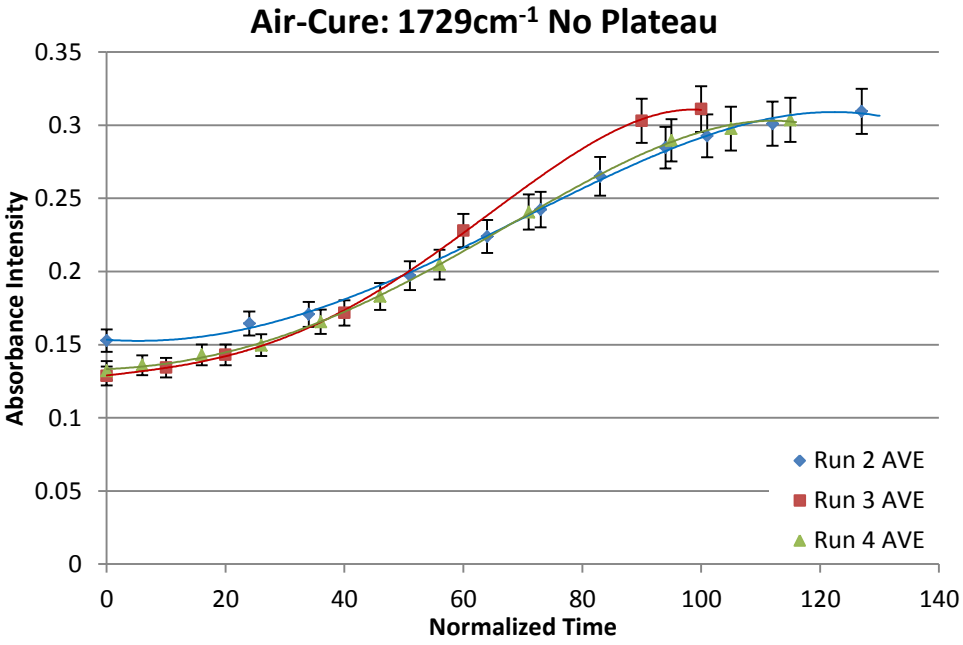

(b)

Figure B2.2: Change in absorbance vs. time for the aliphatic amine at 1729cm^{-1} in air-cured GL-4850 polyurethane: (a) all data; (b) normalized time steps after eliminating plateaus.

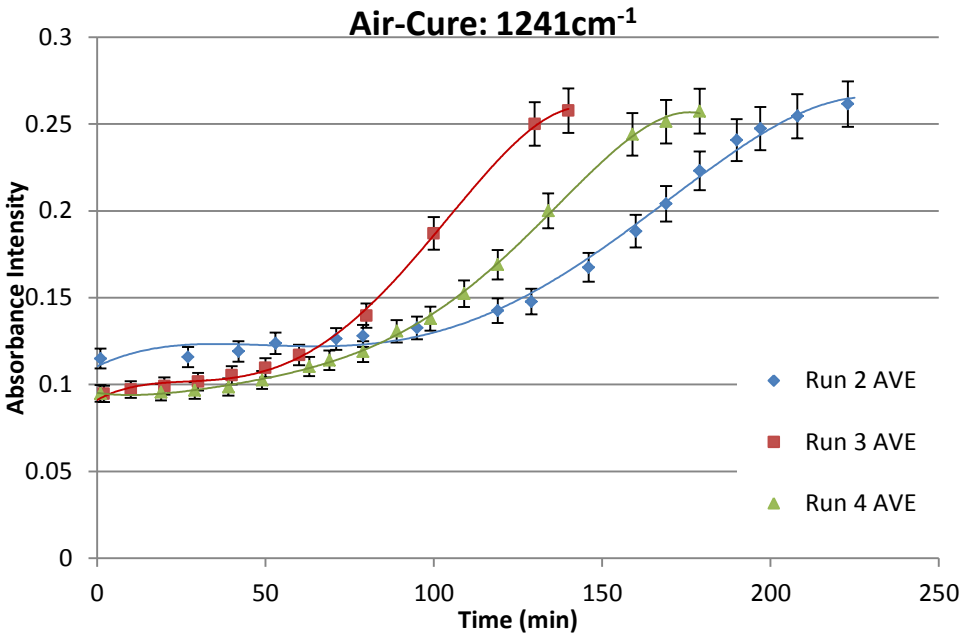

(a)

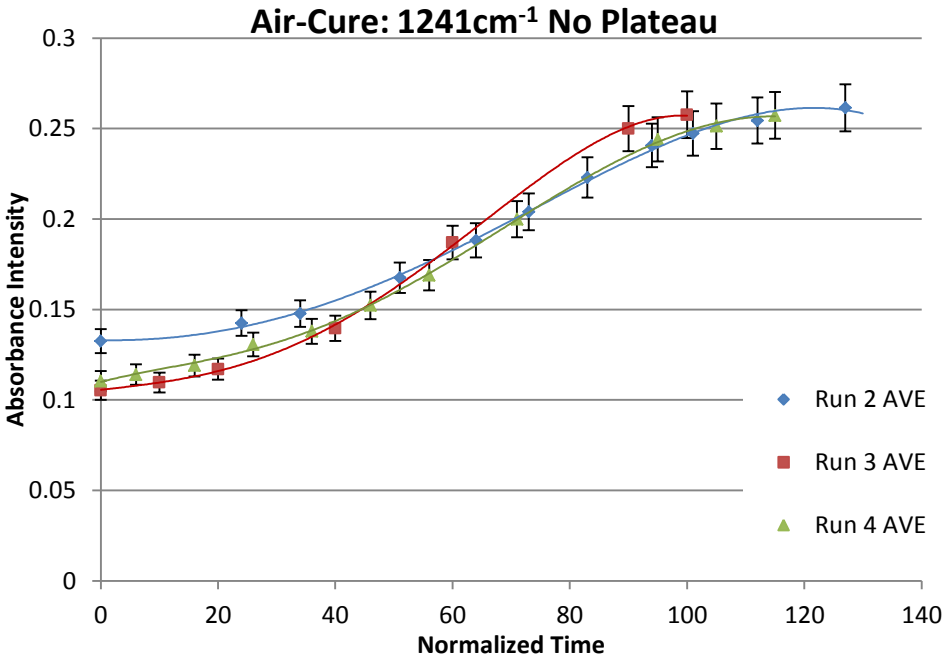

(b)

Figure B2.3: Change in absorbance vs. time for the aliphatic amine at 1241cm^{-1} in air-cured GL-4850 polyurethane: (a) all data; (b) normalized time steps after eliminating plateaus.

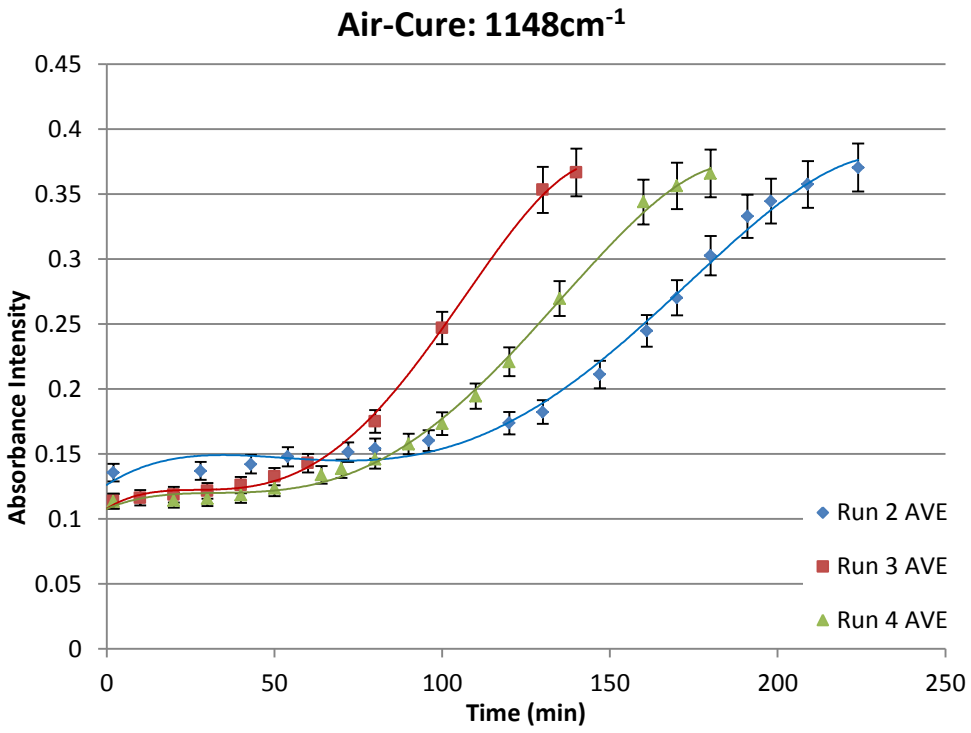

(a)

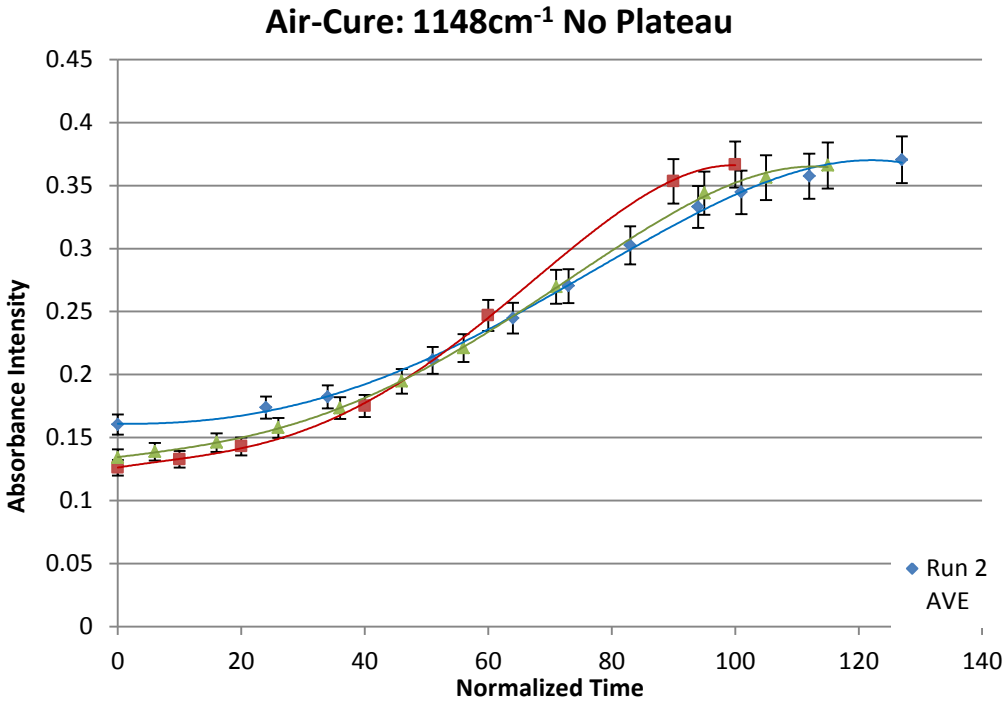

(b)

Figure B2.4: Change in absorbance vs. time for the aliphatic amine at 1148cm^{-1} in air-cured GL-4850 polyurethane: (a) all data; (b) normalized time steps after eliminating plateaus.

Table B2.1: Summary of the plateau times and relative humidity for sample runs 2 through 4.

Sample Run	t(min)	RH (%)
2	100	47
3	42	40
4	64	45

Special thanks to W. Huang and G-L. Jane of the Laboratory for Interdisciplinary Statistical Analysis (LISA) at Virginia Tech for reviewing the methodology used for error analysis in this work.